

**ANTICANCER PROPERTY OF SOME METAL(II) COMPLEXES OF
1, 10-PHENANTHROLINE AND MALTOL**

By

TAN THEAN HENG

A dissertation submitted to the Department of Chemical Engineering,
Faculty of Engineering and Science,
Universiti Tunku Abdul Rahman,
in partial fulfillment of the requirements for the degree of
Master of Science
February 2014

ABSTRACT

ANTICANCER PROPERTY OF SOME METAL(II) COMPLEXES OF 1, 10-PHENANTHROLINE AND MALTOL

TAN THEAN HENG

After the discovery of the novel compound cisplatin, a platinum anticancer agent, scientists have increasing interest in the possibilities of developing other transition metal compound into anticancer agent. In this study copper, cobalt and zinc was chosen and incorporated with organic ligand matol and 1,10-phenanthroline. The three compounds that were screened from this combination were $[M(\text{phen})(\text{ma})\text{Cl}]$ ($M=\text{Cu}(\text{II}), \text{Co}(\text{II}), \text{Zn}(\text{II})$; phen=1,10-phenanthroline; ma=maltolate). Two malignant breast cancer cell lines, MCF-7 and MDA-MB-231, and one non-malignant cell line, MCF10A, were used. MTT assay was done to screen for anticancer properties of $[M(\text{phen})(\text{ma})\text{Cl}]$ with 24 hours, 48 hours and 72 hours duration. The cytotoxicity of $[\text{Cu}(\text{phen})(\text{ma})\text{Cl}]$ were equally potent for malignant and non-malignant cell lines with IC-50 values of MCF-7, MDA-MB-231 and MCF10A for $[\text{Cu}(\text{phen})(\text{ma})\text{Cl}]$ after 24 hours incubation at $4.0\mu\text{M}$, $5.5\mu\text{M}$ and $8.7\mu\text{M}$ respectively. The same trend was recorded for $[\text{Zn}(\text{phen})(\text{ma})\text{Cl}]$ recording IC-50 values of MCF-7, MDA-MB-231 and MCF10A after 48 hours incubation at $7.9\mu\text{M}$, $6.5\mu\text{M}$ and $10.0\mu\text{M}$ respectively. There were considerable difference in $[\text{Co}(\text{phen})(\text{ma})\text{Cl}]$ IC-50 value after 72 hours incubation among MCF-7

(2.9 μ M), MDA-MB-231 (17.8 μ M) and MCF10A (16.9 μ M). Basic morphological study on cells that were treated with [Cu(phen)(ma)Cl] and [Zn(phen)(ma)Cl] showed cytoplasmic enlargement and rupture of the plasma membrane indicating necrosis. Under microscope [Co(phen)(ma)Cl] showed nuclear condensation, cytoplasmic vacuolation, membrane bebbing and presence of apoptotic body on MCF-7 and MDA-MB-231 indicating apoptosis but has relatively low effectiveness towards MCF10A. After preliminary studies on [M(phen)(ma)Cl] results shown that [Cu(phen)(ma)Cl] and [Zn(phen)(ma)Cl] were equally cytotoxic to both malignant and non-malignant cell lines so these two compounds were excluded from further testing. The morphological observation on the effects of [Co(phen)(ma)Cl] was confirmed with Annexin V-FITC/PI apoptosis assay showing [Co(phen)(ma)Cl] induced apoptosis dose dependently on MCF-7 and MDA-MB-231 only and the effect was not as apparent on MCF10A with percentage of viable cells >90% on 3 μ M, 17 μ M and 25 μ M. Cell cycle studies using flow cytometry showed slight arrest in G2/M phrased for MCF-7 and significant arrest on G0/G1 phrase for MDA-MB-231. Meanwhile no cell cycle arrest was found on MCF10A. Proteasome-Glo™ cell-based assay showed that [Co(phen)(ma)Cl] inhibit proteasome activity of MDA-MB-231 on 3 μ M, 17 μ M and 25 μ M in a dose dependent manner while having insignificant effect on MCF-7 and MCF10A. Measurement of Reactive Oxygen Species showed accumulation of intracellular ROS level in MDA-MB-231 after treated with [Co(phen)(ma)Cl] on 3 μ M, 17 μ M and 25 μ M in a dose dependent manner. There was no significant changes in intracellular ROS level in MCF-7 and MCF10A after treated with [Co(phen)(ma)Cl]. The results showed selectivity

on cytotoxicity of [Co(phen)(ma)Cl] towards tumorigenic and non-tumorigenic breast epithelial cells plus distinct difference in mechanism of action between highly invasive breast cancer cell line and non-invasive breast cancer cell line. Better understanding of [Co(phen)(ma)Cl] mechanism of action can lead to the discovery of a novel compound that can target a particular type of cancer cell.

ACKNOWLEDGEMENT

I would like to express my deepest gratitude for my supervisor, Dr Tioh Ngee Heng, for his willingness to take me under his supervision when I was left stranded halfway. Without his guidance and persistent help this thesis would not have been possible.

I am indebted to Dr Alan Khoo Soo Beng for allowing me to use his laboratory for my research and also Dr Munirah Bt. Ahmad for her guidance during my stay in IMR. I am grateful to Mrs Chu Tai Lin for her assistance in providing me with all the materials and cell lines that were required in my research.

Last but not least, a thank you to my ex-supervisor Dr Ng Chew Hee for providing me the opportunity to participate in this interesting yet challenging research.

APPROVAL SHEET

This dissertation/thesis entitled “**ANTICANCER PROPERTY OF SOME METAL(II) COMPLEXES OF 1, 10-PHENANTHROLINE AND MALTOL**” was prepared by TAN THEAN HENG and submitted as partial fulfillment of the requirements for the degree of Master of Science at Universiti Tunku Abdul Rahman.

Approved by:

(Dr. Tioh Ngee Heng)
Supervisor
Department of Chemical Engineering
Faculty of Engineering and Science
Universiti Tunku Abdul Rahman

Date: 27 February 2014

FACULTY OF ENGINEERING AND SCIENCE
UNIVERSITI TUNKU ABDUL RAHMAN

Date: 27 February 2014

SUBMISSION OF DISSERTATION

It is hereby certified that **Tan Thean Heng** (ID No: **08UEM00965**) has completed this dissertation entitled “ANTICANCER PROPERTY OF SOME METAL(II) COMPLEXES OF 1, 10-PHENANTHROLINE AND MALTOL” under the supervision of Dr. Tioh Ngee Heng (Supervisor) from the Department of Chemical Engineering, Faculty of Engineering and Science.

I understand that University will upload softcopy of my thesis in pdf format into UTAR Institutional Repository, which may be made accessible to UTAR community and public.

Yours truly,

(TAN THEAN HENG)

DECLARATION

I hereby declare that the dissertation is based on my original work except for quotations and citations which have been duly acknowledged. I also declare that it has not been previously or concurrently submitted for any other degree at UTAR or other institutions.

(TAN THEAN HENG)

27 February 2014

TABLE OF CONTENTS

	Page
ABSTRACT	ii
ACKNOWLEDGEMENTS	v
APPROVAL SHEET	vi
SUBMISSION SHEET	vii
DECLARATION	viii
TABLE OF CONTENTS	ix
LIST OF TABLES	xii
LIST OF FIGURES	xv
LIST OF ABBREVIATIONS	xix
CHAPTER	
1.0 INTRODUCTION AND OBJECTIVES	1
1.1 Introduction	1
1.2 Objectives of this study	4
1.2.1 To test for anticancer properties of [M(phen)(mal)Cl]	4
1.2.2 To determine the selectivity of the mechanism of action of [M(phen)(mal)Cl] compounds	5
1.2.3 To find out the mechanism of action of [M(phen)(mal)Cl]	5
2.0 LITERATURE REVIEW	6
2.1 Development of new anticancer drugs	6
2.2 Metal based anticancer drugs	7
2.2.1 Copper based anticancer drugs	8
2.2.2 Cobalt based anticancer drugs	10
2.2.3 Zinc based anticancer drugs	11
2.3 Phenanthroline	12
2.4 Maltol	13
2.5 Different types of breast cancer	15
2.6 Apoptosis in cancer	17
2.7 The cell cycle and cancer	20
2.8 Proteasome inhibitors in cancer therapy	22
2.9 ROS and cancer therapeutics	25
3.0 PRELIMINARY STUDIES AND SCREENING OF [M(phen)(ma)Cl]	27
3.1 Material and methods	27
3.1.1 Cell line	27
3.1.2 Culture medium	28
3.1.2.1 RPMI medium preparation	28
3.1.2.2 DMEM preparation	29

	3.1.2.3	F-12 medium preparation	30
	3.1.2.4	DMEM/F-12 medium preparation	30
	3.1.3	Phosphate buffered saline solution preparation	31
	3.1.4	Thawing the cell line	31
	3.1.5	Maintenance of cell culture	31
	3.1.5.1	Medium changing	32
	3.1.5.2	Subculture of confluence cells	32
	3.1.6	Cryopreservation of cell line	33
	3.1.7	Cell count using trypan blue exclusion method	33
	3.1.8	Compound solution preparation	33
	3.1.9	Determination of the cytotoxicity of [M(phen)(ma)Cl]	34
	3.1.9.1	Preparing stock cells	35
	3.1.9.2	MTT assay	35
	3.1.10	Morphological study	36
3.2		Results	38
	3.2.1	Cell viability test using MTT assay	38
	3.2.2	Cell morphological study	65
3.3		Discussion	71
4.0		FURTHER STUDY ON [Co(phen)(ma)Cl]	75
4.1		Material and methods	75
	4.1.1	Cell line	75
	4.1.2	Apoptosis assay	76
	4.1.2.1	Cell preparation and staining of the cell	76
	4.1.3	Cell cycle analysis	77
	4.1.3.1	Hypotonic staining buffer reagent for DNA preparation	77
	4.1.3.2	Cell preparation and staining of the DNA	78
	4.1.4	Proteasome inhibition assay	79
	4.1.4.1	Proteasome-Glo™ Reagent Preparation	79
	4.1.4.2	Cell preparation and staining of the cells	80
	4.1.5	Measurement of Reactive Oxygen Species (ROS)	81
	4.1.5.1	Preparation of Reagents	81
	4.1.5.2	Cell preparation and staining of the cells	81
4.2		Results	83
	4.2.1	Apoptosis assay	83
	4.2.2	Cell cycle analysis	91
	4.2.3	Proteasome inhibition assay	98
	4.2.4	Measurement of Reactive Oxygen Species (ROS)	106
4.3		Discussion	112

5.0	FURTHER STUDIES AND CONCLUSION	118
5.1	Recommendations for further studies	118
5.2	Conclusion	120
	REFERENCES	122
	APPENDICES	137

LIST OF TABLES

Tables	Page
3.1.1 Percentage of viable cells of MCF-7 cells after 24 hours of treatment with increasing concentrations [Cu(phen)(ma)Cl].	40
3.1.2 Percentage of viable cells of MDA-MB-231 cells after 24 hours of treatment with increasing concentrations [Cu(phen)(ma)Cl].	40
3.1.3 Percentage of viable cells of MCF10A cells after 24 hours of treatment with increasing concentrations [Cu(phen)(ma)Cl].	40
3.2.1 Percentage of viable cells of MCF-7 cells after 24 hours of treatment with increasing concentrations [Co(phen)(ma)Cl].	43
3.2.2 Percentage of viable cells of MDA-MB-231 cells after 24 hours of treatment with increasing concentrations [Co(phen)(ma)Cl].	43
3.2.3 Percentage of viable cells of MCF10A cells after 24 hours of treatment with increasing concentrations [Co(phen)(ma)Cl].	43
3.3.1 Percentage of viable cells of MCF-7 cells after 24 hours of treatment with increasing concentrations [Zn(phen)(ma)Cl].	46
3.3.2 Percentage of viable cells of MDA-MB-231 cells after 24 hours of treatment with increasing concentrations [Co(phen)(ma)Cl].	46
3.3.3 Percentage of viable cells of MCF10A cells after 24 hours of treatment with increasing concentrations [Zn(phen)(ma)Cl].	46
3.4.1 Percentage of viable cells of MCF-7 cells after 48 hours of treatment with increasing concentrations [Cu(phen)(ma)Cl].	49
3.4.2 Percentage of viable cells of MDA-MB-231 cells after 48 hours of treatment with increasing concentrations [Cu(phen)(ma)Cl].	49
3.4.3 Percentage of viable cells of MCF10A cells after 48 hours of treatment with increasing concentrations [Cu(phen)(ma)Cl].	49

3.5.1	Percentage of viable cells of MCF-7 cells after 48 hours of treatment with increasing concentrations [Co(phen)(ma)Cl].	52
3.5.2	Percentage of viable cells of MDA-MB-231 cells after 48 hours of treatment with increasing concentrations [Co(phen)(ma)Cl].	52
3.5.3	Percentage of viable cells of MCF10A cells after 48 hours of treatment with increasing concentrations [Co(phen)(ma)Cl].	52
3.6.1	Percentage of viable cells of MCF-7 cells after 48 hours of treatment with increasing concentrations [Zn(phen)(ma)Cl].	55
3.6.2	Percentage of viable cells of MDA-MB-231 cells after 48 hours of treatment with increasing concentrations [Zn(phen)(ma)Cl].	55
3.6.3	Percentage of viable cells of MCF10A cells after 48 hours of treatment with increasing concentrations [Zn(phen)(ma)Cl].	55
3.7.1	Percentage of viable cells of MCF-7 cells after 72 hours of treatment with increasing concentrations [Cu(phen)(ma)Cl].	58
3.7.2	Percentage of viable cells of MDA-MB-231 cells after 72 hours of treatment with increasing concentrations [Cu(phen)(ma)Cl].	58
3.7.3	Percentage of viable cells of MCF10A cells after 72 hours of treatment with increasing concentrations [Cu(phen)(ma)Cl].	58
3.8.1	Percentage of viable cells of MCF-7 cells after 72 hours of treatment with increasing concentrations [Co(phen)(ma)Cl].	61
3.8.2	Percentage of viable cells of MDA-MB-231 cells after 72 hours of treatment with increasing concentrations [Co(phen)(ma)Cl].	61
3.8.3	Percentage of viable cells of MCF10A cells after 72 hours of treatment with increasing concentrations [Co(phen)(ma)Cl].	61
3.9.1	Percentage of viable cells of MCF-7 cells after 72 hours of treatment with increasing concentrations [Zn(phen)(ma)Cl].	64

3.9.2	Percentage of viable cells of MDA-MB-231 cells after 72 hours of treatment with increasing concentrations [Zn(phen)(ma)Cl].	64
3.9.3	Percentage of viable cells of MCF10A cells after 72 hours of treatment with increasing concentrations [Zn(phen)(ma)Cl].	64
4.1.1	Percentage of apoptotic, dead and viable cells of MCF-7 after treated with increasing concentrations of [Co(phen)(ma)Cl] for 72 hours.	90
4.1.2	Percentage of apoptotic, dead and viable cells of MDA-MB-231 after treated with increasing concentrations of [Co(phen)(ma)Cl] for 72 hours.	90
4.1.3	Percentage of apoptotic, dead and viable cells of MCF10A after treated with increasing concentrations of [Co(phen)(ma)Cl] for 72 hours.	90
4.2.1	Percentage of MCF-7 cells in G0/G1, S and G2/M phases after treated with increasing concentrations of [Co(phen)(ma)Cl] for 72 hours.	97
4.2.2	Percentage of MDA-MB-231 cells in G0/G1, S and G2/M phases after treated with increasing concentrations of [Co(phen)(ma)Cl] for 72 hours.	97
4.2.3	Percentage of MCF10A cells in G0/G1, S and G2/M phases after treated with increasing concentrations of [Co(phen)(ma)Cl] for 72 hours.	97
4.3.1	Percentage of trypsin-like proteasome activity of MCF-7, MDA-MB-231 and MCF10A cells after treated with increasing concentrations of [Co(phen)(ma)Cl] for 72 hours.	104
4.3.2	Percentage of chemotrypsin-like proteasome activity of MCF-7, MDA-MB-231 and MCF10A cells after treated with increasing concentrations of [Co(phen)(ma)Cl] for 72 hours.	104
4.3.3	Percentage of caspase-like proteasome activity of MCF-7, MDA-MB-231 and MCF10A cells after treated with increasing concentrations of [Co(phen)(ma)Cl] for 72 hours.	105
4.4.1	Relative DCF fluorescence percentage of MCF-7, MDA-MB-231 and MCF10A cells after treated with increasing concentrations of [Co(phen)(ma)Cl] for 72 hours	111

LIST OF FIGURES

Figures		Page
1.1	The molecular structure of $[M(\text{phen})(\text{mal})\text{Cl}]$ with M as the metal center flanked with 1,10-phenanthroline on the right and maltol on the left as ligand.	3
3.1.1	Viable cells of of MCF-7, MDA-MB-231 and MCF10A cells treated with increasing concentrations of $[\text{Cu}(\text{phen})(\text{ma})\text{Cl}]$ for 24 hours using MTT assay.	39
3.1.2	Viable cells of of MCF-7, MDA-MB-231 and MCF10A cells treated with increasing concentrations of $[\text{Co}(\text{phen})(\text{ma})\text{Cl}]$ for 24 hours using MTT assay.	42
3.1.3	Viable cells of of MCF-7, MDA-MB-231 and MCF10A cells treated with increasing concentrations of $[\text{Zn}(\text{phen})(\text{ma})\text{Cl}]$ for 24 hours using MTT assay.	45
3.1.4	Viable cells of of MCF-7, MDA-MB-231 and MCF10A cells treated with increasing concentrations of $[\text{Cu}(\text{phen})(\text{ma})\text{Cl}]$ for 48 hours using MTT assay.	48
3.1.5	Viable cells of of MCF-7, MDA-MB-231 and MCF10A cells treated with increasing concentrations of $[\text{Co}(\text{phen})(\text{ma})\text{Cl}]$ for 48 hours using MTT assay.	51
3.1.6	Viable cells of of MCF-7, MDA-MB-231 and MCF10A cells treated with increasing concentrations of $[\text{Zn}(\text{phen})(\text{ma})\text{Cl}]$ for 48 hours using MTT assay.	54
3.1.7	Viable cells of of MCF-7, MDA-MB-231 and MCF10A cells treated with increasing concentrations of $[\text{Cu}(\text{phen})(\text{ma})\text{Cl}]$ for 72 hours using MTT assay.	57
3.1.8	Viable cells of of MCF-7, MDA-MB-231 and MCF10A cells treated with increasing concentrations of $[\text{Co}(\text{phen})(\text{ma})\text{Cl}]$ for 72 hours using MTT assay.	60
3.1.9	Viable cells of of MCF-7, MDA-MB-231 and MCF10A cells treated with increasing concentrations of $[\text{Zn}(\text{phen})(\text{ma})\text{Cl}]$ for 72 hours using MTT assay.	63

- 3.2.1 Morphological observations of (a) untreated MCF-7 cells (d) untreated MDA-MB-231 cells (g) untreated MCF10A cells with cells treated with increasing concentrations of [Cu(phen)(ma)Cl] for 72 hours (b) MCF-7 0.05 μ M (c) MCF-7 0.4 μ M (e) MDA-MB-231 0.05 μ M (f) MDA-MB-231 0.4 μ M (h) MCF10A 0.05 μ M (i) MCF10A 0.4 μ M. Arrow (A) apoptotic body (C) condensation of chromatin (D) dead cell (E) detachment from surface (L) elongation of cell (M) enlargement of cytoplasm (V) vacoulation. Images were captured using phase-contrast inverted microscope at 200x magnification. 68
- 3.2.2 Morphological observations of (a) untreated MCF-7 cells (d) untreated MDA-MB-231 cells (g) untreated MCF10A cells with cells treated with increasing concentrations of [Co(phen)(ma)Cl] for 72 hours (b) MCF-7 2.9 μ M (c) MCF-7 17.8 μ M (e) MDA-MB-231 2.9 μ M (f) MDA-MB-231 17.8 μ M (h) MCF10A 2.9 μ M (i) MCF10A 17.8 μ M. Arrow (A) apoptotic body (C) condensation of chromatin (D) dead cell (E) detachment from surface (L) elongation of cell (M) enlargement of cytoplasm (V) vacoulation. Images were captured using phase-contrast inverted microscope at 200x magnification. 69
- 3.2.3 Morphological observations of (a) untreated MCF-7 cells (d) untreated MDA-MB-231 cells (g) untreated MCF10A cells with cells treated with increasing concentrations of [Zn(phen)(ma)Cl] for 72 hours (b) MCF-7 2.7 μ M (c) MCF-7 7.7 μ M (e) MDA-MB-231 2.7 μ M (f) MDA-MB-231 7.7 μ M (h) MCF10A 2.7 μ M (i) MCF10A 7.7 μ M. Arrow (A) apoptotic body (C) condensation of chromatin (D) dead cell (E) detachment from surface (L) elongation of cell (M) enlargement of cytoplasm (V) vacoulation. Images were captured using phase-contrast inverted microscope at 200x magnification. 70
- 4.1.1 Flow cytometric analysis of annexin V-FITC/PI double-staining: MCF-7 cells were left untreated or treated for 72 hours with (a) 3 μ M (b) 17 μ M or (c) 25 μ M of [Co(phen)(ma)Cl]. Cells were incubated with Annexin V-FITC in a buffer containing PI and analyzed by flow cytometry. The y axis denotes cells stained with PI and the x axis represents cells stained in Annexin V-FITC. 84

4.1.2	Flow cytometric analysis of annexin V-FITC/PI double-staining: MDA-MB-231 cells were left untreated or treated for 72 hours with (a) 3 μ M (b) 17 μ M or (c) 25 μ M of [Co(phen)(ma)Cl]. Cells were incubated with Annexin V-FITC in a buffer containing PI and analyzed by flow cytometry. The y axis denotes cells stained with PI and the x axis represents cells stained in Annexin V-FITC.	86
4.1.3	Flow cytometric analysis of annexin V-FITC/PI double-staining: MCF10A cells were left untreated or treated for 72 hours with (a) 3 μ M (b) 17 μ M or (c) 25 μ M of [Co(phen)(ma)Cl]. Cells were incubated with Annexin V-FITC in a buffer containing PI and analyzed by flow cytometry. The y axis denotes cells stained with PI and the x axis represents cells stained in Annexin V-FITC.	88
4.1.4	Percentage of apoptotic, dead and viable cells of MCF-7, MDA-MB-231 and MCF10A after treated with increasing concentrations of [Co(phen)(ma)Cl] for 72 hours.	89
4.2.1	Cell cycle analysis of MCF-7 after treated with increasing concentrations of [Co(phen)(ma)Cl] for 72 hours detected using flow cytometry with PI staining. The y axis denotes cell count and the x axis represents DNA content.	93
4.2.2	Changes in DNA content of MDA-MB-231 after treated with increasing concentrations of [Co(phen)(ma)Cl] for 72 hours detected using flow cytometry with PI staining. The y axis denotes cell count and the x axis represents DNA content.	94
4.2.3	Changes in DNA content of MCF10A after treated with increasing concentrations of [Co(phen)(ma)Cl] for 72 hours detected using flow cytometry with PI staining. The y axis denotes cell count and the x axis represents DNA content.	95
4.2.4	Percentage of MCF-7, MDA-MB-231 and MCF10A cells in G0/G1, S and G2/M phases after treated with increasing concentrations of [Co(phen)(ma)Cl] for 72 hours.	96

4.3.1	Percentage of trypsin-like proteasome activity of MCF-7, MDA-MB-231 and MCF10A cells after treated with increasing concentrations of [Co(phen)(ma)Cl] for 72 hours.	101
4.3.2	Percentage of chemotrypsin-like proteasome activity of MCF-7, MDA-MB-231 and MCF10A cells after treated with increasing concentrations of [Co(phen)(ma)Cl] for 72 hours.	102
4.3.3	Percentage of caspase-like proteasome activity of MCF-7, MDA-MB-231 and MCF10A cells after treated with increasing concentrations of [Co(phen)(ma)Cl] for 72 hours.	103
4.4.1	Relative DCF fluorescence percentage of MCF-7 cells after treated with increasing concentrations of [Co(phen)(ma)Cl] for 72 hours.	108
4.4.2	Relative DCF fluorescence percentage of MDA-MB-231 cells after treated with increasing concentrations of [Co(phen)(ma)Cl] for 72 hours.	109
4.4.3	Relative DCF fluorescence percentage of MCF10A cells after treated with increasing concentrations of [Co(phen)(ma)Cl] for 72 hours.	110

LIST OF ABBREVIATIONS

Phen	1,10-Phenanthroline
DCFH-DA	2',7'-dichlorofluorescein-diacetate
MTT	3-(4,5-dimethylthiazol-2-yl)-2,5-diphenyltetrazolium bromide
ATP	Adenosine-5'-triphosphate
Al ³⁺	Aluminum ion
Annexin V	Annexin A5
ATM	Ataxia telangiectasia mutated
bcl-2	B-cell lymphoma 2
CO ₂	Carbon dioxide
CDC7	Cell division cycle 7-related protein
°C	Celsius
Cl	Chlorine
CD95	Cluster of differentiation 95
Co	Cobalt
Cu(II)	Copper(II)
Cu	Copper
Co(II)	Cobalt(II)
CDK	Cyclin-dependent kinase
p15	Cyclin-dependent kinase 4 inhibitor B
p27	Cyclin-dependent kinase inhibitor 1B
p16	Cyclin-dependent kinase inhibitor 2A
COX	Cyclooxygenase
DNA	Deoxyribonucleic acid

EMT	Epithelial-mesenchymal transition
ER+	Estrogen receptor positive
ER-	Estrogen receptor negative
FITC	Fluorescein isothiocyanate
Ga ³⁺	Gallium ion
IC-50	Half maximal inhibitory concentration
HER2/ErbB2/neu	Human Epidermal Growth Factor Receptor 2
H ₂ O ₂	Hydrogen peroxide
OH [•]	Hydroxyl radical
IARC	International Agency For Research On Cancer
Fe ³⁺	Iron ion
MDA-MB-231	M.D. Anderson - Metastatic Breast - 231
Ma	Maltol
M	Metal center
MCF10A	Michigan Cancer Foundation - 10A
MCF-7	Michigan Cancer Foundation - 7
μM	Micromolar
mL	Millilitre
mm	Millimeter
MAPK	Mitogen-activated protein kinase
NFκB	Nuclear factor kappa-light-chain-enhancer of activated B cells
p38MAPK	P38 mitogen-activated protein kinase
PTEN	Phosphatase and tensin homolog
PI3K	Phosphatidylinositide 3-kinase
PBS	Phosphate buffer saline

PI	Propidium iodide
Akt	Protein Kinase B
RhoA	Ras homolog gene family, member A
ROS	Reactive oxygen species
Rb	Retinoblastoma
pRb	Retinoblastoma protein
rpm	Revolutions per minute
ATR	Serine/threonine-protein kinase
Chk1	Serine/threonine-protein kinase
$O_2^{\bullet-}$	Superoxide radical
p53	Tumor protein 53
UCH-L1	Ubiquitin carboxy-terminal hydrolase L1
VO^{2+}	Vanadium ion
Zn	Zinc
Zn(II)	Zinc(II)

CHAPTER 1

INTRODUCTION AND OBJECTIVES

1.1 Introduction

Cancer is one of the major causes of death in both developed and developing countries (World Health Organization, 2014). The risk of cancer is rising in developing countries as a result of aging population and growth as well as living cancer-related lifestyle choices including smoking, sedentary, and unhealthy diets. Breast cancer is by far the most common cancer diagnosed and cause of death in women worldwide, ranking second in both sexes combined (Ferlay et al., 2010). The incidence of breast cancer has increased in most countries worldwide in the last decades, with the most rapid increase occurring in many of the developing countries (IARC, 2012). The treatment given for cancer is variable and dependent on a number of factors including the type, location and amount of disease and the health status of the patient.

One of the treatments is chemotherapy which incorporates a broad spectrum of drugs used to treat cancer. These drugs typically function by inducing death on dividing cells. Since cancer cells have lost most of the regulatory functions available in normal cells, they will continue to try to divide when other cells do not. This characteristic causes cancer cells vulnerable to a broad spectrum of cellular poisons. However chemotherapeutic techniques have a number of side-effects that depend on the type of medication used. Most of the regular

medications used affect primarily the fast-dividing cells of the body, such as blood cells and the cells lining the intestines, stomach, and mouth. Some of the most commonly reported side effects are nausea and vomiting, alopecia, fatigue, ototoxicity, neutropenia, thrombocytopenia, anemia, mucositis, loss of appetite, cognitive problems, low libido and infertility, bowel movement problems, depression and also neurotoxicity (American Cancer Society). Even with such adverse list of side effects chemotherapy are plagued with pharmacological deficiencies and limitations. Chemotherapy is not always effectual, and even when it does, it may not entirely eliminate the cancer (Weeks et al., 2012). The prevalence of cancer and all associated costs, both in human and financial terms, drives the search for new therapeutic drugs and treatments.

Transition metals have a valued place in medicinal chemistry. The initial reports on the therapeutic exploit of transition metal complexes in cancer and leukemia timed back to the sixteenth century. In the 60s the anti-tumor activity of cis-diammine-dichloroplatinum(II) or better known as cisplatin was discovered (Rosenberg et al., 1969). Cisplatin was developed into one of the most regularly utilized and most efficient cytostatic drug for treatment of solid carcinomas. Cisplatin is particularly effective against testicular and ovarian cancer (Wong and Giandomenico, 1999; Giaccone, 2000). Cisplatin is also used in combination regimens for other carcinomas, including bladder and non small cell lung and head and neck cancers (Weiss and Christian 1993; Ho et al., 2003). However there are limitations the usage of cisplatin due to developed resistance to cisplatin

(Wernyj and Morin 2004), had to be administered intravenously due to its insolubility in water (Wong and Giandomenico 1999) and also significant side effects that comes with it (Marzano *et al.*, 2002). The discovery of cisplatin encouraged anticancer research on other metal complexes (Thati, et al., 2007) like titanium (Kopf and Kopf-Maier, 1979), gold (Mirabelli *et al.*, 1986), germanium (Schein *et al.*, 1980), copper (Yoon *et al.*, 1990), iron (Carter *et al.*, 1989), ruthenium (Mirabelli *et al.*, 1986), cobalt (Carter *et al.*, 1989), vanadium (Larsen *et al.*, 1990).

The compounds that were used in this study are [M(phen)(ma)Cl]. Below is the image of the molecular structure of [M(phen)(ma)Cl].

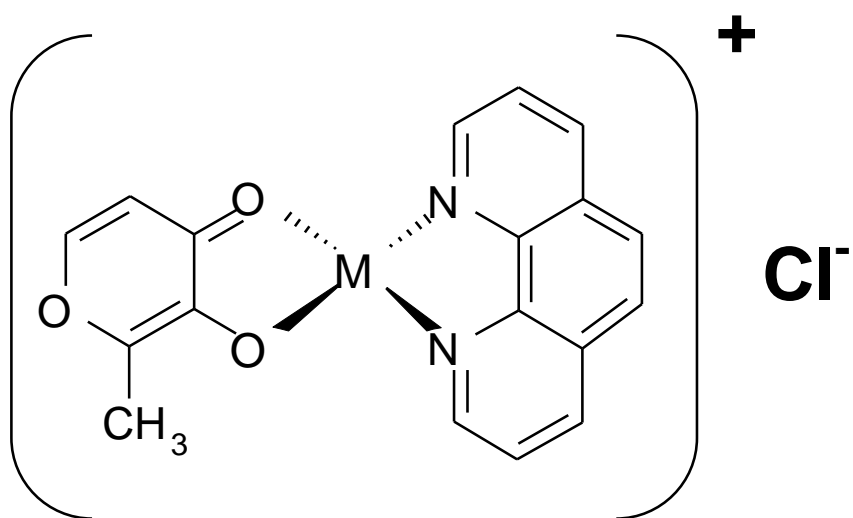


Figure 1.1: The molecular structure of [M(phen)(ma)Cl] with M as the metal center flanked with 1,10-phenanthroline on the right and maltol on the left as ligand.

[M(phen)(ma)Cl] is a compound with a transition metal as the center. Copper, cobalt and zinc were use as the metal center. The compound were flanked with two ligands which were 1,10-phenanthroline and maltol.

Three different breast epithelial cell lines were used in this study. Two different malignant cell lines that were chosen were MCF-7 and MDA-MB-231. A non-malignant cell line MCF10A was used as a comparison. MCF-7 cell line is one of the commonly used breast cancer cell line as a non-invasive and estrogen receptor positive while MDA-MB-231 is an invasive and estrogen receptor negative breast cancer cell line. These three cell lines were specifically chosen so that a comparison between malignant cell lines can also be made instead of just a comparison of malignant and non-malignant cell lines.

The first objective of this study is to test for anticancer properties of [M(phen)(ma)Cl]. Cell viability test were utilized to measure the IC-50 of the cell lines with MTT assay and changes in the morphology of cell lines were observed under phase-contrast inverted microscope. The second objective is to determine the selectivity of the mechanism of action of [M(phen)(ma)Cl] compounds. Three different breast epithelial cell lines were chosen for their distinctive attributes. MCF-7 was chosen as a non- invasive and estrogen receptor positive malignant cell line while MDA-MB-231 was chosen as an invasive and estrogen receptor negative malignant cell line. MCF10A was chosen as a non-malignant cell line. The last objective is to find out the mechanism of action of [M(phen)(ma)Cl]. In

order to discover the mechanism of action of [M(phen)(ma)Cl] four different assays will be used to analyze. Annexin V-FITC/PI assay will be used to find for evidence of cell death via apoptosis. Cell cycle analysis will be used to determine whether there is any occurrence of cell cycle arrest or any anomalies in DNA replication cycle. Proteasome-Glo™ cell-based assay will be used to determine whether the proteasome activity of the cells will be affected by [M(phen)(ma)Cl]. OxiSelect™ Intracellular ROS Assay Kit (Cell Biolabs, Inc.) will be used to measure the intracellular ROS level of the cells to find the difference in measurement with and without the treatment of [M(phen)(ma)Cl].

CHAPTER 2

LITERATURE REVIEW

2.1 Development of new anticancer drugs

The center of attention of conventional anticancer drug research and development was to discover an agent with cytotoxic property. The paradigms of discovering anticancer drugs are to focus on agents chosen for its considerable cytostatic or cytotoxic activity on tumor cell lines (Faber et al., 1948). That is why my research was started off with cell viability test using MTT assay, a colorimetric assay that is commonly used for measuring the activity of cellular enzymes (Berridge et al., 2005). This is to check for the cytotoxicity of [Cu(phen)(mal)Cl], [Co(phen)(mal)Cl] and [Zn(phen)(mal)Cl] complexes.

Even though this conventional approach was able to attain significant achievements, the modern breakthroughs in molecular biology and a deeper understanding of the pharmacology of cancer at a molecular level have demanded researchers to discover drugs that are target-based (Takimoto and Calvo, 2008). Numerous target-based compounds have surfaced recently and one of it is Bortezomib, a small-molecule proteasome inhibitor used for the treatment of multiple myeloma refractory to other treatments (Adams and Kauffman, 2004). Anticancer agents with proteasome inhibitor properties are an increasing popular aspect to be worked on by researchers. This reason has prompted me to

incorporate a test into my research to measure proteasome activity of the cell lines to check for any inhibition in proteasome activity.

After the chosen complex gone through the preliminary testing and came out with promising results then it will go through the process of being a new drug. Each new drug or drug combinations needs to be assessed for safety and potency prior to be approved. The assessment of new anticancer drugs or drug combinations typically goes through three main phases. The procedures of clinical drug development need to be meticulous and thorough as each phase of analysis can direct to permanent discontinuation of the compound of interest (Di Masi and Grabowski, 2007).

2.2 Metal based anticancer drugs

Since the earliest times of human medical history, metal compounds have been utilized successfully for treating various kinds of diseases. Ancient Egyptians physicians recognized the therapeutic prospect of gold salts (Nobili et al., 2009). Arsenic drugs like arsenic trioxide had been used widely in traditional Chinese medicine as antiseptic agents and also in the treatment of syphilis, psoriasis and even cancer (Dilda and Hogg, 2007; Gielen and Tiekink, 2005). Arsenic trioxide was among the first few compounds that was recommended for anticancer treatment. Around 18th and 19th century arsenic trioxide was widely used as a primary treatment for leukemia (Zhu et al., 2002). In the 1960s when Barnett Rosenberg discovered cisplatin, a platinum(II) complex marked the modern era of

metal-based anticancer drugs (Rosenberg et al., 1969), At the present time cisplatin and its successors carboplatin and oxaliplatin are among the main chemotherapeutics used to treated various kinds of cancers (Kelland 2007). Encouraged by the success of cisplatin, attention was also diverted to other metal-based complexes as a viable source of development of anticancer drugs like ruthenium, gold, titanium, copper, rhodium, vanadium and cobalt (Clarke et al., 1999; Eastman 1987; Kostova 2006; Ott and Gust 2007; Shaw 1999)

2.2.1 Copper based anticancer drugs

Copper displays significant biochemical action either as an essential trace nutrient or as a component of various exogenously delivered into humans (Brewer 2009). Present attention in copper complexes is on their prospective exploit as antimicrobial, antiviral, anti-inflammatory, enzyme inhibitors and even antitumor agents (Weder et al., 2002).

Numerous copper(II) chelate complexes was found to show evidence of cytotoxic activity through cell apoptosis or enzyme inhibition (Tripathi et al., 2007). These complexes containing bi-Schiff bases as ligands are efficient in shrinking tumor size, slowing of metastasis and considerably decrease the mortality rate of the hosts. Copper(II) chelates of salcaldoxime and resorcylaldoxime expressed antiproliferative and strong cytotoxic effects at par of that of adriamycin by causing cell cycle arrest and apoptosis (Elo 2004). These complexes demonstrate a

diverse biological activity that is comparable to one of the commonly used platinum anticancer drugs cisplatin.

The complex 2,6-bis(benzimidazo-2-yl)pyridine copper(II) chloride has proven to show metalloprotease activity (Shrivastava et al., 2002). It binds to bovine serum albumin leading to site-specific cleavage of protein. The complexes of carboxamidrazones have been shown to increase antiproliferative activity against B16F10 mouse melanoma cells (Gokhale et al., 2001). This shows that the combination of Cu(II) with carboxamidrazon ligands might cause intracellular transportation and block estrogen receptors. Cu(II) compound of chlorophyllin proven to induce apoptosis in human colon cancer cells through caspase-8 and apoptosis-inducing factor activation in a cytochrome *c*-independent manner (Díaz et al., 2003).

Despite the fact that copper is a crucial cofactor for tumor angiogenesis development, numerous Cu(II) complexes have proven to exhibit proteasome inhibition traits and also inducing apoptosis in different types of human cancer cells (Daniel et al., 2004). The metal in these complexes is incorporated with neutral heteroatomic molecules like 1,10-phenanthroline or to anionic organic ligands like pyrrolidine dithiocarbamate. It is obvious that the ligand themselves are not proficient inhibitors and complex formation is fundamental for mobilization of copper ions through the cell membrane to cause proteasome

inhibition (Hindo et al., 2009). This is caused by the increased of lipophilicity of metal when incorporated with ligands.

2.2.2 Cobalt based anticancer drugs

Cobalt based compounds lately drawn a sizable amount of attention as systemic anticancer agents. Cobalamin is used in conjunction with folic acid in chemotherapy utilize antimetabolites to bring down the adverse side effects. In view of the fact that fast growing cells need higher dosage of cobalamin than normal cells, cobalamin-conjugates with radioisotopes or cytotoxic compounds like nitrosylcobalamin has shown to increase tumor accumulation (Bauer et al., 2007; Gupta et al., 2008; Ruiz-Sanchez et al., 2011).

Cobalt alkyne complexes have shown to enhance anticancer activity both *in vitro* and *in vivo* especially against breast cancer cells (Jung et al., 1997). Small changes on the molecule of the complexes can lead to distinct variation in the mode of action (Ott and Gust 2007). Studies on the mode of action found that cobalt alkyne complexes do not largely target DNA in viable cells. Numerous research shows that the activity of [2-Acetoxy(2-propynyl)benzoate]-hexacarbonyldicobalt] may be due to the interaction of the ligand acetylsalicylic acid with cyclooxygenase enzymes (COX-1 and COX-2). This is best suited for targeting breast cancer cells as it is known that it is hypersensitive against COX inhibitors (Ott et al., 2005). This emerges to be a prospective approach because

inhibition of cyclooxygenase slows tumor growth as well as improves response to conventional cancer therapies.

Several redox-active cobalt(II) and cobalt(III) complexes have shown significant antitumor activity and DNA damage in numerous rodent tumor models (Vol'pin et al., 1999; Osinsky et al., 2003; Osinsky et al., 2004). These redox-active complexes by cytotoxic ligand release and or by other mechanisms like binding of the histidine units of polypeptide chains with metmyoglobin (Blum et al., 1998). Furthermore, these complexes might catalyze auto-oxidation of ascorbic acid involving generation of $O_2^{\bullet-}$, OH^{\bullet} , and H_2O_2 (Vol'pin et al., 1999). Consequently, cobalt complexes that are build up in malignant tissues should display increased antitumor activity in conjunction with ascorbic acid (Osinsky et al., 2004; Vol'pin et al., 1999).

2.2.3 Zinc based anticancer drugs

Even though with the various of physiological roles of zinc(II) ion (Thorp, 1998) and the broad range of Zn(II) complexes used in various fields like radioprotective agents (Emami et al., 2007) tumor photo sensitizer (Huang et al., 2006) and antimicrobial agents (Chohan et al., 2007) but there is very limited information on the cytotoxicity of zinc-based compounds on human cancer cell lines (Jiang et al., 2008). Zinc is a low cost, biocompatible metal with a large coordinative chemistry, interesting photophysical properties and is very promising for inorganic medicinal chemistry (Clarke et al., 1999). The use of Zn(II) species

as antitumour drugs is very interesting because of bioavailability and versatile coordination ability Zn(II) complexes could show interesting cytotoxic ability with low toxicity (Benedetti et al., 2010)

Currently, zinc oxide nanoparticles have garnered lots of attention for their implication in cancer therapy (Zhang et al., 2011). Research have proven that these complexes possesses cytotoxic properties to cell-specific and proliferation-dependent manner with fast multiplying cancer cells most vulnerable and quiescent cells least susceptible (Hanley et al., 2008; Ostrovsky et al., 2009; Premanathan et al., 2011). Zinc(II) complexes containing 4,4 dinonyl-2,2-bipyridine as main ligand and tropolones or 1-phenyl-3-methyl-4-R-5-pyrazolones as ancillary ligands have shown selective toxicity toward prostate cancer cells lines. Studies confirmed that the nature of the central metal ion as well as its coordination environment induce significant changes in the biological activity of resulting complexes (Paola et al., 2010)

2.3 Phenanthroline

Phenanthrolines are a group of compounds with unique mode of action (Kemp et al., 2007). These compounds have garnered much interest for their prospective properties against cancer as well as to viral, bacterial and fungal infections. Unlike cisplatin, intercalating ligands like phenanthrolines and their metal complex derivatives binds with DNA by aromatic p stacking between base pairs. This mode of action causes the helix to lengthen, stiffen and unwind (Kemp et al.,

2007). One of the phenanthroline derivative, phenanthroline-5,6-dione have shown considerable anticancer activity both with and without metal incorporated into it (Devereux et al., 2007).

A few phenanthroline complexes are already renowned for their excellent cytotoxic properties. Phenanthroline itself have shown high potency against neoplastic cell lines with IC-50 values of phenanthroline in L1210, HepG2 and A498 cell lines reported to be as low as 4.5µM (Thati et al., 2007; McFadyen et al., 1985). However phenanthroline is less effective towards leukemia cell lines than cisplatin while in other cell lines it shows 2.5- to 3.3- fold of increased activity (Garza-Ortiz et al., 2007). Another complex incorporated with 1,10-phenanthroline have shown potent cytotoxicity against human cancer cells at low micromolar concentrations. This complex also did not cause acute or subacute toxicity in mice at the range of practical clinical dose level (Narla et al., 2001).

2.4 Maltol

Maltol (3-hydroxy-2-methyl-4-pyrone) is one of the well known hydroxypyrones that is widely used for flavour enhancer and also its antioxidant properties (Gralla et al., 1969). It is found in the bark of larch tree, in pine needles, and in roasted malt and is common added as an additive in food, beverage, tobacco, brewing and also cosmetics (Bjeldanes and Chew 1979). Maltol possesses a high bioavailability and favourable toxicity profiles making it a suitable component to incorporate into a complex to reduce its toxicity. Maltol readily binds to hard

metal centers such as Fe^{3+} , Ga^{3+} , Al^{3+} , and VO^{2+} (Liboiron et al., 2005). Due to this property, maltol has been proven to significantly increase aluminum uptake in the body (Kaneko et al., 2004) and also increases the oral bioavailability of gallium (Bernstein et al., 2000) and iron (Reffitt et al., 2000)

Recently, maltol was found to exhibit significant antineoplastic activities towards different cancer cell lines (Hironishi et al., 1996). DNA breakage due to the generation of reactive oxygen species was deduced to be one of the probable mode of action undertaken by maltol complexes (Yasumoto et al., 2004). Besides that, a couple of maltol-derived compounds were synthesized and tested in the formulation of new prospective metal-based antitumor drugs that can hinder with DNA replication came up with promising results (Jakupec and Keppler 2004; Barve et al., 2009; Kandioller et al., 2009).

Hypothesizing that these compounds have good potential as anticancer agents, $[\text{Cu}(\text{phen})(\text{mal})\text{Cl}]$, $[\text{Co}(\text{phen})(\text{mal})\text{Cl}]$ and $[\text{Zn}(\text{phen})(\text{mal})\text{Cl}]$ were screened for their biological activity. Copper, cobalt and zinc were chosen as the center of the metal complex due to its low cost in synthesizing and proven tract records on anticancer activity. 1,10-phenanthroline was incorporated as one of the ligand to increase the binding of the complexes to targeted DNA thus increasing its potency. Maltol was used as another ligand to increase the complexes bioavailability and reducing their toxic side effects while at the same time enhancing their anticancer activities.

2.5 Different types of breast cancer

According to National Center for Biotechnology Information (www.ncbi.nlm.nih.gov) breast cancer usually starts either in the cells of the lobules, which are the milk-producing glands, or the ducts, which is the passages that drain the milk from the lobules to the nipple. A pathology report will show whether the cancer has spread beyond the milk ducts or lobules of the breast where it originated.

Basically there are two types of breast cancer, invasive and non-invasive. Non-invasive cancers stay within the milk ducts or lobules in the breast and they do not grow into or invade normal tissues within or beyond the breast. Non-invasive cancers are commonly called as carcinoma in situ. Ductile carcinoma in situ is breast cancer in the lining of the milk ducts that have not metastasize to adjacent tissues. It may develop to invasive cancer if untreated. However lobular carcinoma in situ is an indicator for a heightened risk of escalating into invasive cancer in the same or both breasts. Invasive cancers will spread to normal and healthy tissues. There are different regiments of treatments for invasive and non-invasive cancers (Koutsilieris et al., 1999).

Most breast cancers are sensitive to the hormone estrogen. The presence of estrogen will enhance the growth of breast cancer tumor. These cancers have estrogen receptors on the surface of their cells. These cancers are characterized as

estrogen receptor positive cancer (ER+). Even though breast cancer is linked to exposure to estrogen however not every breast cancers are responsive to estrogen and its analogs. Some cancers are lacking of the estrogen receptor and is classified as estrogen receptor negative cancer (ER-). Classifying breast cancers by ER+ or ER- can aid in the selection of proper therapies like some ER+ cancers are responsive positively to hormone blockers while ER- cancers do not. Such classification system also provides a better understanding into the possible pathophysiology of these tumors. Numerous studies have shown that ER+ and ER- breast cancers have specifically different risk factors and with that a possibility of different etiologies (Althuis et al., 2004; Korde et al., 2010).

What makes metastatic breast cancer distinctive from other solid tumors is that ER+ breast cancer patients have a better reaction to chemotherapy and favorable prognosis (Sherry et al., 1986; Coleman and Rubens 1987; Diel et al., 1992). Regrettably this is not the scenario for patients ER- breast cancer (Anderson et al., 2005). Facts presented by epidemiological studies have shown that breast cancer risk factors vary by tumor characteristic (Althuis et al., 2004; Yang et al., 2011). With these in mind I have specifically chosen 3 different cell lines to represent each type of breast cancer. MCF-7 is a non-invasive and also a ER+ breast cancer cell line while MDA-MB-231 is an invasive and also a ER- breast cancer cell line (Nagaraja et al., 2006). While MCF10A, a non-tumorigenic epithelial cell line (Nagaraja et al., 2006), is used as a comparison to determine whether

[Cu(phen)(mal)Cl], [Co(phen)(mal)Cl] and [Zn(phen)(mal)Cl] are cytotoxic to normal and healthy cells.

2.6 Apoptosis in cancer

There are a few ways that apoptotic cells can be identified from normal healthy cells. One of the easiest method is to observe the morphological changes of the cells .Apoptosis was originally identified by its morphological changes, such as cell shrinkage, chromatin condensation, membrane blebbing and nuclear fragmentation (Kerr et al., 1972; Wyllie et al.; 1980; Kerr et al., 1994). The understanding that apoptosis is a gene-directed program has had insightful implications for comprehending the developmental biology and tissue homeostasis, for it means that cell numbers can be controlled by factors that influence cell survival as well as those that manage proliferation and differentiation. Besides that, the genetic basis for apoptosis showed that cell death, like any other metabolic or developmental program, can be interrupted by mutation. In fact, flaws in apoptotic pathways are now considered to cause numerous of human diseases, ranging from neurodegenerative disorders to malignancy (Thompson 1995).

Among the most important advances of cancer biology and cancer genetics is the breakthrough is that malignant phenotype is significantly influenced by apoptosis and genes that control the pathway. The significance *bcl-2* oncogene in tumor development was established after the cloning and characterization of this gene

(Tsujiimoto et al., 1984; Tsujiimoto et al., 1985). Other than that, the initial tumor suppressor gene that was being related to apoptosis was *p53*. *p53* mutations occur in the most of human tumors and usually connected with higher tumor stage and poor patient prognosis (Wallace-Brodeur and Lowe 1999).

Eventhough the early studies on Bcl-2 and p53 recognized the significance of apoptosis in carcinogenesis, it is now obvious that mutations in many cancer-related genes can interrupt apoptosis, leading to tumor initiation, progression or metastasis. For instance, the Fas/CD95 receptor usually regulates the number of cells in the immune system by killing cells through apoptosis, and interruption of this pathway can cause lymphoproliferative disorders and even cancers (Beltinger et al., 1998). Besides that, a few signal transduction pathways support cell survival in reaction to growth and/or survival factors. Signaling through PI-3 kinase is one of the significant pathway (Marte and Downward, 1997), which able to be started by Ras and is down regulated by the PTEN tumor suppressor (Cantley and Neel, 1999). Ras activation and PTEN loss are ordinary in human cancers.

Last but not least, apoptosis is know to be caused by highly cytotoxic compounds, which might suggest the possibility that flaws in apoptotic programs add to unsuccessful treatment. Because decrease in treatment sensitivity is also caused by the similar mutation that represses apoptosis, cancer genetics is able to be connected to cancer therapy. Since apoptotic pathways can be maneuvered to

create huge alteration in cell death, the genes and proteins regulating apoptosis are possible drug targets. A lot of empirically derivative cytotoxic drugs by now can aim apoptosis, although not directly and non-exclusively. Those drugs are also mutagenic and toxic to healthy tissues. In comparison, drugs that directly cause apoptosis may present fewer chances for gaining drug resistance, reduce mutagenesis and decrease toxicity. Numerous present strategies are targeting anti-apoptotic activities (Tai et al., 1999), restoring pro-apoptotic activities (Spitz et al., 1996; Badie et al., 1998), through death ligands (Wold 1993; Dong et al., 1997), enhancing the effects of pro-apoptotic mutations (Samuelson and Lowe 1997) and chemoprotection (Komarov et al., 1999).

The understanding of apoptosis and its roll in cancer and cancer therapy was highly increased in recent year. In addition, a clearer picture of the molecular mechanisms that manage and perform apoptotic cell death was achieved. Apoptosis opens up opportunities for cancer prognosis, diagnostics and therapy with the current understanding we achieved even though there is much more to be learned. Finding out whether [Mphen)(mal)Cl] compounds induce cell death via apoptosis will be a key step in finding the mechanism of action of these compounds.

2.7 The cell cycle and cancer

Superficially, the correlation between the cell cycle and cancer is apparent: cell cycle machinery regulates cell proliferation, and cancer is a disease of uncontrolled cell proliferation. Basically, all cancers allow the existence of too many cells. However, this cell number surplus is associated in a vicious cycle with a decrease in sensitivity to signals that normally signal a cell to adhere, differentiate, or die. This arrangement of altered properties amplifies the complexity of deciphering which changes are mainly accountable for causing cancer (Nasmyth 1996).

Unregulated cell cycle mechanism activates the uncontrolled cell propagation that differentiates the malignant phenotype. Mitogens let loose the stops of cell cycle development by upregulating G1–S CDK actions, in response causing phosphorylation of pRB proteins, resulting in disturbance of its interface with the E2F family of transcription factors. In tumorigenic cells, pRB regulators are frequently faulty, ensuing in E2F-dependent G1–S gene expression even in without the presence of mitogens (Harbour and Dean 2000). This might occur as a consequence of activating tumourigenic mutations that was recognized in varied tumours at different advances in the mitogenic signalling pathways from ligands and receptors like HER2/ErbB2/neu receptor mutations or *HER2* gene upregulation to downstream signalling pathways like Ras–Raf–MAPK (Zhang et al., 2009; Freier et al., 2003; Huang et al., 2002). Abnormal signalling helps in commencement of CDK–cyclin, which phosphorylate Rb and stimulate

transcriptional repression. The idea that Rb phosphorylation is a convergence spot for oncogenic signalling pathways is in accordance with the truth that down regulation of the RB gene by methylation is a normal incidence in cancer (Malumbres and Barbacid 2001). The inactivation of tumour suppressor genes that encode CDKIs such as p15, p16 and p27 are also ordinary occurrence in diverse tumour types. This releases the brakes on cell cycle progression, and further abrogation of checkpoint control mechanisms direct to the attainment of genomic instability, which drives tumour evolution (Malumbres and Barbacid 2009).

Cdc7 kinase has surfaced as a predominantly appealing anti-cancer aim for DNA duplication initiation pathway due to the reason it can be repressed using ATP-competitive SMIs. A number of biopharmaceutical firms have commence Cdc7 drug improvement ventures, a number of which have entered preliminary clinical trials (Swords et al., 2010; Montagnoli, et al., 2010). Cdc7 inhibitors contain wide tumour range action in preclinical models, in accordance with absence of the defensive mechanism in most tumorigenic cancer. Apoptotic cancer cell death in retort to Cdc7 inhibition is p53-independent is controlled through the p38MAPK in an ATM- and Rad3-related (ATR)-dependent manner (Im and Lee 2008). Fascinatingly, in conjunction to its function in origin firing, Cdc7 kinase has been revealed to engage in a vital role in controlling the ATR–Chk1 pathway by phosphorylating the Chk1 activator Claspin (Kim et al., 2008; Matsumoto et al., 2010). Therefore, the double consequence of Cdc7 inhibitors on DNA duplication

and DNA damage reaction pathways might advance potentiate cancer cell elimination.

The cell cycle mechanism is a prospective beneficial aim in cancer because it is situated downstream at the junction of intricate oncogenic signalling pathways and its deregulation is important to the abnormal cell growth (Williams and Stoeber 1999; Tudzarova et al., 2010; Montagnoli et al., 2004; Montagnoli et al., 2008). Furthermore, numerous mechanisms are evolutionarily preserved and consequently clinical implications are probable to be suitable to varied types tumour. It will be interesting to find whether [M(phen)(mal)Cl] compounds mechanism of action involves the cell cycle engine.

2.8 Proteasome inhibitors in cancer therapy

The ubiquitin proteasome pathway is responsible for controlling a lot of activities in the cell which are vital for tumor cell enlargement. Inhibition of proteasome function has become an effective approach for cancer treatment. Clinical corroboration of the proteasome to be viable therapeutic aim was accomplished with the compound bortezomib and has driven the growth of newer kinds of proteasome inhibitors with enhanced anti-cancer property.

Proteasome inhibitors were not originally developed to be utilized for clinical application. Proteasome inhibitors were first used as vitro probes for examining the role of the proteasome in catalyst action. When the indispensable function by

proteasome in cell activity unveiled, researchers considered the option of inhibiting proteasome as a therapeutic use. Studies shown that proteasome inhibitors were able to induce apoptosis on leukemic cell lines (Imajoh-Ohmi et al., 1995; Drexler 1997) and in Burkitt's lymphoma in vivo models (Shinohara et al., 1996). Deeper in vitro analysis confirmed that proteasome inhibitors exhibited a wide range anti-proliferative and pro-apoptotic activities.

Proteasome inhibition has more effect on malignant cells than non-malignant cells in pre-clinical studies. What causes the elevated effectiveness on malignant cells is uncertain. The most likely reason is the advantage of the proteasome to control propagation plus affecting apoptosis in a negative way. Majority of cancer cells has high growth rate and have a higher necessity for synthesizing proteins and cause the cells to be more susceptible to proteasome inhibition. A research has established that higher proteasome activity in leukaemic cell lines is associated with heighten sensitivity to proteasome inhibitors (Crawford et al., 2009). In accordance with this, a research has revealed a direct connection between proteasome inhibitor sensitivity and rates of translation in multiple myeloma cells (Nawrocki et al., 2008). Nonetheless, proteasome inhibitors displayed better efficacies in a few malignancies than others and there are clearly other determinants that account for this. It is possible that the relative significance of the mechanisms correlates with the tumor type. Inhibition of NF κ B activity (Traenckner et al.,1994), altered degradation of cell cycle related proteins (Sherr and Roberts 1999), altered pro-apoptotic and anti-apoptotic protein balance

(McConkey and Zhu, 2008), endoplasmic reticulum stress (Morgillo et al., 2010) and inhibition of angiogenesis (Tamura et al., 2010) and DNA repair (Motegi et al., 2009) have all been reported to contribute to the apoptotic affect of proteasome inhibitors in tumour cells.

Even though most of these researches recognized the prospect of proteasome inhibitors as therapeutic compounds, due to lack of effectiveness, specificity or stability many of these compounds were stuck in laboratory studies. This prompted scientists to go back to the drawing board to come up with something different. To solve this problem more potent and selective activity of inhibitors was designed to compensate for these shortcomings.

The ubiquitin proteasome pathway is now highly valued for its significant role in regulating various cellular processes. Although the exact mechanisms of action of proteasome inhibitors are not yet fully definite, there are various of pathways that become visibly vital in the selectivity for malignant cells. Testing [Mphen)(mal)Cl] using Proteasome-Glo™ 3-Substrate System (Promega™) will give some important insight on whether these compounds induce death following this unique pathway.

2.9 ROS and cancer therapeutics

Tumor biology has discovered that cancer cells are known to display heightened intrinsic oxidative stress. In contrast with the normal counterparts, the majority of cancer cells have inherently increased amounts of reactive oxygen species (ROS), for instance superoxide, H₂O₂ and the hydroxyl radicals (Kawanishi et al., 2006; Szatrowski and Nathan 1991; Hileman et al., 2004; Toyokuni et al., 1995). Nucleic acids, proteins and lipids were found to be highly reactive to these oxygen-containing reactive chemicals. Cancer-cell proliferation, metastasis, angiogenesis and alternation in the cellular sensitivity to anticancer agents were found to be closely connected to the high level of ROS in cancer cells. (Arnold et al., 2001; Ishikawa et al., 2008). ROS usually available in the environment, but in cells the main source is through the mitochondrial respiratory chain (King et al., 2009). However, there are other sources and examples for ROS in cells and especially in cancer cells (Tsang et al., 2003).

Cancer therapies are practically as toxic to healthy cells as to cancer cells and a main objective in the development of novel therapeutics is to make use of disparities in cancer cells so that therapies can be highly targeted. Heightened ROS level could be used for therapeutic targeting of tumor tissue. ROS generation, as well as reduction below a threshold, impacts cancer cell killing, both strategies which are pro-oxidant and antioxidant approaches have been employed (Trachootham et al., 2006; Wang and Yi 2008; Alexandre et al., 2006). The elevated level of ROS in cancer cells has been exploited for developing novel

therapeutic strategies to preferentially kill cancer cells (Hileman et al., 2004; Tsang et al., 2003; Pelicano et al., 2003). Various drugs were designed to eliminate cancer cells by increasing oxidant stress by directly produce ROS or by inhibiting antioxidant activities (Schumacker, 2006; Jing et al., 1999; Miyajima et al., 1997). This is based on their susceptibility to additional ROS insults. Testing for intracellular level of ROS after treatment with [Mphen)(mal)Cl] compounds will give insight on whether these compounds are pro-oxidant, antioxidant or follow a ROS independent pathway.

CHAPTER 3

PRELIMINARY STUDIES AND SCREENING OF [M(phen)(ma)Cl]

[Cu(phen)(ma)Cl], [Co(phen)(ma)Cl] and [Zn(phen)(ma)Cl] are novel compounds that had not been tested on before by other researchers. The screening these compounds were done using two tumorigenic breast cancer cell lines MCF7 and MDA-MB-231 with one non-tumorigenic breast cell line MCF10A. A common cell viability test, MTT assay, was done and in conjunction with it the morphology of the cells were also observed throughout the duration of the studies. Three different time frame 24, 48 and 72 hours were used to observe the effects of [M(phen)(ma)Cl] on the cells over time.

3.1 Material and methods

3.1.1 Cell line

This study was carried out using MCF-7 (Michigan Cancer Foundation - 7), MDA-MB-231 (M.D. Anderson - Metastatic Breast – 231) and MCF10A (Michigan Cancer Foundation – 10A) obtained from ATCC (American Type Culture Collection).

3.1.2 Culture medium

MCF-7 cell line was cultured in RPMI (Roswell Park Memorial Institute) 1640 medium (Gibco[®]) supplemented with 10% (v/v) FBS (Foetal Bovine Serum) (Gibco[®]). MDA-MB-231 cell line was cultured in DMEM (Dulbecco's Modified

Eagle Medium) 10% (v/v) FBS (Foetal Bovine Serum) (Gibco®). MCF10A cell line was cultured in DMEM:F-12 (Ham's F-12 Nutrient Mixture) medium (Gibco®) supplemented with 5% HS (Horse Serum) (Gibco®).

3.1.2.1 RPMI medium preparation

A pack of RPMI 1640 powder (Gibco®) for 1L preparation was emptied into a 1L volumetric flask together with 2g NaHCO₃ (Sigma®) and 5.95g/25mM HEPES (Sigma®). Deionized water was added up to 80% of the flask. The packet was rinsed with deionized water and poured into the flask and repeated until the packet was clean. The flask was sealed and the contents were shook gently until all ingredients were dissolved. The pH of the solution was adjusted to pH7 using filtered 1M NaOH or 1M HCl. The volumetric flask was topped up with deionized water up to the 1L mark. The flask was again sealed and shook gently. The solution was then filtered using a sterilized filter unit with 0.2µm Cellulose Nitrate Membrane Filter (Nalgene®) into a 1 litre sterile Schott Duran bottle using a positive pressure system. One millilitre of the filtered medium mixture was pipetted into a 40 x 11 mm culture dish (Nunc™) and incubated overnight for detection of any contamination for the stock medium. The stock medium was stored in 4°C. A small amount of the stock medium was aliquot out for weekly usage. The medium was supplemented with 10% FBS (Gibco®), 1% of penicillin10.000IU/streptomycin10.000µg/ml (Sigma®) and 1% of GlutaMAX™ (Gibco®).

3.1.2.2 DMEM preparation

A pack of DMEM powder (Gibco®) for 1L preparation was emptied into a 1L volumetric flask together with 2.18g NaHCO₃ (Sigma®). Deionized water was added up to 80% of the flask. The packet was rinsed with deionized water and poured into the flask and repeated until the packet was clean. The volumetric flask was topped up with deionized water up to the 1L mark. The flask was sealed and the contents were shook gently until all ingredients were dissolved. The solution was then filtered using a sterilized filter unit with 0.2µm Cellulose Nitrate Membrane Filter (Nalgene®) into a 1 litre sterile Schott Duran bottle using a positive pressure system. One millilitre of the filtered medium mixture was pipetted into a 40 x 11 mm culture dish (Nunc™) and incubated overnight for detection of any contamination for the stock medium. The stock medium was stored in 4°C. A small amount of the stock medium was aliquot out for weekly usage. The medium was supplemented with 10% FBS (Gibco®), 1% of penicillin10.000IU/streptomycin10.000µg/ml (Sigma®) and 1% of GlutaMAX™ (Gibco®).

3.1.2.3 F-12 medium preparation

A pack of F-12 powder (Gibco®) for 1L preparation was emptied into a 1L volumetric flask together with 1.18g NaHCO₃ (Sigma®). Deionized water was added up to 80% of the flask. The packet was rinsed with deionized water and poured into the flask and repeated until the packet was clean. The volumetric flask was topped up with deionized water up to the 1L mark. The flask was sealed and

the contents were shook gently until all ingredients were dissolved. The solution was then filtered using a sterilized filter unit with 0.2µm Cellulose Nitrate Membrane Filter (Nalgene®) into a 1 litre sterile Schott Duran bottle using a positive pressure system. One millilitre of the filtered medium mixture was pipetted into a 40 x 11 mm culture dish (Nunc™) and incubated overnight for detection of any contamination for the stock medium. The stock medium was stored in 4°C.

3.1.2.4 DMEM/F-12 medium preparation

DMEM stock medium and F-12 stock medium were individually prepared and mixed together in a sterile Schott Duran bottle when usage was needed. For steps on preparation of DMEM and F-12 stock medium please refer to procedure 3.1.2.3 (DMEM Preparation) and 3.2.4 (F-12 Medium Preparation) respectively. The ratio of DMEM and F-12 is 1:1. Medium were prepared fresh weekly. The medium was supplemented with 20ng/ml of human recombinant EGF (Gibco®), hydrocortisone (Sigma®), 10µg/ml of insulin (Gibco®), 1% of penicillin10.000IU/streptomycin10.000µg/ml (Sigma®), 1% of GlutaMAX™ (Gibco®) and 5% HS (Horse Serum) (Gibco®). One millilitre of the filtered medium mixture was pipetted into a 40 x 11 mm culture dish (Nunc™) and incubated overnight for detection of any contamination for the stock medium.

3.1.3 Phosphate buffered saline solution preparation

For each 200mL, 1 tablet of PBS (Phosphate Buffered Saline) (Sigma[®]) was used. The PBS tablet was dissolved in deionized water in a suitable size of Schott Duran bottle. The bottle containing PBS solution was then autoclaved under 121 °C for 15 minutes.

3.1.4 Thawing the cell line

One vial of cryopreserved cell line was thawed in a 37°C water bath immediately after retrieving it from the liquid nitrogen tank. The cryovial was then sprayed with 70% ethanol after thawing in the water bath. The cells inside the vial were transferred into a 90 x 15 mm tissue culture dish (Nunc[™]) and cultured in 5mL of medium specified for each cell line. The first millilitre of the DMEM medium was added drop by drop and mixed thoroughly by gently shaking the T-flask. The T-flask was gently shaken in circular motion and the cells were viewed under inverted microscope (Olympus, Model CKX31) at low power to ensure even distribution of cells on the T-flask surface. Incubate the culture in 5% CO₂ humidified incubator at 37°C.

3.1.5 Maintenance of cell culture

All liquid reagents that were used in culturing cells including medium, PBS solution and trypsin EDTA were warmed in water bath to 37°C before usage.

3.1.5.1 Medium changing

Medium changing was carried out when the cells were not confluence and the colour of the culture medium had changed from red to orange or it has been 3 days or more since the last medium change or subculture. The existing medium was drained. Then same amount of fresh medium was added back. The culture was then re-incubated in the 5% CO₂ humidified incubator at 37°C.

3.1.5.2 Subculture of confluence cells

Subculture was carried out when the cells reached confluence. Existing medium was drained from the culture dish. The culture dish was washed with 3ml of sterile PBS. The PBS solution was drained. The washing procedures were repeated one more time. After washing, 1.5mL of trypsin EDTA (Gibco®) was added. The culture dish was then incubated in the 5% CO₂ humidified incubator at 37°C until all of the cells were fully suspended. The suspended cells were transferred into a sterile Falcon™ tube and topped up with 3mL of medium solution specified for each cell line. The centrifuge tube was centrifuged at 1000rpm for 5 minutes using centrifuge machine. After centrifugation, the pellet of cells was obtained. All supernatant was discarded and the pellet was suspended with medium. The cells were cultured into culture dish or used for tests throughout this study.

3.1.6 Cryopreservation of cell line

The procedure 3.1.5.2 (Subculture of Confluence Cells) was followed until the pellet was obtained. The pellet was then mixed thoroughly in 1mL of 5% DMSO in medium specified for each cell line. The mixture of cells were transferred into a sterile cryovial (Nunc™) and stored in -80°C for short term storage. For long term storage, the cells were stored in liquid nitrogen tank.

3.1.7 Cell count using trypan blue exclusion method

The haemocytometer (HIRSCHMANN®) and cover slip was sprayed with 70% alcohol. The alcohol was wiped off from the haemocytometer and cover slip. The procedure 3.1.5.2 (Subculture of Confluence Cells) was followed until the pellet was obtained. The pellet was then mixed thoroughly with a known amount of medium specified for each cell line. Ten micro litres of the cells were pipetted into a microcentrifuge tube. The cells were then mixed with 10µL of trypan blue solution (Gibco™). Ten micro litres of cells were pipetted on to the haemocytometer and viable cells were counted. The culture will be diluted with medium if the cell concentration obtained is more than 1×10^6 cells/mL. Desired amount of cells was cultured into culture dish or culture plates for testing.

3.1.8 Compound solution preparation

During the course of this study, [Cu(phen)(ma)Cl], [Co(phen)(ma)Cl] and [Zn(phen)(ma)Cl] was used. These compounds were prepared fresh and was used immediately to prevent degradation. The compounds were measured in a

microcentrifuge tube and the amount of distilled deionized water needed to be added was calculated using this formula:

$$V = \frac{n_i}{C_i}$$

Where C_i = Molarity or concentration in mol/L

V = volume of the mixture

n_i = mole of the constituent

3.1.9 Determination of the cytotoxicity of [M(phen)(ma)Cl]

The optimum cell plating numbers were obtained for each individual cell line and each different incubation period for the test. The incubation periods for this study were 24, 48 and 72 hours. This was obtained by seeding the cells in 96-wells plate in increasing number without any treatment from any compound. The cells were left for 24 hours to recover from cell harvest procedure. The medium were drained and replaced with fresh medium. The cells were observed for the condition and confluence level. The viability of the cells were obtained using MTT assay after incubated for designated time frame. A standard curve was plotted and a pointed at the middle of the slope where the confluence level is around 70% was chosen to be the optimum plating number for the specified cell line and duration of the test. For the procedure of MTT assay, please refer to procedure 3.9.2 (MTT assay)

3.1.9.1 Preparing stock cells

The procedure 3.1.7 (Cell Count Using Trypan Blue Exclusion Method) was followed until the number of cells harvested was obtained. Then, medium was added to make a stock concentration of cells of 1×10^6 cells/mL. The amount of medium needed to add was calculated using the following formula:

$$\text{Amount of medium needed in mL} = \frac{\text{the number of cells}}{\text{desired concentration of cells}}$$

3.1.9.2 MTT assay

The procedure 3.1.9.1 (Preparing Stock Cells) was followed to obtain stock concentration of cells of 1×10^6 cells/mL. Then the designated plating cell numbers for each cell line for each incubation period were pipetted into 96-wells flat-bottom plate (Nunc™). Each wells were topped up to 100 μ L with medium. The plate was incubated for 24 hours in the 5% CO₂ humidified incubator at 37°C for the cells to recover from harvesting procedure. For the treatment of the [M(phen)(ma)Cl] compounds, existing medium was replaced with fresh medium before the intended concentrations of [M(phen)(ma)Cl] compounds were added into each wells. For each concentration a triplicate were done to find the average and standard deviation of the results. The cells were then incubated in the 5% CO₂ humidified incubator at 37°C for designated incubation period. The cell

confluence for the untreated was observed under inverted microscope. The procedure will only advance if the confluence of the untreated cells reaches 70%~80%. The plate will be discarded if the confluence level is lower or higher than 70%~80%. After that 20 μ L of MTT (Sigma[®]) were pipetted into each well. The plate was incubated for another 2 hours. For each incubation period, the test for all 3 cell lines were done together to reduce variables among each cell line. Then, all supernatant was drained from the wells and 100 μ L of DMSO was added. The plate was agitated gently to facilitate the mixing of DMSO and formazan blue crystals. Absorbance reading was taken using multiplate reader (BIO-RAD model 680). Each experiment were repeated two more times to get three sets of results.

3.1.10 Morphological study

The procedure 3.1.9.1 (Preparing Stock Cells) was followed to obtain stock concentration of cells of 1×10^6 cells/mL. The cells were cultured in 60 x 15 mm culture dish (Nunc[™]) with cell number enough to achieve 70%~80% cell confluence for untreated cells at the end of the each designated incubation period. The cells were then incubated in the 5% CO₂ humidified incubator at 37°C for 24 hours to let it recover from harvesting procedure. The existing medium were drained and replaced with fresh medium before various concentrations of [M(phen)(ma)Cl] compounds were added into each culture dish. The cells were then incubated in the 5% CO₂ humidified incubator at 37°C for designation incubation period. The cells were then observed under inverted microscope (Nikon ECLIPSE Ti-E) at 200x magnification and numerous pictures were

capture using built-in digital microscope camera and edited using microscope imaging software provided. The picture with the best representation of the cells condition at that time was chosen.

3.2 Results

3.2.1 Cell viability test using MTT assay

[Cu(phen)(ma)Cl] , [Co(phen)(ma)Cl] and [Zn(phen)(ma)Cl] were tested for their effect on viability of malignant cell lines which is MCF-7 and MDA-MB-231. It was also tested on non-malignant cell line MCF10A to test for selectivity of its effect. Cells were treated with increasing concentrations of these compounds for 24 hours, 48 hours and 72 hours and then compared with untreated cells. With the absorbance reading of untreated cells set as reference point the percentages of viable cells of treated cells were calculated.

For 24 hours incubation time the concentrations used for [Cu(phen)(ma)Cl] were 1 μ M, 3 μ M, 5 μ M, 7 μ M, 9 μ M and 11 μ M (Figure 3.1.1). Both MCF-7 and MDA-MB-231 cell lines show a similar trend of decreased in cell viability when the concentration of [Cu(phen)(ma)Cl] increases. However at 5 μ M and higher the percentage of cell viability for MCF-7 became slightly constant while for MDA-MB-231 cells the trend remains and the cell viability continues to pl μ Mmet following the increasing concentration of [Cu(phen)(ma)Cl] . There is no apparent effect on MCF10A by [Cu(phen)(ma)Cl] up until 7 μ M where the percentage of cell viability dropped to 79.91%. From that point onwards the percentage of cell viability for MCF10A cells also plunge. The IC-50 recorded for [Cu(phen)(ma)Cl] after 24 hours treatment for MCF-7, MDA-MB-231 and MCF10A were 5 μ M, 5.5 μ M and 8.7 μ M respectively.

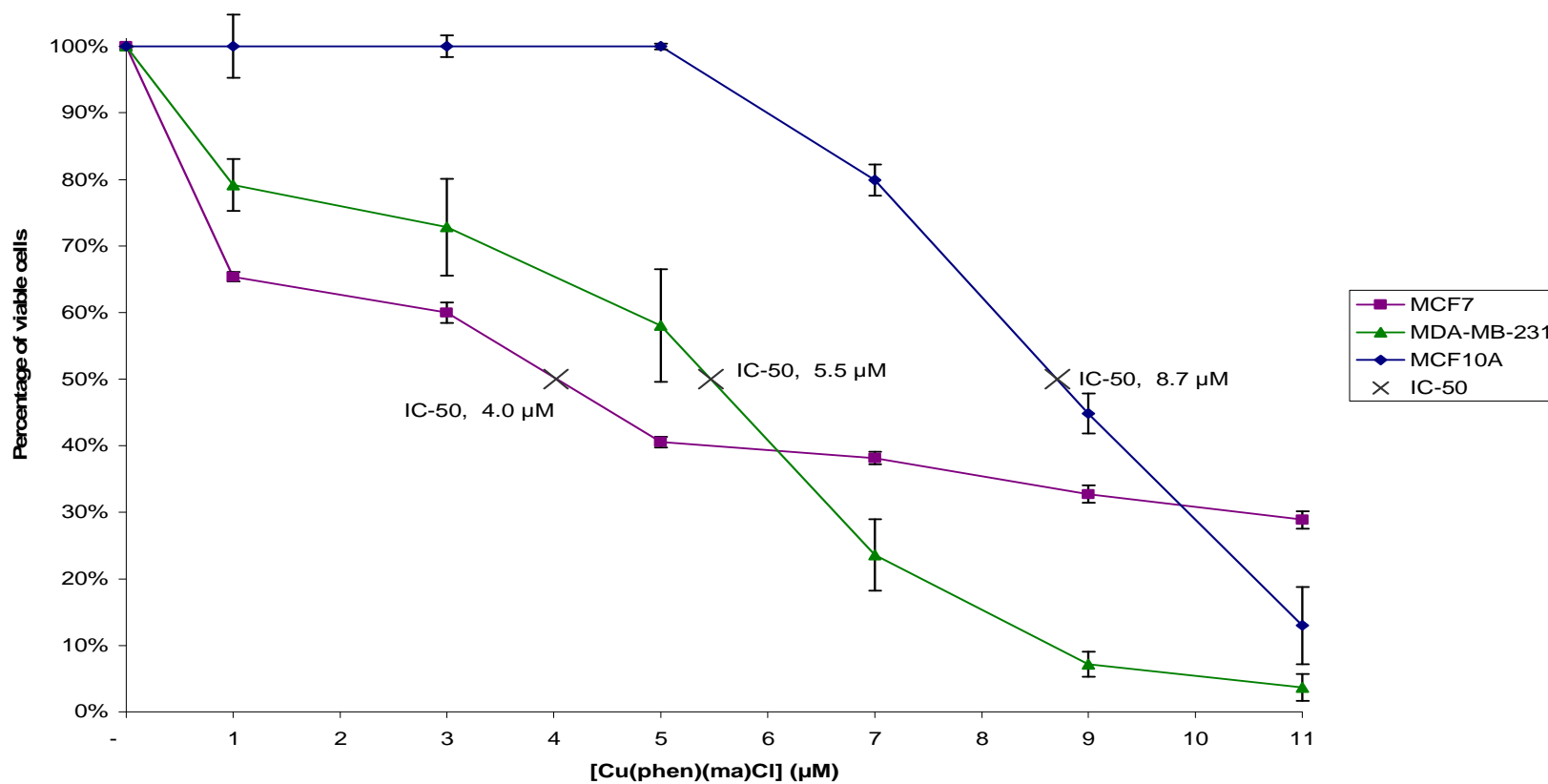


Figure 3.1.1 Viable cells of MCF-7, MDA-MB-231 and MCF10A cells treated with increasing concentrations of [Cu(phen)(ma)Cl] for 24 hours using MTT assay.

Concentrations of [Cu(phen)(ma)Cl] (μM)	^a Percentage of viable cells (%)
0	100
1	65.39 \pm 0.68
3	59.97 \pm 1.55
5	40.56 \pm 0.82
7	38.12 \pm 0.94
9	32.72 \pm 1.31
11	28.86 \pm 1.32

Table 3.1.1 Percentage of viable cells of MCF-7 cells after 24 hours of treatment with increasing concentrations [Cu(phen)(ma)Cl].

Concentrations of [Cu(phen)(ma)Cl] (μM)	^a Percentage of viable cells (%)
0	100
1	79.19 \pm 3.89
3	72.83 \pm 7.25
5	58.03 \pm 8.45
7	23.59 \pm 5.34
9	7.16 \pm 1.86
11	3.70 \pm 2.00

Table 3.1.2 Percentage of viable cells of MDA-MB-231 cells after 24 hours of treatment with increasing concentrations [Cu(phen)(ma)Cl].

Concentrations of [Cu(phen)(ma)Cl] (μM)	^a Percentage of viable cells (%)
0	100
1	100.00 \pm 4.76
3	100.00 \pm 1.59
5	100.00 \pm 0.45
7	79.91 \pm 2.36
9	44.86 \pm 3.01
11	12.98 \pm 5.82

Table 3.1.3 Percentage of viable cells of MCF10A cells after 24 hours of treatment with increasing concentrations [Cu(phen)(ma)Cl].

^a Percentage of viable cells is obtained from mean \pm standard deviation values of three independent experiments.

MCF-7, MDA-MB-231 and MCF10A cell lines were all treated with the same variant of concentrations of [Co(phen)(ma)Cl] for 24 hours which were 100 μ M, 200 μ M, 300 μ M, 400 μ M, 500 μ M and 600 μ M (Figure 3.1.2). All three cell lines also show similar trend of decreasing in the percentage of cell viability when the concentration of [Co(phen)(ma)Cl] increased. At 400 μ M of [Co(phen)(ma)Cl] the percentage of cell viability of MCF10A cells had drop down to 0% while MCF-7 and MDA-MD-231 cells still stand at 23.87% and 30.43% respectively. The figure continued to drop until 13.83% and 12.10% at 600 μ M of [Co(phen)(ma)Cl] for MCF-7 and MDA-MB-231 cells respectively. The IC-50 value after treatment of [Co(phen)(ma)Cl] for 24 hours for MCF-7 cells at 245 μ M, MDA-MB-231 cells at 345 μ M and MCF10A cells at 187 μ M.

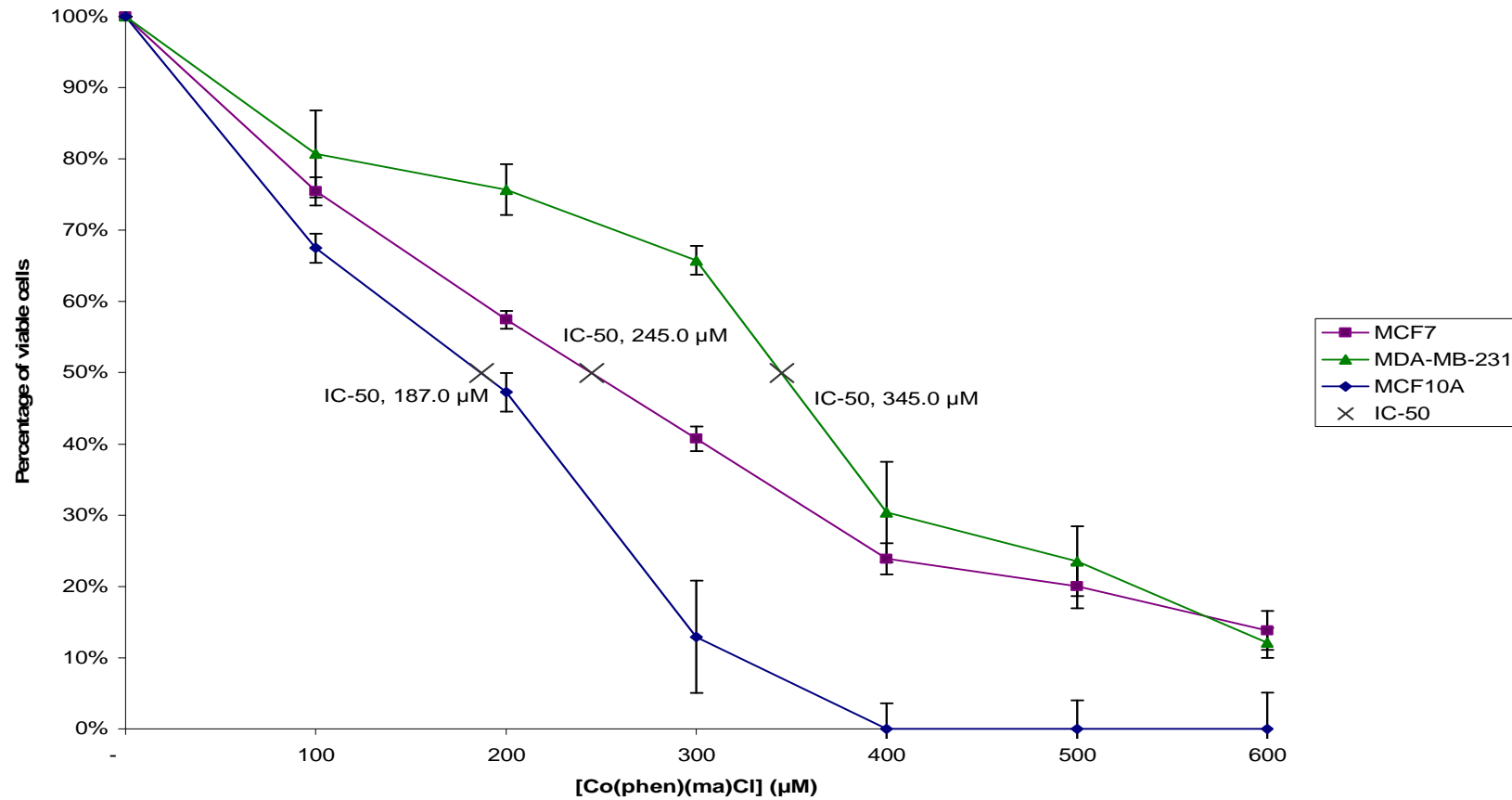


Figure 3.1.2 Viable cells of MCF-7, MDA-MB-231 and MCF10A cells treated with increasing concentrations of [Co(phen)(ma)Cl] for 24 hours using MTT assay.

Concentrations of [Co(phen)(ma)Cl] (μM)	^a Percentage of viable cells (%)
0	100
100	75.47 \pm 1.96
200	57.44 \pm 1.26
300	40.74 \pm 1.75
400	23.87 \pm 2.19
500	20.03 \pm 3.06
600	13.83 \pm 2.75

Table 3.2.1 Percentage of viable cells of MCF-7 cells after 24 hours of treatment with increasing concentrations [Co(phen)(ma)Cl].

Concentrations of [Co(phen)(ma)Cl] (μM)	^a Percentage of viable cells (%)
0	100
100	80.73 \pm 6.12
200	75.72 \pm 3.56
300	65.78 \pm 2.03
400	30.43 \pm 7.05
500	23.55 \pm 4.92
600	12.10 \pm 2.10

Table 3.2.2 Percentage of viable cells of MDA-MB-231 cells after 24 hours of treatment with increasing concentrations [Co(phen)(ma)Cl].

Concentrations of [Co(phen)(ma)Cl] (μM)	^a Percentage of viable cells (%)
0	100
100	67.49 \pm 2.03
200	47.27 \pm 2.70
300	12.93 \pm 7.89
400	0 \pm 3.61
500	0 \pm 4.03
600	0 \pm 5.12

Table 3.2.3 Percentage of viable cells of MCF10A cells after 24 hours of treatment with increasing concentrations [Co(phen)(ma)Cl].

^a Percentage of viable cells is obtained from mean \pm standard deviation values of three independent experiments.

A different set of varying concentrations was used for [Zn(phen)(ma)Cl] on MCF-7, MDA-MB-231 and MCF10A cell lines for 24 hours treatment period. The concentrations were 50 μ M, 100 μ M, 150 μ M, 200 μ M, 250 μ M and 300 μ M (Figure 3.1.3). MCF-7 cells showed a distinct drop in percentage of viable cells to 52.97% at first concentration in the set (50 μ M of [Zn(phen)(ma)Cl]) compared to MDA-MB-231 and MCF10A cells which recorded a higher percentage of viable cells at 88.60% and 86.90% respectively. MCF10A cells showed a sharp decrease of percentage of viable cells after 100 μ M from 82.13% at 100 μ M to 14.69% at 200 μ M. After this point all three cell lines showed a steady drop of percentage of cell viability up to 300 μ M of [Zn(phen)(ma)Cl] . The IC-50 found for MCF-7, MDA-MB-231 and MCF10A cell lines after treated with [Zn(phen)(ma)Cl] for 24 hours were 65 μ M, 174 μ M and 138.5 μ M respectively.

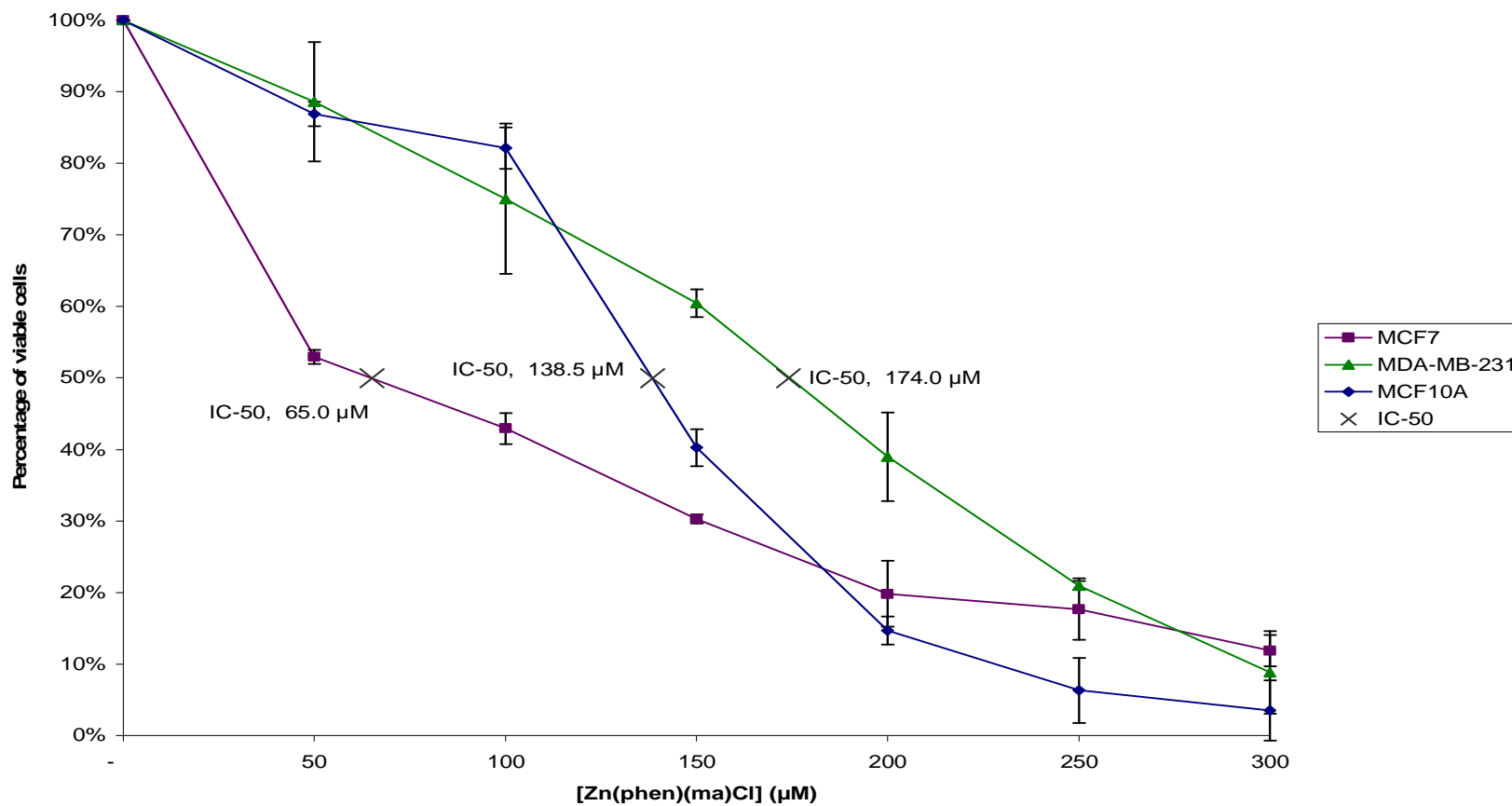


Figure 3.1.3 Viable cells of MCF-7, MDA-MB-231 and MCF10A cells treated with increasing concentrations of [Zn(phen)(ma)Cl] for 24 hours using MTT assay.

Concentrations of [Zn(phen)(ma)Cl] (μM)	^a Percentage of viable cells (%)
0	100
50	52.97 \pm 0.97
100	42.93 \pm 2.16
150	30.28 \pm 0.60
200	19.84 \pm 4.62
250	17.69 \pm 4.28
300	11.89 \pm 2.21

Table 3.3.1 Percentage of viable cells of MCF-7 cells after 24 hours of treatment with increasing concentrations [Zn(phen)(ma)Cl].

Concentrations of [Zn(phen)(ma)Cl] (μM)	^a Percentage of viable cells (%)
0	100
50	88.60 \pm 8.34
100	75.04 \pm 10.53
150	60.45 \pm 1.93
200	38.98 \pm 6.20
250	20.98 \pm 0.65
300	8.84 \pm 5.80

Table 3.3.2 Percentage of viable cells of MDA-MB-231 cells after 24 hours of treatment with increasing concentrations [Zn(phen)(ma)Cl].

Concentrations of [Zn(phen)(ma)Cl] (μM)	^a Percentage of viable cells (%)
0	100
50	86.90 \pm 1.73
100	82.13 \pm 2.88
150	40.27 \pm 2.60
200	14.69 \pm 1.94
250	6.31 \pm 4.54
300	3.56 \pm 4.20

Table 3.3.3 Percentage of viable cells of MCF10A cells after 24 hours of treatment with increasing concentrations [Zn(phen)(ma)Cl].

^a Percentage of viable cells is obtained from mean \pm standard deviation values of three independent experiments.

The concentration used on MCF-7, MDA-MB231 and MCF10A cell lines for 48 hours treatment of [Cu(phen)(ma)Cl] were 0.25 μ M, 0.5 μ M, 0.75 μ M, 1.00 μ M, 3.00 μ M and 5.00 μ M (Figure 3.1.4). MCF-7 cells showed a sharp drop in the percentage of viable cells from 0.25 μ M at 83.30% to 1 μ M at 28.97%. MDA-MB-231 also showed the same trend from 0.25 μ M at 76.44% to 1 μ M at 48.40%. From this point onwards both MCF-7 and MDA-MB-231 percentage of viable cells drop gradually up to the concentration of 5 μ M. The trend was not observed in MCF10A cell line. [Cu(phen)(ma)Cl] had no apparent effect on MCF10A up until 1 μ M. Even at 3 μ M the percentage of viable cells of MCF10A only dropped slightly to 95.00%. From 3 μ M to 5 μ M the figure dropped drastically to 34.86%. The IC-50 value for MCF-7, MDA-MB-231 and MCF10A cell lines after 48 hours incubation of [Cu(phen)(ma)Cl] were 0.5 μ M, 1.0 μ M and 4.5 μ M respectively.

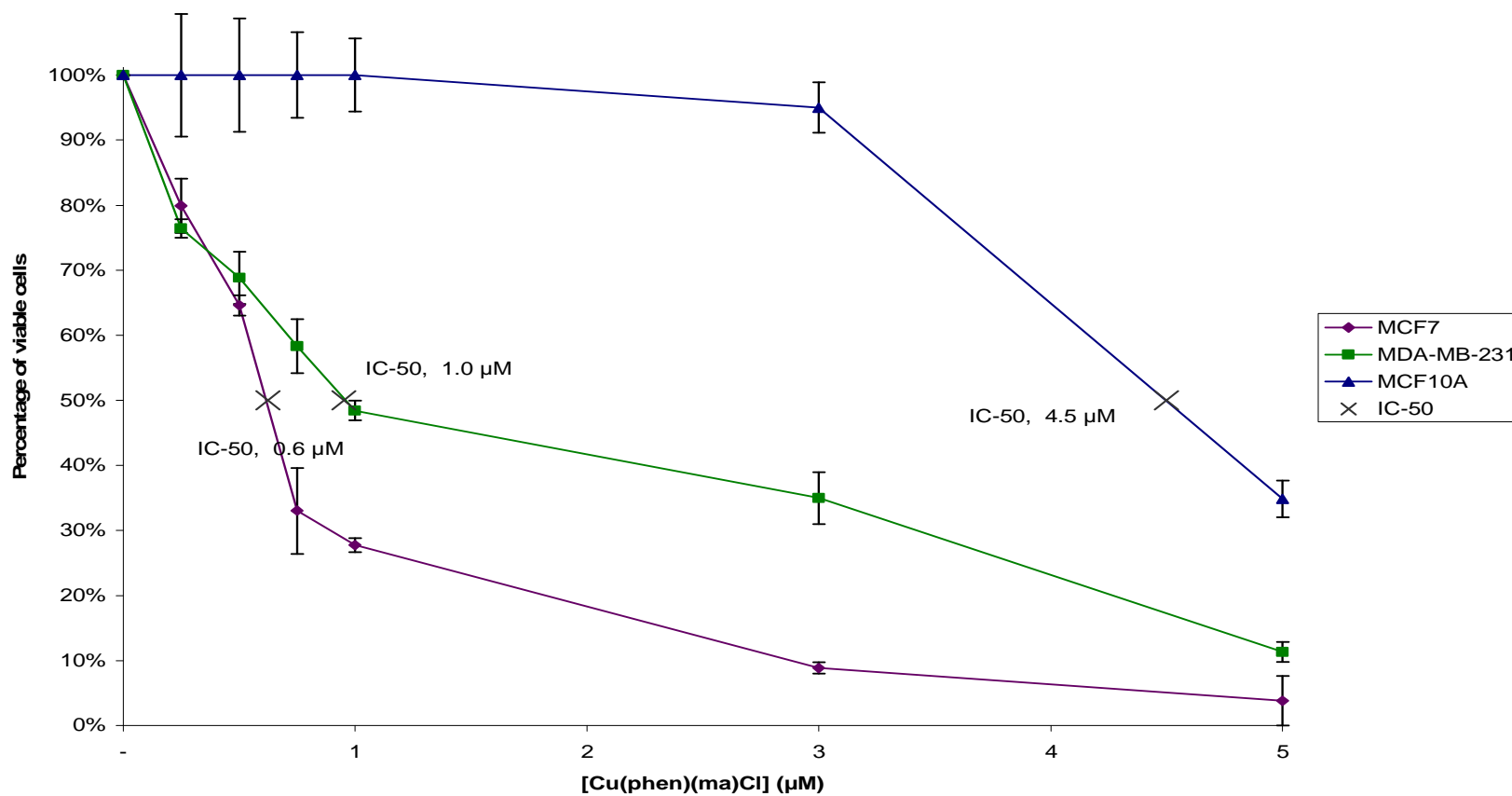


Figure 3.1.4 Viable cells of MCF-7, MDA-MB-231 and MCF10A cells treated with increasing concentrations of [Cu(phen)(ma)Cl] for 48 hours using MTT assay.

Concentrations of [Cu(phen)(ma)Cl] (μM)	^a Percentage of viable cells (%)
0	100
0.25	83.30 \pm 4.18
0.5	65.55 \pm 1.57
0.75	37.68 \pm 6.62
1.00	28.97 \pm 1.09
3.00	9.88 \pm 0.89
5.00	5.07 \pm 3.81

Table 3.4.1 Percentage of viable cells of MCF-7 cells after 48 hours of treatment with increasing concentrations [Cu(phen)(ma)Cl].

Concentrations of [Cu(phen)(ma)Cl] (μM)	^a Percentage of viable cells (%)
0	100
0.25	76.44 \pm 1.40
0.5	68.82 \pm 4.01
0.75	58.33 \pm 4.16
1.00	48.40 \pm 1.51
3.00	34.96 \pm 4.00
5.00	11.31 \pm 1.55

Table 3.4.2 Percentage of viable cells of MDA-MB-231 cells after 48 hours of treatment with increasing concentrations [Cu(phen)(ma)Cl].

Concentrations of [Cu(phen)(ma)Cl] (μM)	^a Percentage of viable cells (%)
0	100
0.25	100.00 \pm 9.41
0.5	100.00 \pm 8.73
0.75	100.00 \pm 6.55
1.00	100.00 \pm 5.65
3.00	95.00 \pm 3.85
5.00	34.86 \pm 2.82

Table 3.4.3 Percentage of viable cells of MCF10A cells after 48 hours of treatment with increasing concentrations [Cu(phen)(ma)Cl].

^a Percentage of viable cells is obtained from mean \pm standard deviation values of three independent experiments.

At 48 hours incubation with [Co(phen)(ma)Cl] 10 μ M, 20 μ M, 30 μ M, 40 μ M, 50 μ M and 60 μ M were the concentrations used on MCF-7, MDA-MB-231 and MCF10A cell lines (Figure 3.1.5). A very similar trend was obtained for MCF-7 and MDA-MB-231 cell lines with the graph for each cell line intertwine with each other. The percentage of viable cells can be seen gradually decreasing from 87.31% for MCF-7 cell line and 91.36% for MDA-MB-231 at 10 μ M to 5.40% for MCF-7 cell line and 7.93% for MDA-MB-231 at 60 μ M. MCF10A can be seen to be slightly less susceptible to the effects of [Co(phen)(ma)Cl] . At 10 μ M there was no apparent effect of [Co(phen)(ma)Cl] on MCF10A cell lines. After that the percentage of viable cells for MCF10A gradually decreased from 79.57% at 20 μ M to 21.00% at 60 μ M. The IC-50 value obtained for [Co(phen)(ma)Cl] 48 hours treatment were 26.5 μ M for MCF-7 cell line, 27.2 μ M for MDA-MB-231 cell line and 32.2 μ M for MCF10A cell line.

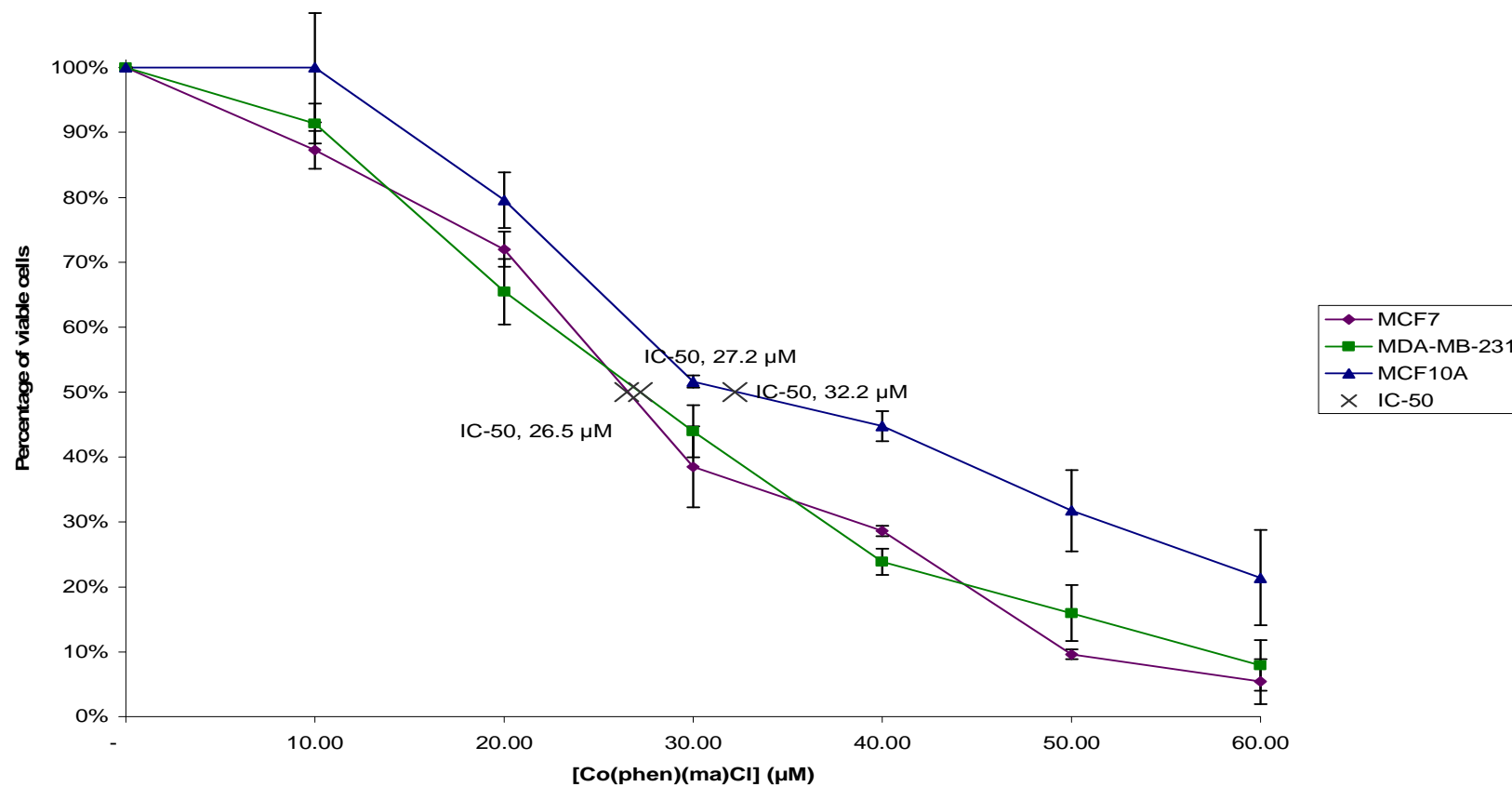


Figure 3.1.5 Viable cells of of MCF-7, MDA-MB-231 and MCF10A cells treated with increasing concentrations of [Co(phen)(ma)Cl] for 48 hours using MTT assay.

Concentrations of [Co(phen)(ma)Cl] (μM)	^a Percentage of viable cells (%)
0	100
10	87.31 \pm 2.92
20	72.00 \pm 2.72
30	38.47 \pm 6.23
40	28.64 \pm 0.80
50	9.62 \pm 0.79
60	5.40 \pm 3.44

Table 3.5.1 Percentage of viable cells of MCF-7 cells after 48 hours of treatment with increasing concentrations [Co(phen)(ma)Cl].

Concentrations of [Co(phen)(ma)Cl] (μM)	^a Percentage of viable cells (%)
0	100
10	91.36 \pm 3.09
20	65.47 \pm 5.07
30	43.96 \pm 4.00
40	23.84 \pm 2.02
50	15.96 \pm 4.32
60	7.93 \pm 3.90

Table 3.5.2 Percentage of viable cells of MDA-MB-231 cells after 48 hours of treatment with increasing concentrations [Co(phen)(ma)Cl].

Concentrations of [Co(phen)(ma)Cl] (μM)	^a Percentage of viable cells (%)
0	100
10	100.00 \pm 8.41
20	79.57 \pm 4.28
30	51.61 \pm 0.96
40	45.00 \pm 2.31
50	32.00 \pm 6.27
60	21.00 \pm 7.35

Table 3.5.3 Percentage of viable cells of MCF10A cells after 48 hours of treatment with increasing concentrations [Co(phen)(ma)Cl].

^a Percentage of viable cells is obtained from mean \pm standard deviation values of three independent experiments.

The series of concentrations used for [Zn(phen)(ma)Cl] treatment for 48 hours on MCF-7, MDA-MB-231 and MCF10A cell lines were 3 μ M, 6 μ M, 9 μ M, 12 μ M, 15 μ M and 18 μ M (Figure 3.1.6). The pattern of the graph for MCF-7 and MDA-MB-231 is quite similar until it nearly overlapped each other at certain points especially at 12 μ M where MCF-7 and MDA-MB-231 cell lines recorded 28.64% and 29.17% of viable cells respectively. MCF10A cell line show relatively resistant towards [Zn(phen)(ma)Cl] compared to its non-malignant counterpart. This is evidently showed where MCF10A cells are in 100% cell viability while MCF-7 and MDA-MB-231 had dropped to 83.35% and 66.12% each. Besides that MCF10A cell line also had a higher IC-50 value at 10.0 μ M compared to MCF-7 cell line at 6.5 μ M and MDA-MB-231 cell line at 7.9 μ M.

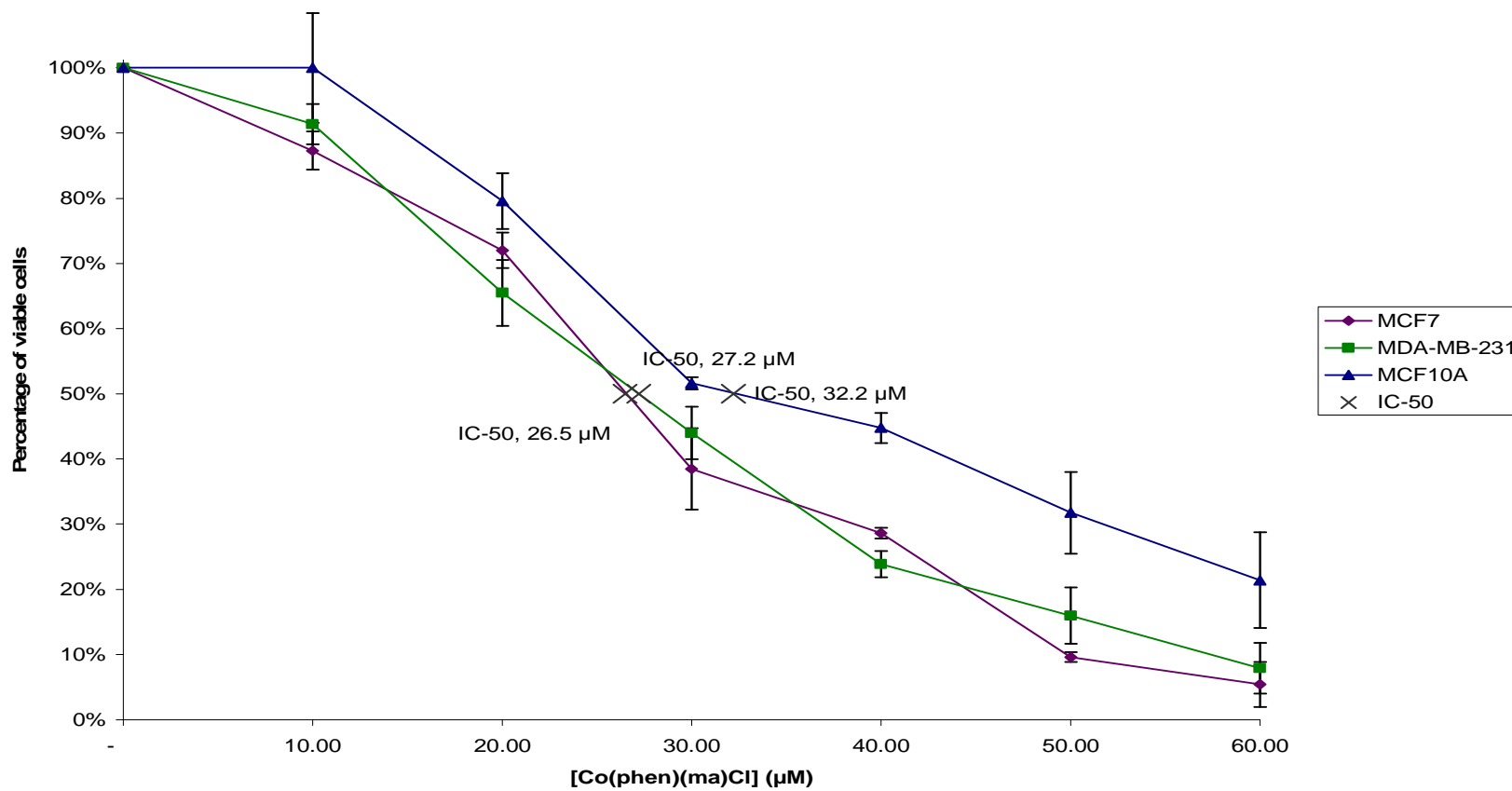


Figure 3.1.6 Viable cells of MCF-7, MDA-MB-231 and MCF10A cells treated with increasing concentrations of [Zn(phen)(ma)Cl] for 48 hours using MTT assay.

Concentrations of [Zn(phen)(ma)Cl] (μM)	^a Percentage of viable cells (%)
0	100
3	83.35 \pm 2.07
6	69.56 \pm 4.74
9	38.06 \pm 5.17
12	28.64 \pm 0.80
15	9.30 \pm 0.86
18	4.43 \pm 4.25

Table 3.6.1 Percentage of viable cells of MCF-7 cells after 48 hours of treatment with increasing concentrations [Zn(phen)(ma)Cl].

Concentrations of [Zn(phen)(ma)Cl] (μM)	^a Percentage of viable cells (%)
0	100
3	66.12 \pm 1.02
6	51.33 \pm 4.04
9	43.32 \pm 4.90
12	29.17 \pm 2.02
15	14.68 \pm 3.49
18	9.92 \pm 6.00

Table 3.6.2 Percentage of viable cells of MDA-MB-231 cells after 48 hours of treatment with increasing concentrations [Zn(phen)(ma)Cl].

Concentrations of [Zn(phen)(ma)Cl] (μM)	^a Percentage of viable cells (%)
0	100
3	100.00 \pm 2.86
6	86.70 \pm 8.32
9	52.32 \pm 0.92
12	45.98 \pm 0.67
15	34.45 \pm 4.25
18	31.48 \pm 0.55

Table 3.6.3 Percentage of viable cells of MCF10A cells after 48 hours of treatment with increasing concentrations [Zn(phen)(ma)Cl].

^a Percentage of viable cells is obtained from mean \pm standard deviation values of three independent experiments.

MDA-MB-231 cell line showed different sensitivity towards [Cu(phen)(ma)Cl] compared to the other two cell lines after 72 hours of incubation (Figure 3.1.7). With that reason, MDA-MB-231 cell line was treated with a different set of varying concentrations of [Cu(phen)(ma)Cl] . MCF-7 and MCF10A cell lines were treated at 0.01 μ M, 0.025 μ M, 0.05 μ M, 0.10 μ M, 0.50 μ M and 1.00 μ M while MDA-MB-231 at 0.01 μ M, 0.03 μ M, 0.07 μ M, 0.10 μ M, 0.30 μ M, 0.70 μ M and 1.00 μ M. MCF-7 cell line showed the highest sensitivity towards [Cu(phen)(ma)Cl] after 72 hours with an IC-50 value of 0.05 μ M then followed by MCF10A cell line with an IC-50 of 0.1 μ M. MDA-MB-231 cell line is the least susceptible to the effects of [Cu(phen)(ma)Cl] with the highest IC-50 value of all three cell lines at 0.4 μ M.

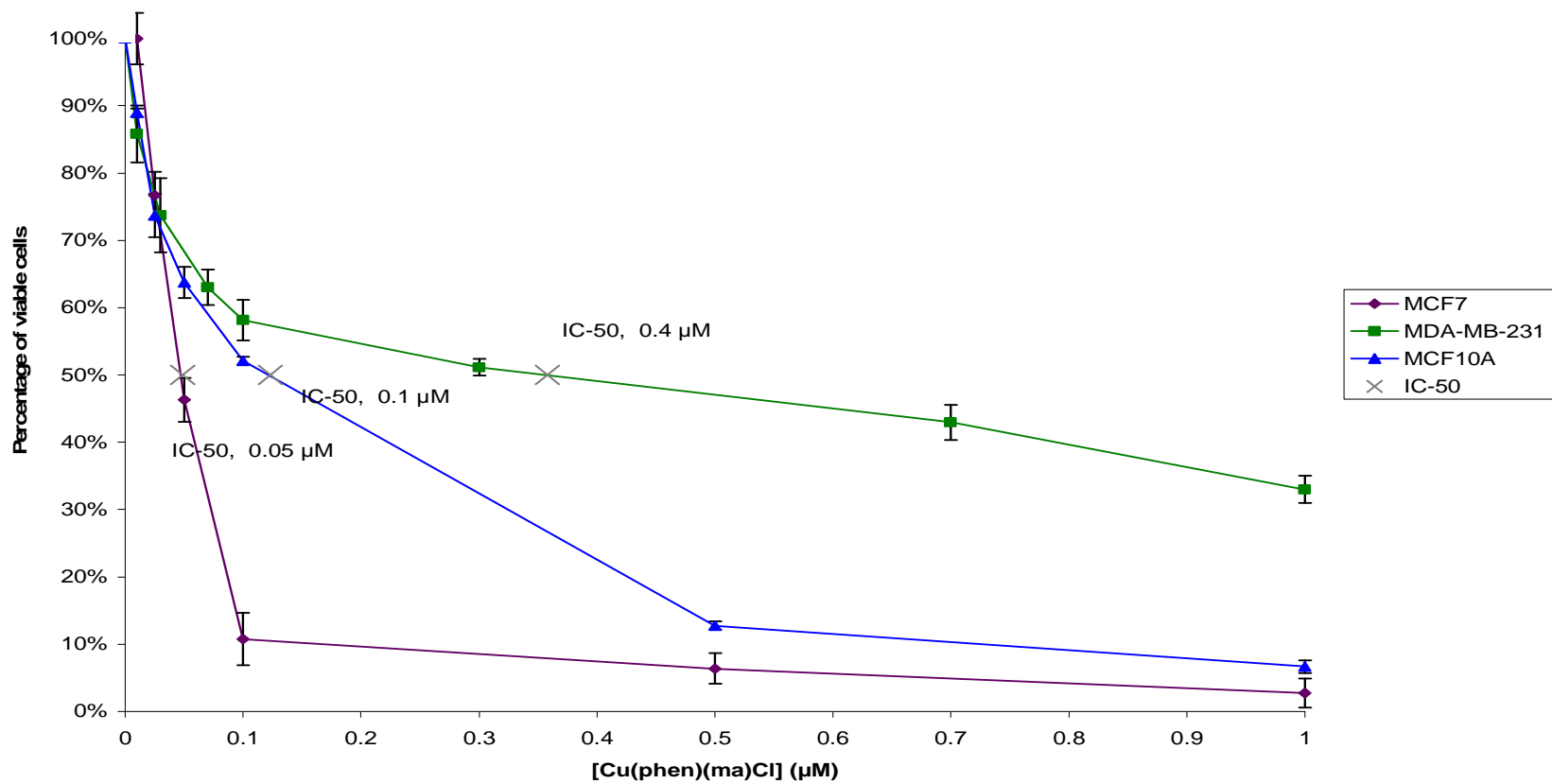


Figure 3.1.7 Viable cells of MCF-7, MDA-MB-231 and MCF10A cells treated with increasing concentrations of [Cu(phen)(ma)Cl] for 72 hours using MTT assay.

Concentrations of [Cu(phen)(ma)Cl] (μM)	^a Percentage of viable cells (%)
0	100
0.01	99.92 \pm 3.80
0.025	76.67 \pm 3.51
0.05	46.31 \pm 3.24
0.10	10.81 \pm 3.88
0.50	6.40 \pm 2.29
1.00	2.77 \pm 2.19

Table 3.7.1 Percentage of viable cells of MCF-7 cells after 72 hours of treatment with increasing concentrations [Cu(phen)(ma)Cl].

Concentrations of [Cu(phen)(ma)Cl] (μM)	^a Percentage of viable cells (%)
0	100
0.01	85.80 \pm 4.25
0.03	73.73 \pm 5.51
0.07	63.01 \pm 2.64
0.10	58.17 \pm 3.01
0.30	51.16 \pm 1.24
0.70	42.95 \pm 2.62
1.00	33.00 \pm 2.00

Table 3.7.2 Percentage of viable cells of MDA-MB-231 cells after 72 hours of treatment with increasing concentrations [Cu(phen)(ma)Cl].

Concentrations of [Cu(phen)(ma)Cl] (μM)	^a Percentage of viable cells (%)
0	100
0.01	88.96 \pm 0.62
0.025	73.67 \pm 3.21
0.05	63.74 \pm 2.30
0.10	52.09 \pm 0.60
0.50	12.77 \pm 0.62
1.00	6.69 \pm 0.97

Table 3.7.3 Percentage of viable cells of MCF10A cells after 72 hours of treatment with increasing concentrations [Cu(phen)(ma)Cl].

^a Percentage of viable cells is obtained from mean \pm standard deviation values of three independent experiments.

The concentrations for [Co(phen)(ma)Cl] treatment for 72 hours period were 1 μ M, 5 μ M, 10 μ M, 15 μ M, 20 μ M, 25 μ M and 30 μ M (Figure 3.1.8). MDA-MB-231 and MCF10A cell lines had a very similar trend. There are several points that both graphs almost merge with each other like at 1 μ M with MDA-MB-231 at 85.47% and MCF10A at 85.67% of viable cells. Besides that the IC-50 value of both of the cell lines are very closed to each other with MDA-MB-231 IC-50 value at 17.8 μ M and MCF10A IC-50 value at 16.9 μ M. On the contrary MCF-7 showed a less resistant trend towards [Co(phen)(ma)Cl] after 72 hours of treatment. The IC-50 value of MCF-7 which was at 2.9 μ M is much lower than the other two cell lines.

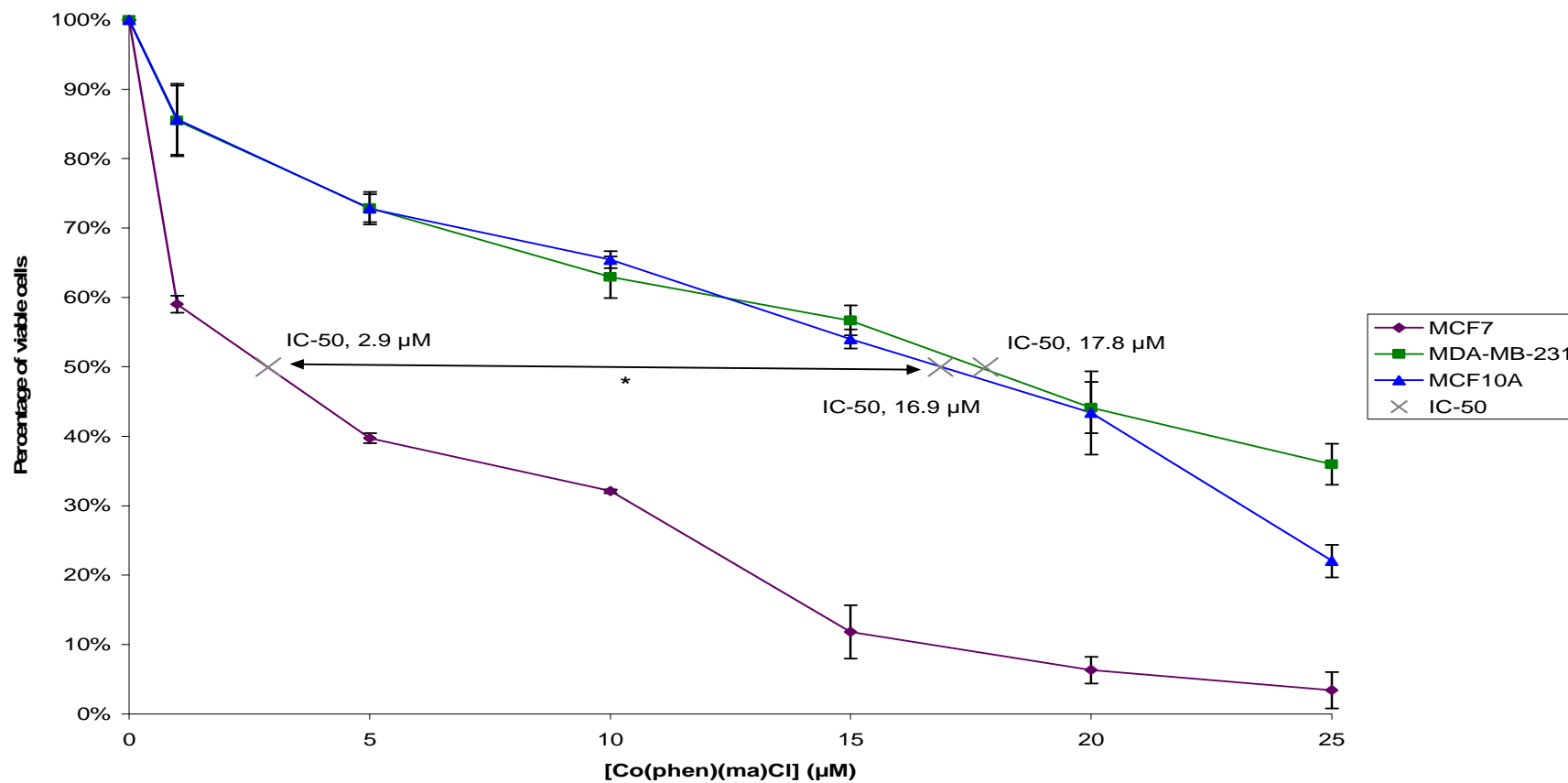


Figure 3.1.8 Viable cells of of MCF-7, MDA-MB-231 and MCF10A cells treated with increasing concentrations of [Co(phen)(ma)Cl] for 72 hours using MTT assay. * $P < 0.05$

Concentrations of [Co(phen)(ma)Cl] (μM)	^a Percentage of viable cells (%)
0	100
1	59.07 \pm 1.21
5	39.73 \pm 0.74
10	32.09 \pm 0.26
15	11.81 \pm 3.83
20	6.31 \pm 1.94
25	3.40 \pm 2.64

Table 3.8.1 Percentage of viable cells of MCF-7 cells after 72 hours of treatment with increasing concentrations [Co(phen)(ma)Cl].

Concentrations of [Co(phen)(ma)Cl] (μM)	^a Percentage of viable cells (%)
0	100
1	85.47 \pm 5.06
5	72.87 \pm 2.01
10	62.93 \pm 3.00
15	56.70 \pm 2.14
20	44.14 \pm 3.67
25	35.97 \pm 2.95

Table 3.8.2 Percentage of viable cells of MDA-MB-231 cells after 72 hours of treatment with increasing concentrations [Co(phen)(ma)Cl].

Concentrations of [Co(phen)(ma)Cl] (μM)	^a Percentage of viable cells (%)
0	100
1	85.67 \pm 5.13
5	72.84 \pm 2.34
10	65.46 \pm 1.23
15	54.00 \pm 1.40
20	43.00 \pm 6.01
25	22.00 \pm 2.34

Table 3.8.3 Percentage of viable cells of MCF10A cells after 72 hours of treatment with increasing concentrations [Co(phen)(ma)Cl].

^a Percentage of viable cells is obtained from mean \pm standard deviation values of three independent experiments.

The concentrations used for [Zn(phen)(ma)Cl] treatment for 72 hours were 1 μ M, 3 μ M, 5 μ M, 7 μ M, 9 μ M and 11 μ M (Figure 3.1.9). The percentage of MCF-7, MDA-MB-231 and MCF10A cells were gradually dropping when the concentration of [Zn(phen)(ma)Cl] increases. MCF-7 cell line was the most susceptible to [Zn(phen)(ma)Cl] treatment with total cell death at 11 μ M while MDA-MB-231 and MCF10A cell lines still had 35.66% and 8.67% of cells left each. The IC-50 value of MCF-7, MDA-MB-231 and MCF10A were 2.7 μ M, 5.5 μ M and 7.7 μ M respectively.

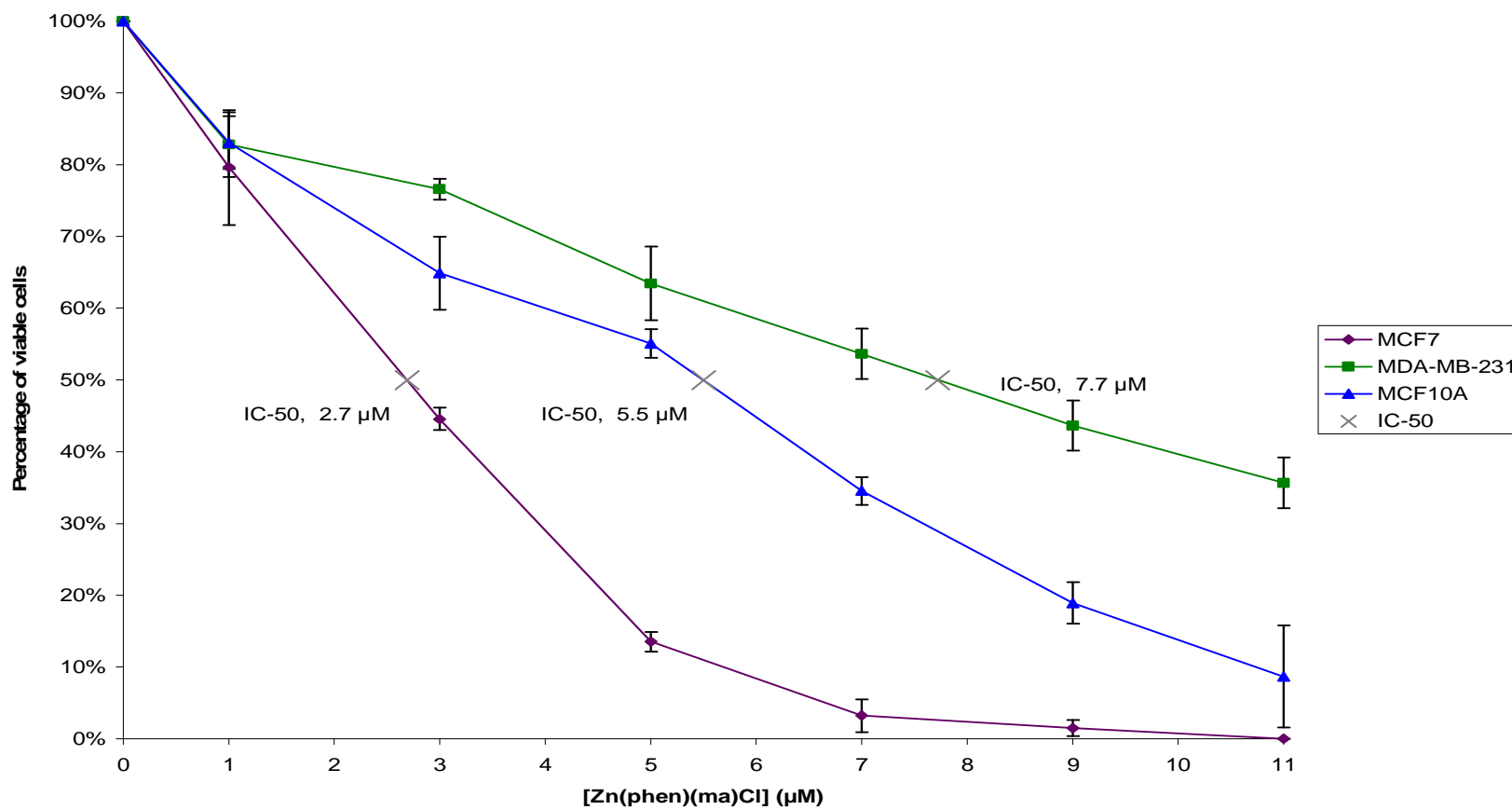


Figure 3.1.9 Viable cells of MCF-7, MDA-MB-231 and MCF10A cells treated with increasing concentrations of [Zn(phen)(ma)Cl] for 72 hours using MTT assay.

Concentrations of [Zn(phen)(ma)Cl] (μ M)	^a Percentage of viable cells (%)		
0	100		
1	79.62	\pm	7.99
3	44.57	\pm	1.57
5	13.50	\pm	1.38
7	3.21	\pm	2.27
9	1.48	\pm	1.14
11	0.00	\pm	0.00

Table 3.9.1 Percentage of viable cells of MCF-7 cells after 72 hours of treatment with increasing concentrations [Zn(phen)(ma)Cl].

Concentrations of [Zn(phen)(ma)Cl] (μ M)	^a Percentage of viable cells (%)		
0	100		
1	82.80	\pm	4.50
3	76.61	\pm	1.45
5	63.46	\pm	5.15
7	53.64	\pm	3.51
9	43.65	\pm	3.51
11	35.66	\pm	3.52

Table 3.9.2 Percentage of viable cells of MDA-MB-231 cells after 72 hours of treatment with increasing concentrations [Zn(phen)(ma)Cl].

Concentrations of [Zn(phen)(ma)Cl] (μ M)	^a Percentage of viable cells (%)		
0	100		
1	83.08	\pm	3.70
3	64.87	\pm	5.06
5	55.09	\pm	2.02
7	34.54	\pm	1.92
9	18.90	\pm	2.89
11	8.67	\pm	7.09

Table 3.9.3 Percentage of viable cells of MCF10A cells after 72 hours of treatment with increasing concentrations [Zn(phen)(ma)Cl].

^a Percentage of viable cells is obtained from mean \pm standard deviation values of three independent experiments.

3.2.2 Cell morphological study

MCF-7, MDA-MB-231 and MCF10A cell lines were used and the cells were left untreated or treated with 0.05 μ M and 0.4 μ M of [Cu(phen)(ma)Cl], 2.9 μ M and 17.8 μ M of [Co(phen)(ma)Cl], 2.7 μ M and 7.7 μ M [Zn(phen)(ma)Cl] for 72 hours. The concentrations chosen were taken from the lowest and highest IC-50 value of the compound among the three cell lines. Then the cells were viewed under phase-contrast inverted microscope. Pictures were taken at 200x magnification. A part of the picture was cropped out without altering its image size to represent the condition of majority of the cells that were in.

The untreated MCF-7 cells exhibited typical growth patterns and a smooth, flattened morphology with normal nuclei. It has branch-like structure extending outwards connecting to neighbouring cells and grows in clusters (Figure 3.2.1a, Figure 3.2.2a and Figure 3.2.3a). When MCF-7 cells were treated 0.05 μ M of [Cu(phen)(ma)Cl] the first most apparent change was the distortion of its normal shape. The cells were turning round and condensation of the chromatin was observable (Figure 3.2.1b). When the concentration of [Cu(phen)(ma)Cl] increased to 0.4 μ M most of the cells floated up detached from the surface. This indicates that the cells were dead. Some of the cells' cytoplasm were getting enlarged (Figure 3.2.1c). When MCF-7 cells were treated with 2.9 μ M [Co(phen)(ma)Cl] the shape of the cells were also distorted and turning roundish. Nuclear condensation was also observable in this condition. Besides that the cells also appeared to be brighter around the membrane indicating it is detaching from the surface (Figure 3.2.2b). At the concentration of 17.8 μ M of [Co(phen)(ma)Cl] most of the cells were

completely detached from the surface and appeared dead (Figure 3.2.2c). When treated with $2.7\mu\text{M}$ of $[\text{Zn}(\text{phen})(\text{ma})\text{Cl}]$ nuclear condensation was also present. Besides that the cells also undergo vacuolation and some of the cells were enlarged. The shape of the cells were quite similar to the untreated ones though slight deformation can be seen (Figure 3.2.3b). The confluence level of the cells were clearly lower than the untreated one when the treatment concentration of $[\text{Zn}(\text{phen})(\text{ma})\text{Cl}]$ increased to $7.7\mu\text{M}$. More dead cells were floating around and the size of the cells were relatively larger compared to the healthy ones (Figure 3.2.3c).

The untreated MDA-MB-231 cells showed normal growth patterns in spindle shape with normal nuclei grew near to each other (Figure 3.2.1d, Figure 3.2.2d, Figure 3.2.3d). After treated with $0.05\mu\text{M}$ of $[\text{Cu}(\text{phen})(\text{ma})\text{Cl}]$ the most conspicuous change in the cell morphology included losing the distinct spindle shape and extensive detachment from the culture plate surface (Figure 3.2.1e). When the concentration increased to $0.4\mu\text{M}$ of $[\text{Cu}(\text{phen})(\text{ma})\text{Cl}]$ increased dead cells were observed floating in the medium (Figure 3.2.1f). Treatment with $2.9\mu\text{M}$ of $[\text{Co}(\text{phen})(\text{ma})\text{Cl}]$ caused some of the cells to detach from the surface (Figure 3.2.2e). At $17.8\mu\text{M}$ of $[\text{Co}(\text{phen})(\text{ma})\text{Cl}]$ apoptotic bodies were spotted indicating apoptosis was induced (Figure 3.2.3f). After incubated with $2.7\mu\text{M}$ of $[\text{Zn}(\text{phen})(\text{ma})\text{Cl}]$ the cells undergo cytoplasm enlargement and also elongation of the cells (Figure 3.2.3e). When the concentration increased to $7.7\mu\text{M}$ more dead cells were spotted and the confluence level dropped (Figure 3.2.3f).

The untreated MCF10A cells showed normal growth rate shaped in spindle like typical epithelial cells with normal nuclei grew near to each other (Figure 3.2.1g, Figure 3.2.2g and Figure 3.2.3g). Treating the cells with 0.05 μ M of [Cu(phen)(ma)Cl] caused the cells to lose its spindle shape and enlargement of the cytoplasm (Figure 3.2.1h). When the concentration increased to 0.4 μ M widespread of cell detachment was observed with a large quantity of dead cells floating. The confluence level was visibly lower (Figure 3.2.1i). [Co(phen)(ma)Cl] seems to have minimal effect on changing the cell morphology. When incubated in 2.9 μ M of [Co(phen)(ma)Cl] the confluence level of the cells drop slightly and some cells were elongated (Figure 3.2.2h). Even at 17.8 μ M the distinct spindle shape can still be seen though the confluence level further decreased (Figure 3.2.2i). After treatment 2.7 μ M of [Zn(phen)(ma)Cl] the size of the cells were larger and condensation of the chromatin was apparent (Figure 3.2.3h). When the concentration of the treatment increased to 7.7 μ M the cells lose its spindle shape and no longer stick to each other. Dead cells were spotted and cells showed early signs of detachment from the surface (Figure 3.2.3i).

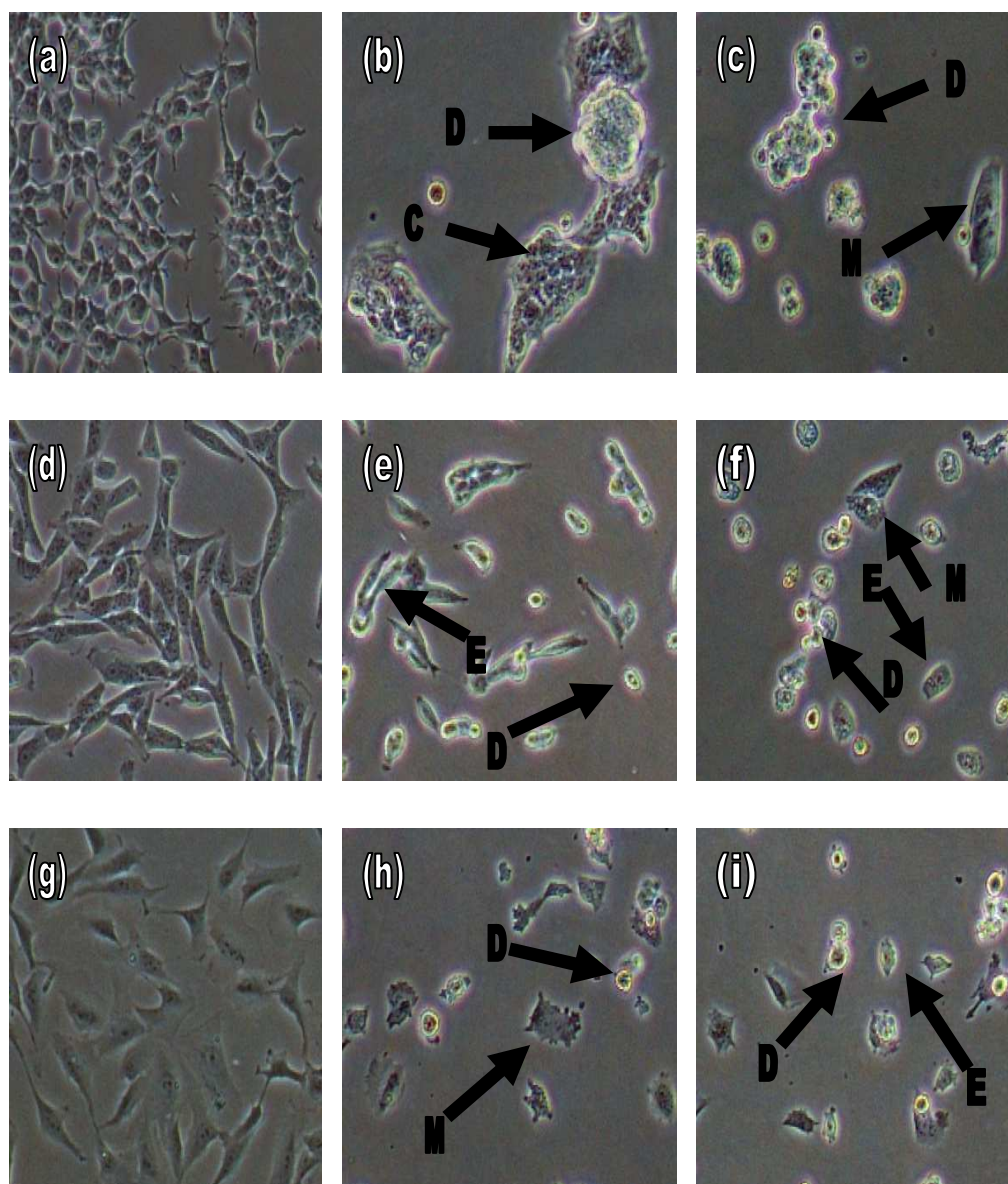


Figure 3.2.1 Morphological observations of: (a) untreated MCF-7 cells (d) untreated MDA-MB-231 cells (g) untreated MCF10A cells with cells treated with increasing concentrations of $[\text{Cu}(\text{phen})(\text{ma})\text{Cl}]$ for 72 hours (b) MCF-7 $0.05\mu\text{M}$ (c) MCF-7 $0.4\mu\text{M}$ (e) MDA-MB-231 $0.05\mu\text{M}$ (f) MDA-MB-231 $0.4\mu\text{M}$ (h) MCF10A $0.05\mu\text{M}$ (i) MCF10A $0.4\mu\text{M}$. Arrow (A) apoptotic body (C) condensation of chromatin (D) dead cell (E) detachment from surface (L) elongation of cell (M) enlargement of cytoplasm (V) vacuolation. Images were captured using phase-contrast inverted microscope at 200x magnification.

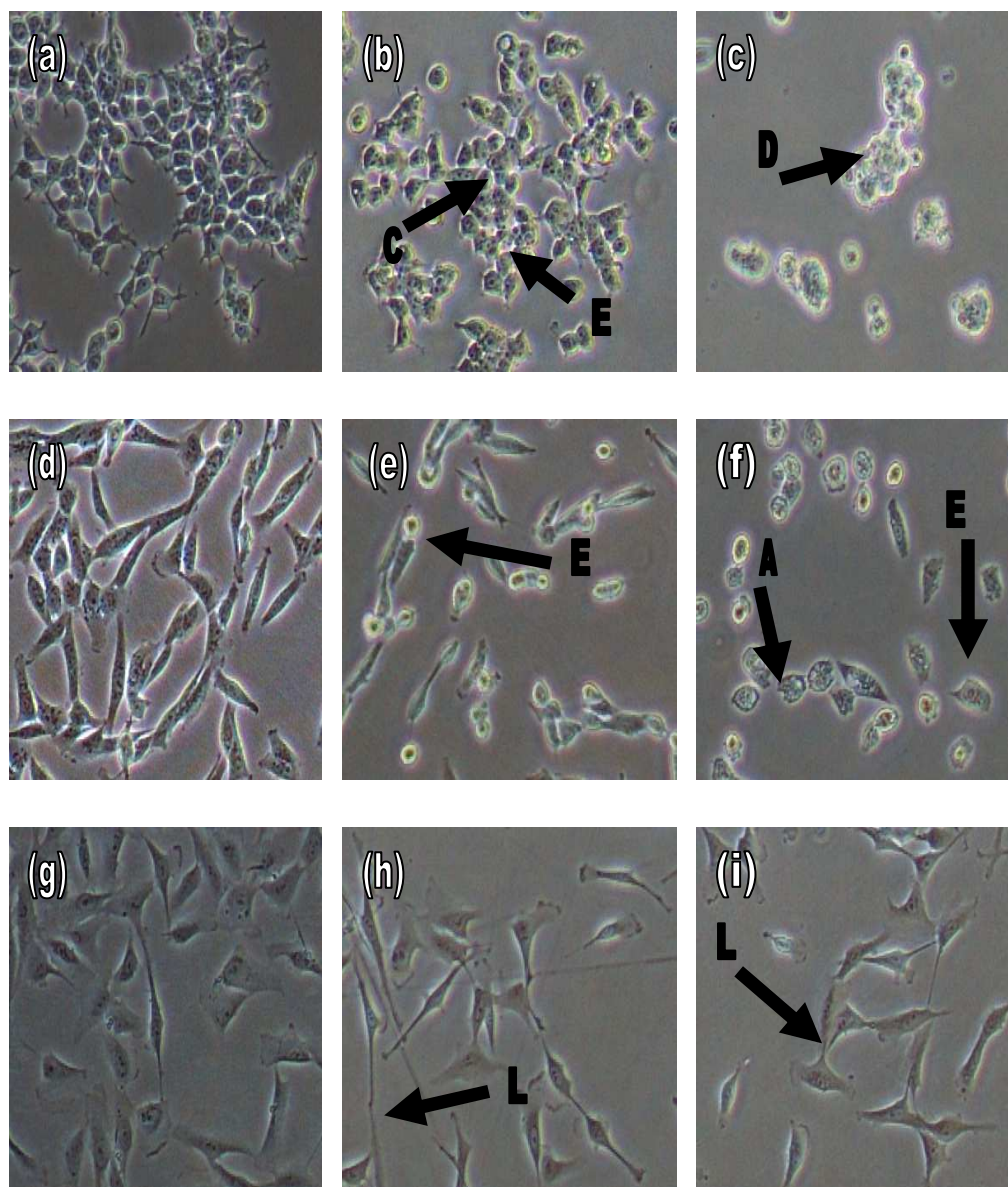


Figure 3.2.2 Morphological observations of: (a) untreated MCF-7 cells (d) untreated MDA-MB-231 cells (g) untreated MCF10A cells with cells treated with increasing concentrations of $[\text{Co}(\text{phen})(\text{ma})\text{Cl}]$ for 72 hours (b) MCF-7 $2.9\mu\text{M}$ (c) MCF-7 $17.8\mu\text{M}$ (e) MDA-MB-231 $2.9\mu\text{M}$ (f) MDA-MB-231 $17.8\mu\text{M}$ (h) MCF10A $2.9\mu\text{M}$ (i) MCF10A $17.8\mu\text{M}$. Arrow (A) apoptotic body (C) condensation of chromatin (D) dead cell (E) detachment from surface (L) elongation of cell (M) enlargement of cytoplasm (V) vacuolation. Images were captured using phase-contrast inverted microscope at 200x magnification.

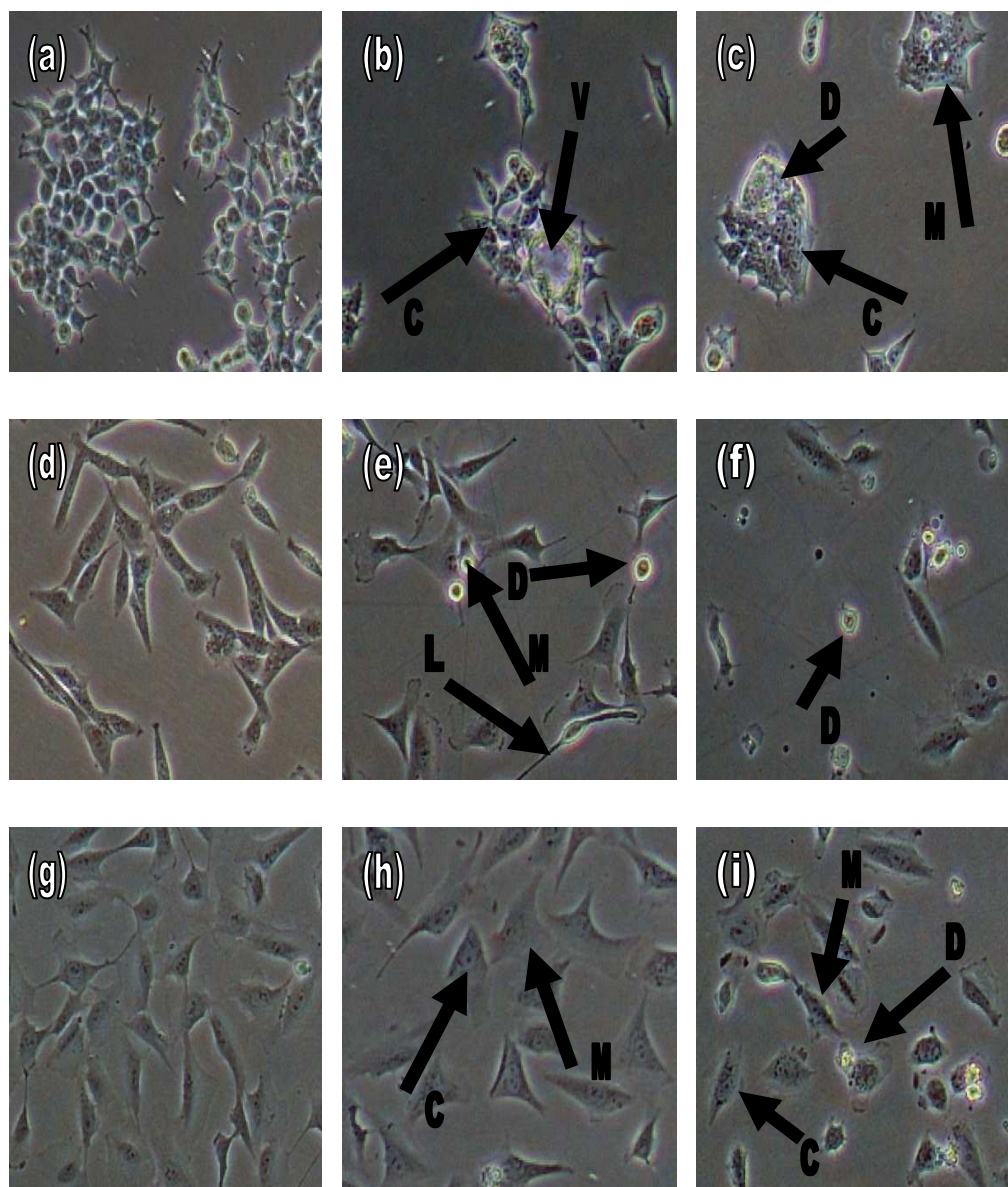


Figure 3.2.3 Morphological observations of: (a) untreated MCF-7 cells (d) untreated MDA-MB-231 cells (g) untreated MCF10A cells with cells treated with increasing concentrations of $[Zn(phen)(ma)Cl]$ for 72 hours (b) MCF-7 $2.7\mu M$ (c) MCF-7 $7.7\mu M$ (e) MDA-MB-231 $2.7\mu M$ (f) MDA-MB-231 $7.7\mu M$ (h) MCF10A $2.7\mu M$ (i) MCF10A $7.7\mu M$. Arrow (A) apoptotic body (C) condensation of chromatin (D) dead cell (E) detachment from surface (L) elongation of cell (M) enlargement of cytoplasm (V) vacuolation. Images were captured using phase-contrast inverted microscope at 200x magnification.

3.3 Discussion

Drugs have the potential to be very harmful to the body unless they are very specific to cancer cells (Schwartzmann et. al., 2002). That is the reason MCF10A cell line was used as a comparative to malignant cell lines used which were MCF-7 and MDA-MB-231. Ultimately, it is preferable to find a compound that has adverse effects on malignant cell lines but has no effect towards non-malignant cell line. The easiest way to determine a compound efficacy towards malignant cell lines is by doing cell viability test via MTT assay. To determine whether there is specificity in the action of the compound the IC-50 value of malignant cell lines were compare with the non-malignant one. A higher IC-50 value on non-malignant cell line compared to malignant cell lines indicates a higher dosage of the compound is needed to have an effect on the non-malignant cells. Therefore, the treatment dosage can be set at lower concentration where it will only affect malignant cell lines but not non-malignant ones.

For the first 24 hours of treatment the $[\text{Co}(\text{phen})(\text{ma})\text{Cl}]$ and $[\text{Zn}(\text{phen})(\text{ma})\text{Cl}]$ were not so reactive with IC-50 values up to the hundreds. So the treatment period were extended up to 48 hours. There was no selectivity for $[\text{Cu}(\text{phen})(\text{ma})\text{Cl}]$ even at 24 hours of treatment as it was equally toxic to malignant and non-malignant cell lines. So $[\text{Cu}(\text{phen})(\text{ma})\text{Cl}]$ was not so suitable to be chosen for further studies. At 48 hours the IC-50 values of $[\text{Co}(\text{phen})(\text{ma})\text{Cl}]$ were still too high to be clinically practicable so the treatment period was further extended to 72 hours. However there was no specificity of the action of $[\text{Zn}(\text{phen})(\text{ma})\text{Cl}]$ compound after comparing the

IC-50 values for the malignant cell lines with non-malignant. So [Zn(phen)(ma)Cl] was also not chosen to be further studied.

MTT assay has shown that [Co(phen)(ma)Cl] significantly suppressed the proliferation of MCF-7, MDA-MB-231 and MCF10A cell lines in a dose and time dependent manner. At 72 hours of treatment there was a significant difference between the IC-50 value of MCF-7 cell line compared to MCF10A cell line with $P < 0.05$. The IC-50 value for MCF-7 cell line after 72 hours of treatment with [Co(phen)(ma)Cl] was $2.9\mu\text{M}$ while for MDA-MB-231 and MCF10A cell lines were $16.9\mu\text{M}$ and $17.8\mu\text{M}$ respectively. Even though the IC-50 value of MDA-MB-231 cell line, one of the malignant cell lines used in this study, was not that different from the IC-50 value of MCF10A which was the non-malignant counterpart but the vast difference compared to the one of MCF-7 cell line indicating there might be different mode of action undertaken by [Co(phen)(ma)Cl] compound in killing these cells. If further analysis on this compound turns to be promising then the original molecular structure of [Co(phen)(ma)Cl] may be modified to create a new compound that has higher selectivity and competency in killing cancer cells.

Necrosis is evidenced by cytoplasmic enlargement, rupture of the plasma membrane, swelling of cytoplasmic organelles particularly mitochondria, and some condensation of nuclear chromatin (Galluzzi et al. 2007). Using this know fact and compare it with the photos taken for morphological studies it can be concluded that [Cu(phen)(ma)Cl] and [Zn(phen)(ma)Cl] induced cell death on MCF-7, MDA-MB-231 and MCF10A primarily through necrosis.

Cells treated with [Cu(phen)(ma)Cl] and [Zn(phen)(ma)Cl] showed signs of cytoplasmic swelling, one of the indications of necrosis. The process of rupturing plasma membrane was very hard to be spotted as it happens spontaneously. However the presence of debris usually is a sign of cells died from lysis process causing the cell contents to be released (Figure 3.2.1 and Figure 3.2.3).

Some of the features of apoptotic cells include cytoplasmic and nuclear condensation, nuclear fragmentation, normal morphological appearance of cytoplasmic organelles, dynamic membrane blebbing and an intact plasma membrane (Kerr et al. 1972; Wyllie et al. 1980; Mathew et al. 2001; Galluzzi et al. 2007). Some of these features like nuclear condensation and intact plasma membrane can be observed when MCF-7 and MDA-MB-231 cell lines were treated with [Co(phen)(ma)Cl] (Figure 3.2.2). The remaining features are very hard if not impossible to be observed under a conventional phase-contrast inverted microscope. Cytoplasmic organelles and nuclear fragmentation cannot be observed clearly without higher magnification microscope and also without the aid of specific dyes. The presence of apoptotic body in MDA-MB-231 cells when treated with 17.8 μ M of [Co(phen)(ma)Cl] clearly confirmed that [Co(phen)(ma)Cl] induced apoptosis on MDA-MB-231 cell line (Figure 3.2.2f). It was vaguer for MCF-7 to conclude whether it undergone apoptosis under the influence of [Co(phen)(ma)Cl] since most of the cells were dead at 17.8 μ M. However the way the dead cells appeared, shrunk and with intact membrane, does not imply it had undergone necrosis suggesting it may have undergone apoptosis (Figure

3.2.2c). [Co(phen)(ma)Cl] appeared to have relatively low effect of MCF10A cell line. There was no distinct change in features observed except elongation of the cells. The cells still maintained its spindle shape. However the confluence of the cells decreased when the concentration of [Co(phen)(ma)Cl] increased. That explains the elongation of the cells as MCF10A cells usually elongates to cover more surface area when the confluence level is low (Figure 3.2.2h and Figure 3.2.2i).

Morphological study can only provide a rough estimation of what were going on when the cell lines were treated with [M(phen)(ma)Cl]. To provide concrete evidence that is acceptable in the scientific community specific tests are needed to be carried out. However after analysing the results obtained from the preliminary studies [Cu(phen)(ma)Cl] and [Zn(phen)(ma)Cl] were not suitable to be continued to be studied on. The IC-50 value of [Cu(phen)(ma)Cl] and [Zn(phen)(ma)Cl] for malignant and non-malignant cell lines were too near to each other. This only meant [Cu(phen)(ma)Cl] and [Zn(phen)(ma)Cl] were equally cytotoxic to both malignant and non-malignant cell lines thus it will be a waste of resources and time to continue on with these two compounds.

CHAPTER 4

FURTHER STUDIES ON [Co(phen)(ma)Cl]

After preliminary studies done [M(phen)(ma)Cl] it was found that [Cu(phen)(ma)Cl] and [Zn(phen)(ma)Cl] were not suitable for further testing because of high cytotoxicity towards non-malignant cell line. So in this chapter only [Co(phen)(ma)Cl] was used for testing with the objective of narrowing down the path of which mechanism of action were taken by [Co(phen)(ma)Cl] to kill the malignant cell lines. Three different concentrations that were used were 3 μ M, 17 μ M and 25 μ M. Three micro molar and 17 μ M were specifically chosen to cover the IC-50 value of [Co(phen)(ma)Cl] on all three of the cell lines and 25 μ M were used to determine the effect of [Co(phen)(ma)Cl] at concentration exceeding the IC-50 value.

4.1 Materials and methods

4.1.1 Cell line

Further studies on [Co(phen)(ma)Cl] were done using MCF-7 (Michigan Cancer Foundation - 7), MDA-MB-231 (M.D. Anderson - Metastatic Breast – 231) and MCF10A (Michigan Cancer Foundation – 10A). Culturing materials and methods can be referred back to Chapter 3.

4.1.2 Apoptosis assay

The assay was done using FITC Annexin V Apoptosis Detection Kit II (BD Pharmingen™) and the protocol as adapted using the protocol provided together with the kit.

4.1.2.1 Cell preparation and staining of the cell

A number of 1×10^6 cells/mL cells were cultured in 100 x 15 mm culture dish (Nunc™) with cell number enough to achieve 70%~80% cell confluence for untreated cells at the end of the 72 hours incubation period. The cells were then incubated in the 5% CO₂ humidified incubator at 37°C for 24 hours to let it recover from harvesting procedure. The existing medium were drained and replaced with fresh medium before various concentrations of [Co(phen)(ma)Cl] compounds were added into each culture dish. The cells were then incubated in the 5% CO₂ humidified incubator at 37°C for 72 hours. The cells were detached using Accutase (Sigma®) to yield cells with better viability than trypsin. Accutase (Sigma®) was thawed in room temperature and warmed at room temperature before usage and cannot be warmed in water bath. The culture dish was then incubated in the 5% CO₂ humidified incubator at 37°C until all of the cells were fully suspended. The suspended cells were transferred into a sterile Falcon™ tube and topped up with 3mL of medium solution specified for each cell line. The centrifuge tube was centrifuged at 1000rpm for 5 minutes using centrifuge machine. After centrifugation, the pellet of cells was obtained. All supernatant was discarded and the pellet was then washed with cold PBS solution twice. The

cells were then resuspend in 1X Binding Buffer at a concentration of 1×10^6 cells/ml. One hundred micro liters of the solution (1×10^5 cells) were transferred to a 12 x 75mm Falcon round-bottom tube with 33 μ M nylon mesh cell strainer cap (BD™). Five micro liters of FITC Annexin V and 5 μ L PI were added to each tube. The cells were gently vortex and incubate in room temperature for 15 minutes in the dark. Four hundred micro liters of 1X Binding buffer were added to each tube and the solution of each tube was strained using the cell strainer cap. The cells were analyzed with flow cytometry (BD FACSCalibur™) as soon as possible. For setting up compensation and quadrants a tube of untreated cells unstained, a tube of untreated cells stained with FITC Annexin V without PI and a tube of untreated cells stained with PI without FITC Annexin V were required. Binding buffer, FITC Annexin V and PI were provided by FITC Annexin V Apoptosis Detection Kit II (BD Pharmingen™).

3.1.3 Cell cycle analysis

The protocol was adapted from the research done by Krishan (1975).

4.1.3.1 Hypotonic staining buffer reagent for DNA preparation

The hypotonic staining buffer reagent was prepared before the hand is kept in a tightly-sealed bottle protected from light. No apparent loss of staining activity was observed for several months. The contents of the reagent are:

Sodium citrate	0.25g
Triton-x 100	0.75ml
Propidium iodide	0.025g
Ribonuclease A	0.005g
Distilled water	250 ml

Sodium citrate, triton-x 100 and ribonuclease A were obtained from Sigma® while propidium iodide was obtained from Calbiochem®.

4.1.3.2 Cell preparation and staining of the DNA

A number of 1×10^6 cells/mL cells were cultured in 100 x 15 mm culture dish (Nunc™) with cell number enough to achieve 70%~80% cell confluence for untreated cells at the end of the 72 hours incubation period. The cells were then incubated in the 5% CO₂ humidified incubator at 37°C for 24 hours to let it recover from harvesting procedure. The existing medium were drained and replaced with fresh medium before various concentrations of [Co(phen)(ma)Cl] compounds were added into each culture dish. The cells were then incubated in the 5% CO₂ humidified incubator at 37°C for 72 hours. The cells were detached using Accutase (Sigma®) to yield cells with better viability than trypsin. Accutase (Sigma®) was thawed in room temperature and warmed at room temperature before usage and cannot be warmed in water bath. The culture dish was then incubated in the 5% CO₂ humidified incubator at 37°C until all of the cells were fully suspended. The suspended cells were transferred into a sterile Falcon™ tube and topped up with 3mL of medium solution specified for each cell line. Around $0.5 - 1 \times 10^6$ cells were transferred into a new tube. The tube was centrifuged at

1000rpm for 5 minutes and the supernatant were aspirated without disturbing the pellet. Five hundred micro liters of the hypotonic DNA staining buffer were added to the pellet. The cells were gently vortex and incubate in room temperature for 10 minutes in the dark. The solution were strained and transferred to a 12 x 75mm Falcon round-bottom tube with 33 μ M nylon mesh cell strainer cap (BD™). The cells were analyzed with flow cytometry (BD FACSCalibur™) as soon as possible.

4.1.4 Proteasome inhibition assay

The assay was done using Proteasome-Glo™ 3-Substrate System (Promega™) and the protocol as adapted using the protocol provided together with the kit.

4.1.4.1 Proteasome-Glo™ Reagent Preparation

Proteasome-Glo™ Buffer was thawed and both buffer and the lyophilized Luciferin Detection Reagent were equilibrated in room temperature before use. Luciferin Detection Reagent was reconstituted into the amber bottle by adding the appropriate volume of Proteasome-Glo™ Buffer. The appropriate substrate were thawed and equilibrated to room temperature before use. For the Chymotrypsin-Like Assay, Suc-LLVY-Glo™ Substrate was used; for the Trypsin-Like Assay, Z-LRR-Glo™ Substrate was used; and for the Caspase-Like Assay, Z-nLPnLD-Glo™ Substrate was used. The solution was mixed well by vortexing briefly. Proteasome-Glo™ Reagent was prepared by adding the Proteasome-Glo™ Substrate to the resuspended Luciferin Detection Reagent. The reagent bottle was

labeled to identify the substrate used. Proteasome-Glo™ Reagent was allowed to sit at room temperature for 60 minutes before use. This allows the removal of any contaminating free aminoluciferin.

4.1.4.2 Cell preparation and staining of the cells

A number of 1×10^6 cells/mL were plated for each cell line for 72 hours incubation period into white 96-well microplate with clear bottom (PerkinElmer™). Each wells were topped up to 100µL with medium. The plate was incubated for 24 hours in the 5% CO₂ humidified incubator at 37°C for the cells to recover from harvesting procedure. For the treatment of the [Co(phen)(ma)Cl] compounds, existing medium was replaced with fresh medium before the intended concentrations of [Co(phen)(ma)Cl] compounds were added into each wells. A know inhibitor epoxomicin was used for comparison with the readings obtained from treatment of the compound. For each sample a triplicate were done to find the average and standard deviation of the results. The cells were then incubated in the 5% CO₂ humidified incubator at 37°C for 72 hours. The cell condition and confluence were observed to make sure the reduction of proteasome activity was not due to the reduction of viable cells. The plate will be discarded if the cell viability is not satisfactory. Fifty micro liters of Proteasome-Glo™ Reagent were added to each well of a white 96-well plate containing blank, control or test sample. Contents of wells were gently mixed using a plate shaker at 300–500rpm for 30 seconds. The plate was incubated at room temperature for 10 minutes to 3 hours depending upon convenience of reading time. The sensitivity

level will reach optimal level typically around 10-30 minutes. The luminescence readings were recording using EnVision® Multilabel Plate Reader (PerkinElmer™).

4.1.5 Measurement of Reactive Oxygen Species (ROS)

The assay was done using OxiSelect™ Intracellular ROS Assay Kit (Cell Biolabs, Inc.) and the protocol as adapted using the protocol provided together with the kit.

4.1.5.1 Preparation of Reagents

The 20X DCFH-DA stock solution was diluted to 1X in culture media without the addition of serum. The 1X reagent was vortex into homogeneity. The reagents were prepared fresh for every application. Hydrogen peroxide was prepared using PBS and was used as positive control in this assay. Solution was prepared fresh for every application. Due to photo-oxidation, DCFH-DA solutions of any concentration were stored protected from light.

4.1.5.2 Cell preparation and staining of the cells

A number of 1×10^6 cells/mL were plated for each cell line for 72 hours incubation period into black 96-well microplate with clear bottom (PerkinElmer™). Each wells were topped up to 100 μ L with medium. The plate was incubated for 24 hours in the 5% CO₂ humidified incubator at 37°C for the cells to recover from harvesting procedure. For the treatment of the [Co(phen)(ma)Cl] compounds, existing medium was replaced with fresh medium

before the intended concentrations of [Co(phen)(ma)Cl] compounds were added into each wells. Hydrogen peroxide solution was used as a positive control for this assay. For each sample a triplicate were done to find the average and standard deviation of the results. The cells were then incubated in the 5% CO₂ humidified incubator at 37°C for 72 hours. The cell condition and confluence were observed and any irregularities were noted. The plate will be discarded if the cell viability is not satisfactory. The medium were drain and cells were washed with PBS. The washing procedure was repeated and the wash was drained. One hundred micro litre of 1X DCFH-DA/medium solution were added into each well and incubated at 37°C for 30 minutes. The solution was drained and the cells were washed with PBS two times. The wash solution was drained and 100µL of fresh medium were added into each well. The fluorescence readings were recording using EnVision® Multilabel Plate Reader (PerkinElmer™). Due to photo-oxidation, the procedures after addition of DCFH-DA solution were performed in dark.

4.2 Results

4.2.1 Apoptosis assay

MCF-7, MDA-MB-231 and MCF10A cells were left untreated or treated for 72 hours with 3 μ M, 17 μ M or 25 μ M of [Co(phen)(ma)Cl]. Cells were incubated with Annexin V-FITC in a buffer containing PI and analyzed by flow cytometry. Untreated cells were primarily Annexin V-FITC and PI negative, indicating that they were viable and not undergoing apoptosis. After treatment, there were primarily four populations of cells: cells that were viable and not undergoing apoptosis (Annexin V-FITC and PI negative), cells undergoing apoptosis (Annexin V-FITC positive and PI negative), cells in end stage or late apoptosis (Annexin V-FITC positive and PI positive) and dead cells (Annexin V-FITC and PI positive).

MCF-7 cells untreated with [Co(phen)(ma)Cl] can be seen not stained by both Annexin V-FITC and PI (Figure 4.1.1a). When treated with 3 μ M of [Co(phen)(ma)Cl] the percentage of dead cells increased to 25.86% compared to 1.52% on the untreated cells (Figure 4.1.1b). The percentage of dead cells continued to climb when the concentration increased with 17 μ M (Figure 4.1.1c) and 25 μ M (Figure 4.1.1d) of [Co(phen)(ma)Cl] recorded 29.52% and 46.51% of dead cells respectively. In contrast the percentage of apoptotic cells only increased slightly when the concentration of [Co(phen)(ma)Cl] increased. From untreated at 0.78% to only 6.68% at 25 μ M.

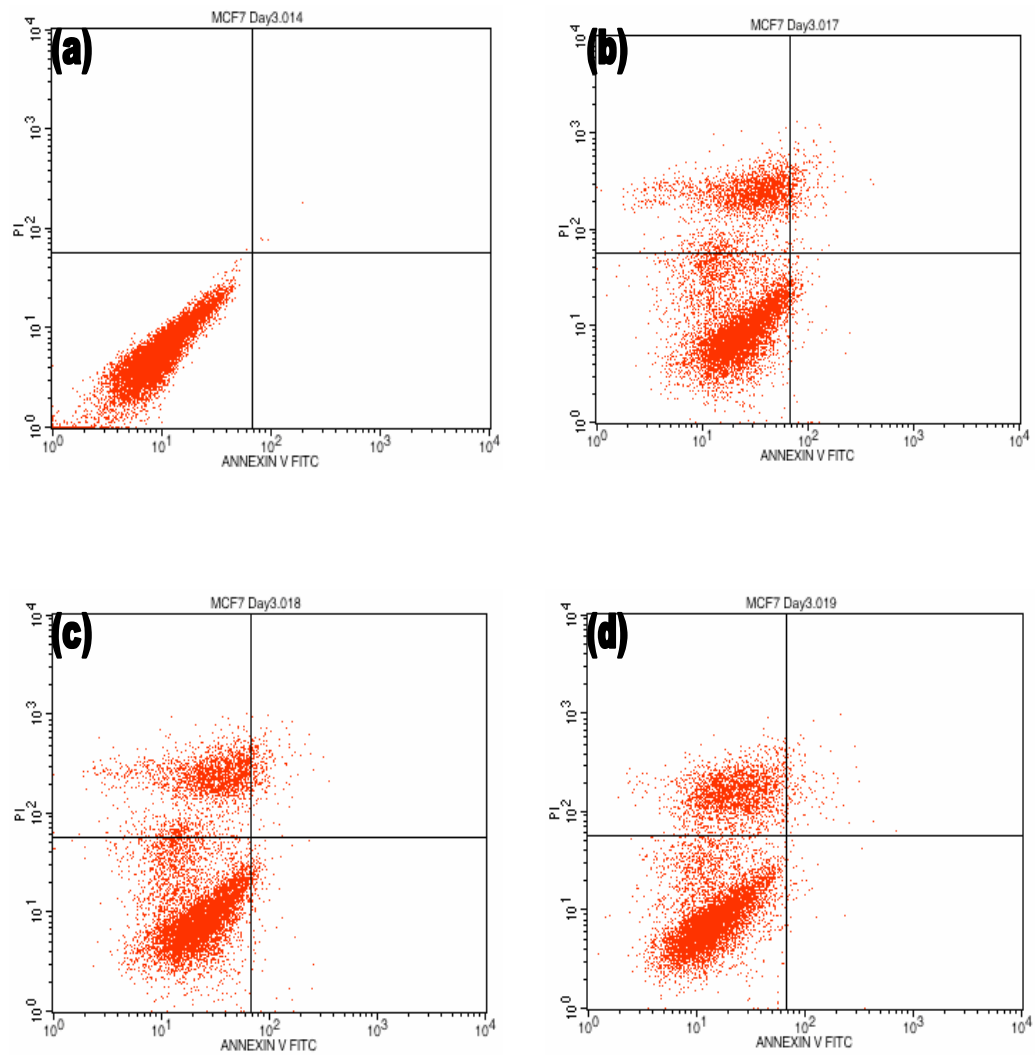


Figure 4.1.1 Flow cytometric analysis of annexin V-FITC/PI double-staining: MCF-7 cells were left untreated or treated for 72 hours with (a) $3\mu\text{M}$ (b) $17\mu\text{M}$ or (c) $25\mu\text{M}$ of $[\text{Co}(\text{phen})(\text{ma})\text{Cl}]$. Cells were incubated with Annexin V-FITC in a buffer containing PI and analyzed by flow cytometry. The y axis denotes cells stained with PI and the x axis represents cells stained in Annexin V-FITC.

Untreated MDA-MB-231 cells showed very few dead or apoptotic cells (Figure 4.1.2a). After treated with 3 μ M of [Co(phen)(ma)Cl] the percentage of apoptotic cells increased tremendously to 44.12% (Figure 4.1.2b). When the concentration of [Co(phen)(ma)Cl] increased the percentage of apoptotic cells also continued to spike with 17 μ M at 57.51% (Figure 4.1.2c) and 25 μ M at 71.58% (Figure 4.1.2d).

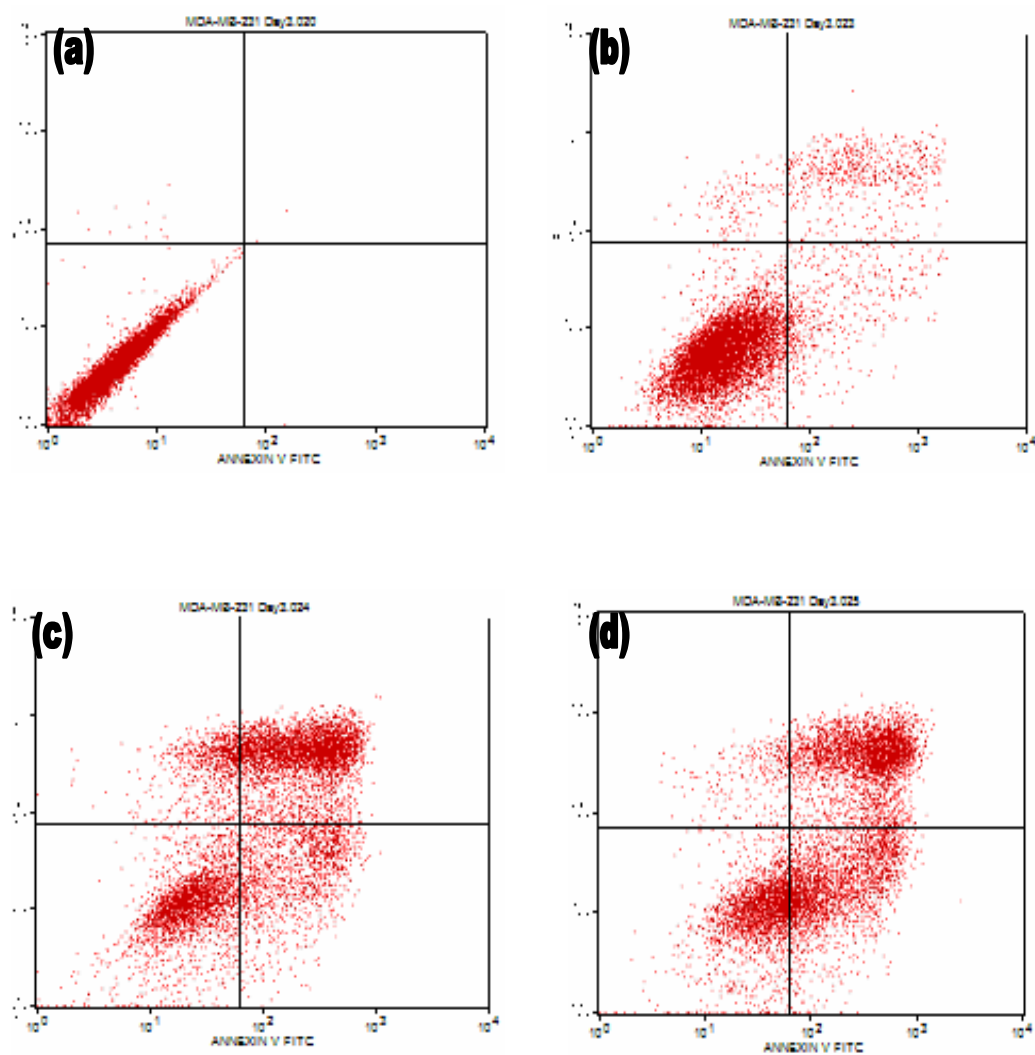


Figure 4.1.2 Flow cytometric analysis of annexin V-FITC/PI double-staining: MDA-MB-231 cells were left untreated or treated for 72 hours with (a) 3 μ M (b) 17 μ M or (c) 25 μ M of [Co(phen)(ma)Cl]. Cells were incubated with Annexin V-FITC in a buffer containing PI and analyzed by flow cytometry. The y axis denotes cells stained with PI and the x axis represents cells stained in Annexin V-FITC.

MCF10A cells untreated with [Co(phen)(ma)Cl] also showed to have very little dead and apoptotic cells (Figure 4.1.3a) like MCF-7 and MDA-MB-231 cells. However the similarity ends here. At 3 μ M of [Co(phen)(ma)Cl] incubated for 72 hours the percentage of apoptotic cells was just at 1.34% while the percentage of dead cells 0.84% (Figure 4.1.3b). The numbers did not increased much when the concentration increased to 17 μ M with percentage of apoptotic cells at 3.18 μ M and percentage of dead cells at 0.44% (Figure 4.1.3c). Even when the concentration of [Co(phen)(ma)Cl] raised up to 25 μ M the percentage of apoptotic cells only peaked at 3.19% while the percentage of dead cells at 2.23% (Figure 4.1.3d).

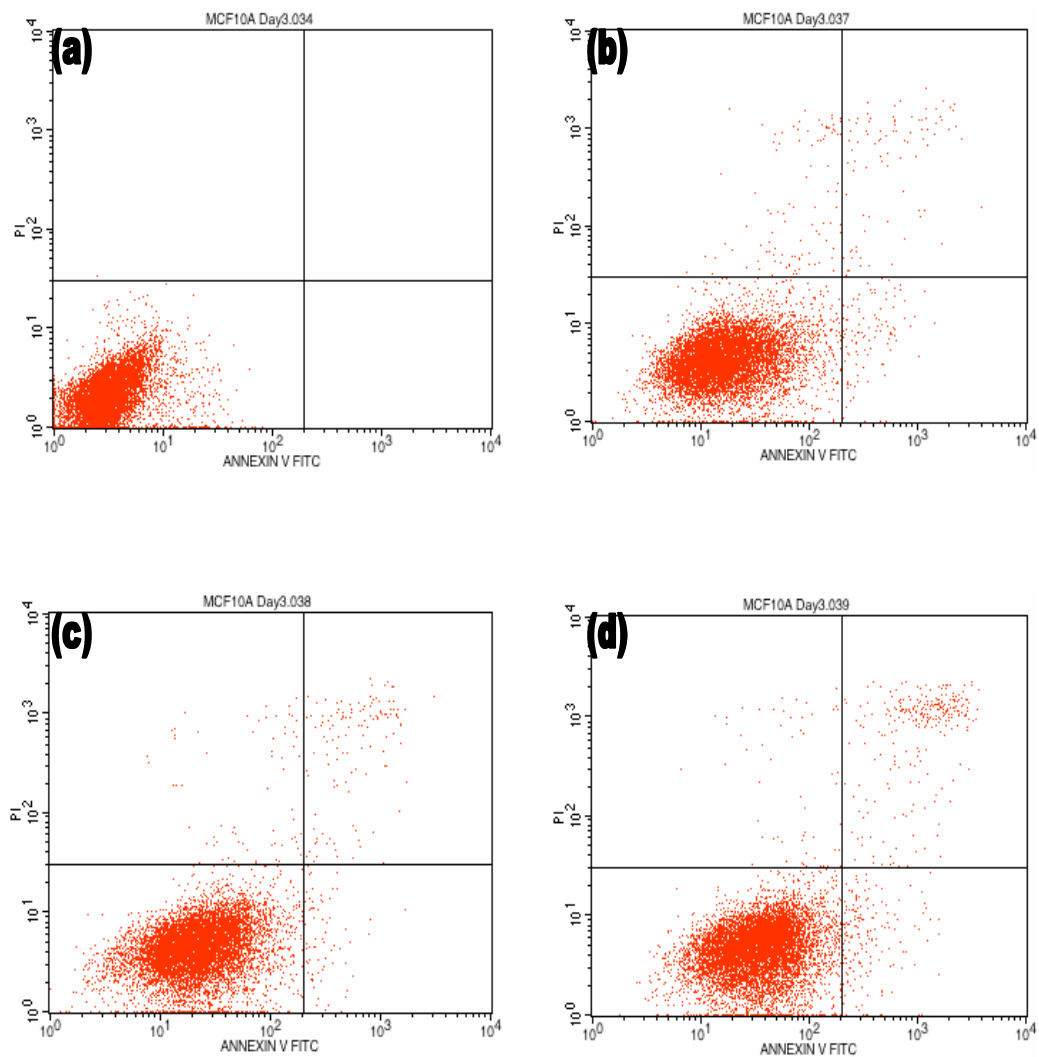


Figure 4.1.3 Flow cytometric analysis of annexin V-FITC/PI double-staining: MCF10A cells were left untreated or treated for 72 hours with (a) $3\mu\text{M}$ (b) $17\mu\text{M}$ or (c) $25\mu\text{M}$ of $[\text{Co}(\text{phen})(\text{ma})\text{Cl}]$. Cells were incubated with Annexin V-FITC in a buffer containing PI and analyzed by flow cytometry. The y axis denotes cells stained with PI and the x axis represents cells stained in Annexin V-FITC.

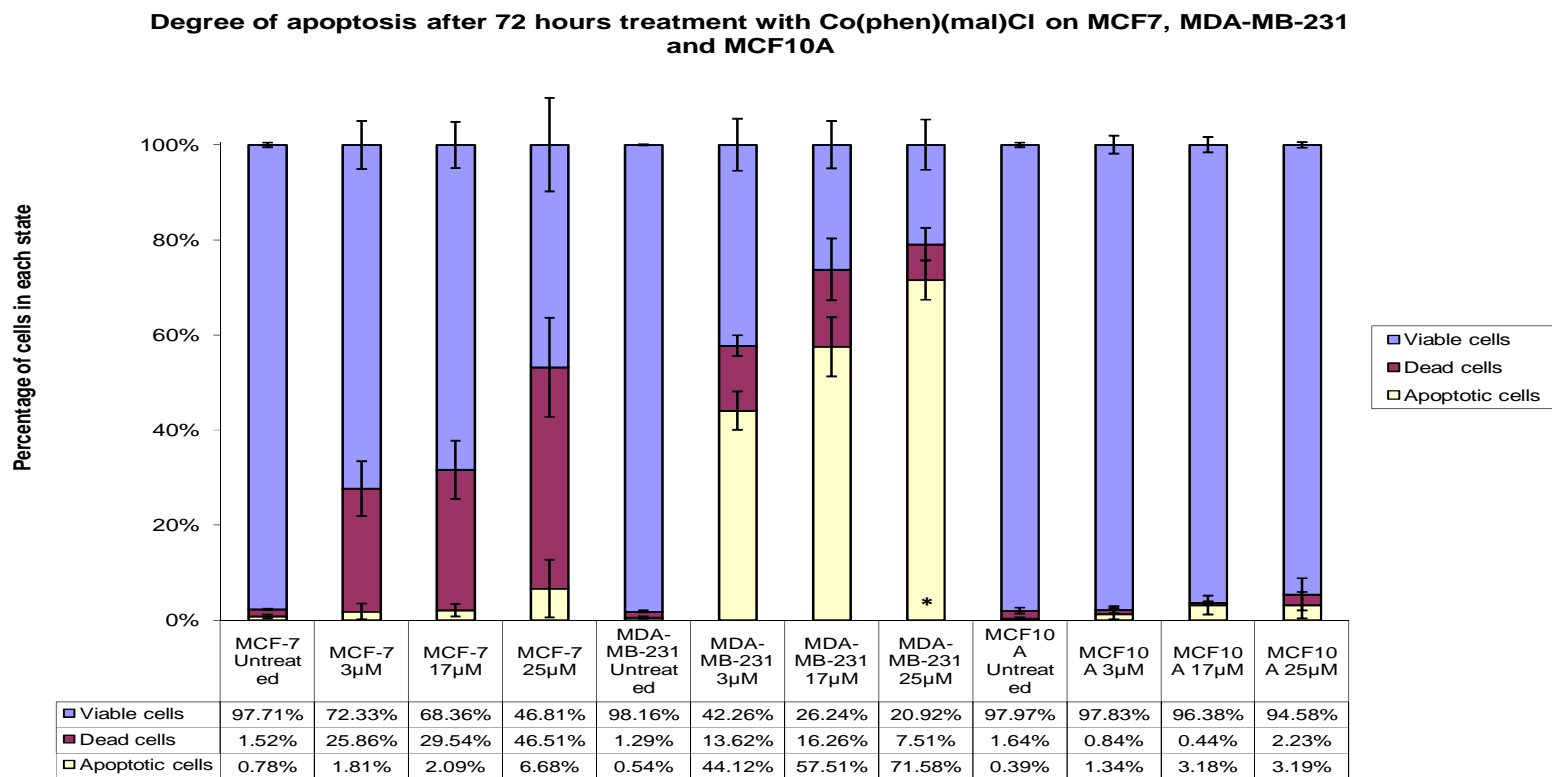


Figure 4.1.4 Percentage of apoptotic, dead and viable cells of MCF-7, MDA-MB-231 and MCF10A after treated with increasing concentrations of [Co(phen)(ma)Cl] for 72 hours. * $P < 0.05$

MCF-7	Untreated	3 μ M	17 μ M	25 μ M
	^a Percentage of cells (%)			
Viable cells	97.71 \pm 0.47	72.33 \pm 5.04	68.36 \pm 4.84	46.81 \pm 9.85
Dead cells	1.52 \pm 0.16	25.86 \pm 5.79	29.54 \pm 6.13	46.51 \pm 10.39
Apoptotic cells	0.78 \pm 0.35	1.81 \pm 1.65	2.09 \pm 1.31	6.68 \pm 6.06

Table 4.1.1 Percentage of apoptotic, dead and viable cells of MCF-7 after treated with increasing concentrations of [Co(phen)(ma)Cl] for 72 hours.

MDA-MB-231	Untreated	3 μ M	17 μ M	25 μ M
	^a Percentage of cells (%)			
Viable cells	98.16 \pm 0.10	42.26 \pm 5.48	26.24 \pm 5.01	20.92 \pm 5.27
Dead cells	1.29 \pm 0.19	13.62 \pm 2.19	16.26 \pm 6.49	7.51 \pm 3.47
Apoptotic cells	0.54 \pm 0.25	44.12 \pm 4.02	57.51 \pm 6.19	71.58 \pm 4.16

Table 4.1.2 Percentage of apoptotic, dead and viable cells of MDA-MB-231 after treated with increasing concentrations of [Co(phen)(ma)Cl] for 72 hours.

MCF10A	Untreated	3 μ M	17 μ M	25 μ M
	^a Percentage of cells (%)			
Viable cells	97.97 \pm 0.47	97.83 \pm 1.91	96.38 \pm 1.61	94.58 \pm 0.61
Dead cells	1.64 \pm 0.63	0.84 \pm 0.76	0.44 \pm 0.38	2.23 \pm 3.37
Apoptotic cells	0.39 \pm 0.16	1.34 \pm 1.16	3.18 \pm 1.99	3.19 \pm 2.76

Table 4.1.3 Percentage of apoptotic, dead and viable cells of MCF10A after treated with increasing concentrations of [Co(phen)(ma)Cl] for 72 hours.

^a Percentage of apoptotic, dead and viable cells is obtained from mean \pm standard deviation values of three independent experiments.

4.2.2 Cell cycle analysis

MCF-7, MDA-MB-231 and MCF10A cells were first serum starved to synchronize the cells to be in the same phase of the cell cycle. Then the cells were either left untreated or treated for 72 hours with 3 μ M, 17 μ M and 25 μ M of [Co(phen)(ma)Cl]. Cells were then incubated in a lysis buffer containing PI, strained to remove clumps and analyzed by flow cytometry. The DNA content of cells duplicates during the S phase of the cell cycle so the relative amount of cells in the G₀ phase and G₁ phase, in the S phase, and in the G₂ phase and M phase can be determined, as the fluorescence of cells in the G₂/M phase will be twice as high as that of cells in the G₀/G₁ phase. The M1 bar showed the area where cells were in G₀/G₁ phase and M2 bar covered the area where cells were in G₂/M phase (Figure 4.2.1, Figure 4.2.2 and Figure 4.2.3). The area in between M1 and M2 is the area where cells in S phase.

Untreated MCF-7 cells showed a low peak at G₂/M phase almost same height as S phase (Figure 4.2.1a). When treated with 3 μ M of [Co(phen)(ma)Cl] the G₂/M phase peak raised and became more apparent and the percentage of cells in G₂/M phase raised from untreated at 0.65% to 5.95% (Figure 4.2.1b). The G₂/M phase peak continued to rise when the concentration of [Co(phen)(ma)Cl] increased to 17 μ M with the percentage of cells at this phase increased to 7.87% (Figure 4.2.1c). The increment percentage of cells in G₂/M phase continued up to 9.01% when the concentration of [Co(phen)(ma)Cl] increased to 25 μ M. The G₂/M phase

peak at 25 μ M concentration of [Co(phen)(ma)Cl] was relatively higher than those at lower concentration and untreated (Figure 4.2.1d).

The trend for MBA-MB-231 cell line was quite different from MCF-7 cell line. Untreated MBA-MB-231 has a clear peak at G2/M phase at 6.64% (Figure 4.2.2a). When treated with 3 μ M of [Co(phen)(ma)Cl] the peak of G2/M phase decreased to 5.40% and cells starting to accumulate at G0/G1 phase (Figure 4.2.2b). At 17 μ M more cells were accumulated at G0/G1 phase at 78.12% compared to 3 μ M at 42.71% (Figure 4.2.2c). The percentage of cells continued to increase in G0/G1 phase for 25 μ M at 85.29% (Figure 4.2.2d).

[Co(phen)(ma)Cl] does not seem to affect the cell cycle process of MCF10A cell line. The percentage of untreated cells at G0/G1 phase was 54.67% (Figure 4.2.3a). Then the figure drop slightly to 51.96% when treated with 3 μ M of [Co(phen)(ma)Cl] (Figure 4.2.3b). However the percentage of cells in G0/G1 phase with 17 μ M of [Co(phen)(ma)Cl] increased to 56.46% (Figure 4.2.3c) then dropped slightly to 56.38% when the concentration of [Co(phen)(ma)Cl] increased to 25 μ M (Figure 4.2.3d). The cells in S and G2/M phase also the same going through slight increase and decrease without a clear pattern when treated with increasing concentrations of [Co(phen)(ma)Cl].

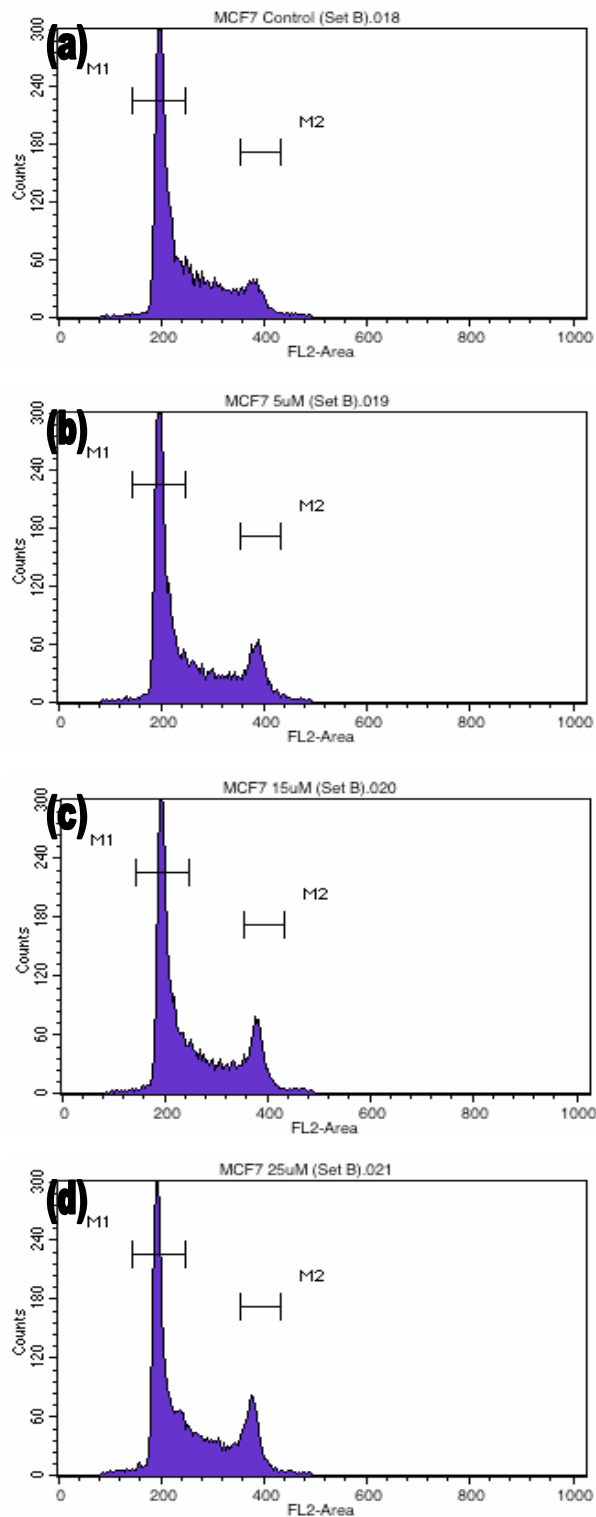


Figure 4.2.1 Cell cycle analysis of MCF-7 after treated with increasing concentrations of [Co(phen)(ma)Cl] for 72 hours detected using flow cytometry with PI staining. The y axis denotes cell count and the x axis represents DNA content.

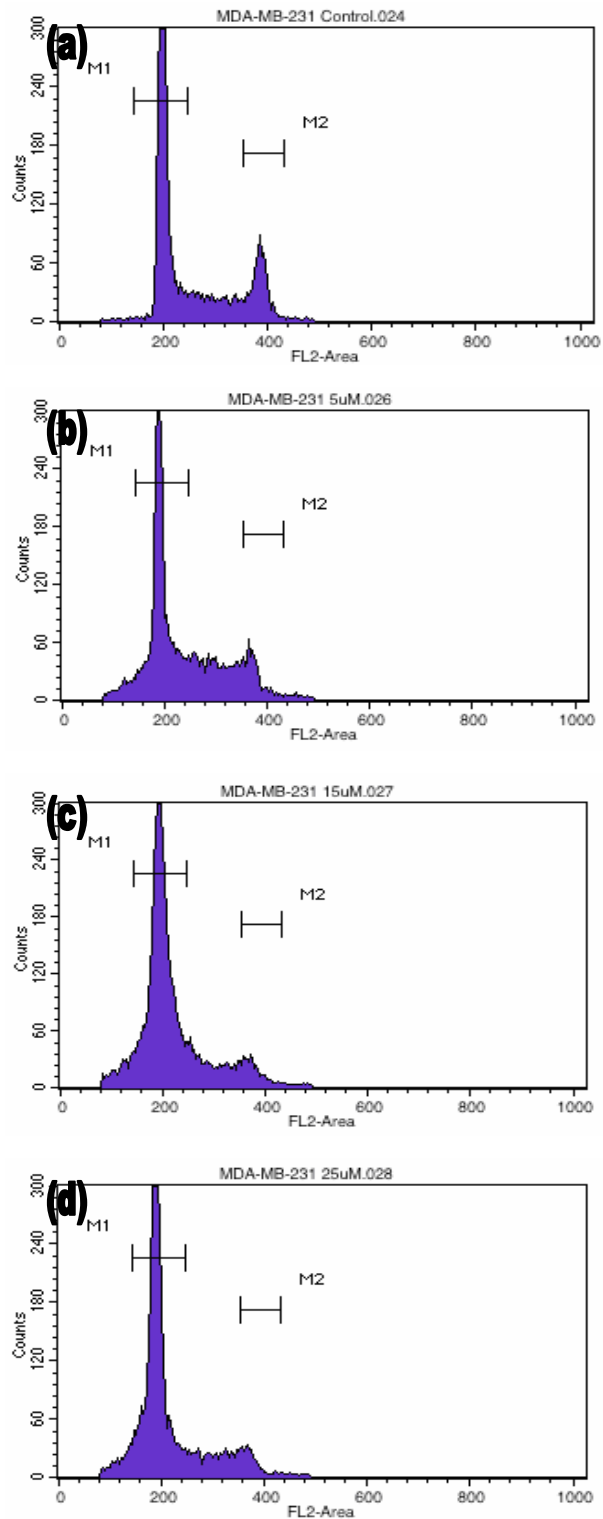


Figure 4.2.2 Changes in DNA content of MDA-MB-231 after treated with increasing concentrations of [Co(phen)(ma)Cl] for 72 hours detected using flow cytometry with PI staining. The y axis denotes cell count and the x axis represents DNA content.

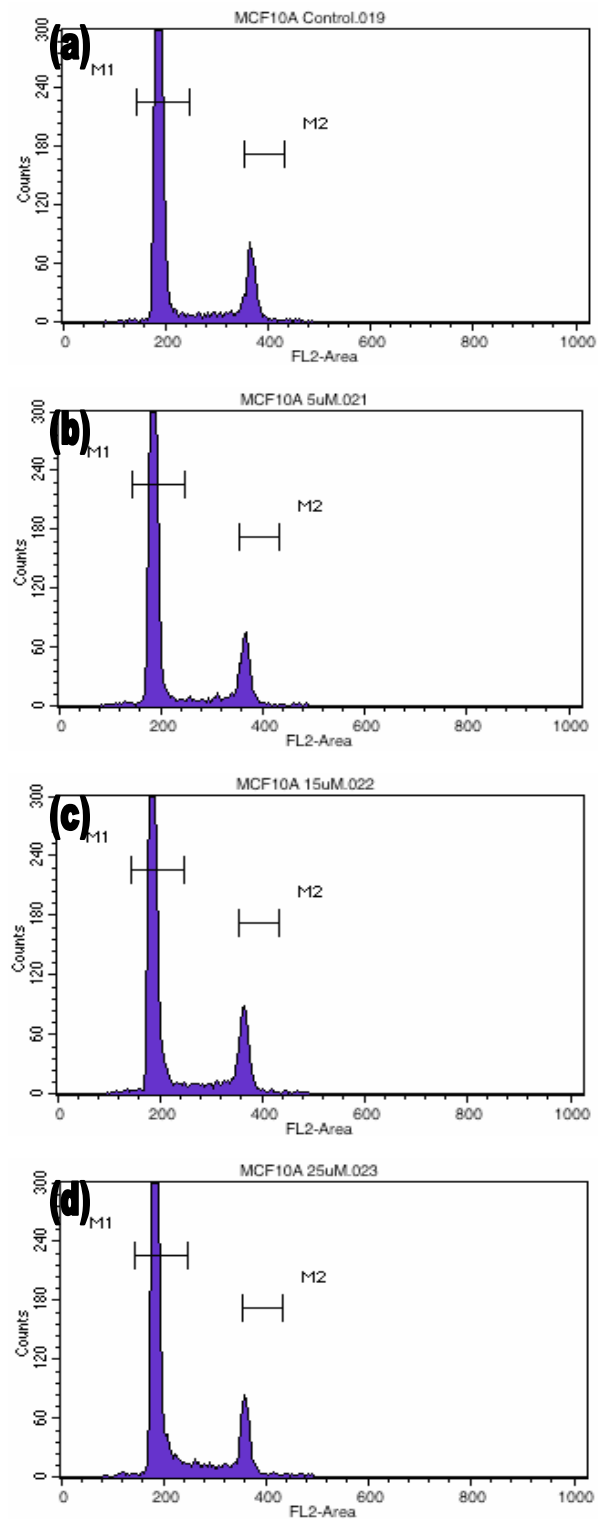


Figure 4.2.3 Changes in DNA content of MCF10A after treated with increasing concentrations of $[\text{Co}(\text{phen})(\text{ma})\text{Cl}]$ for 72 hours detected using flow cytometry with PI staining. The y axis denotes cell count and the x axis represents DNA content.

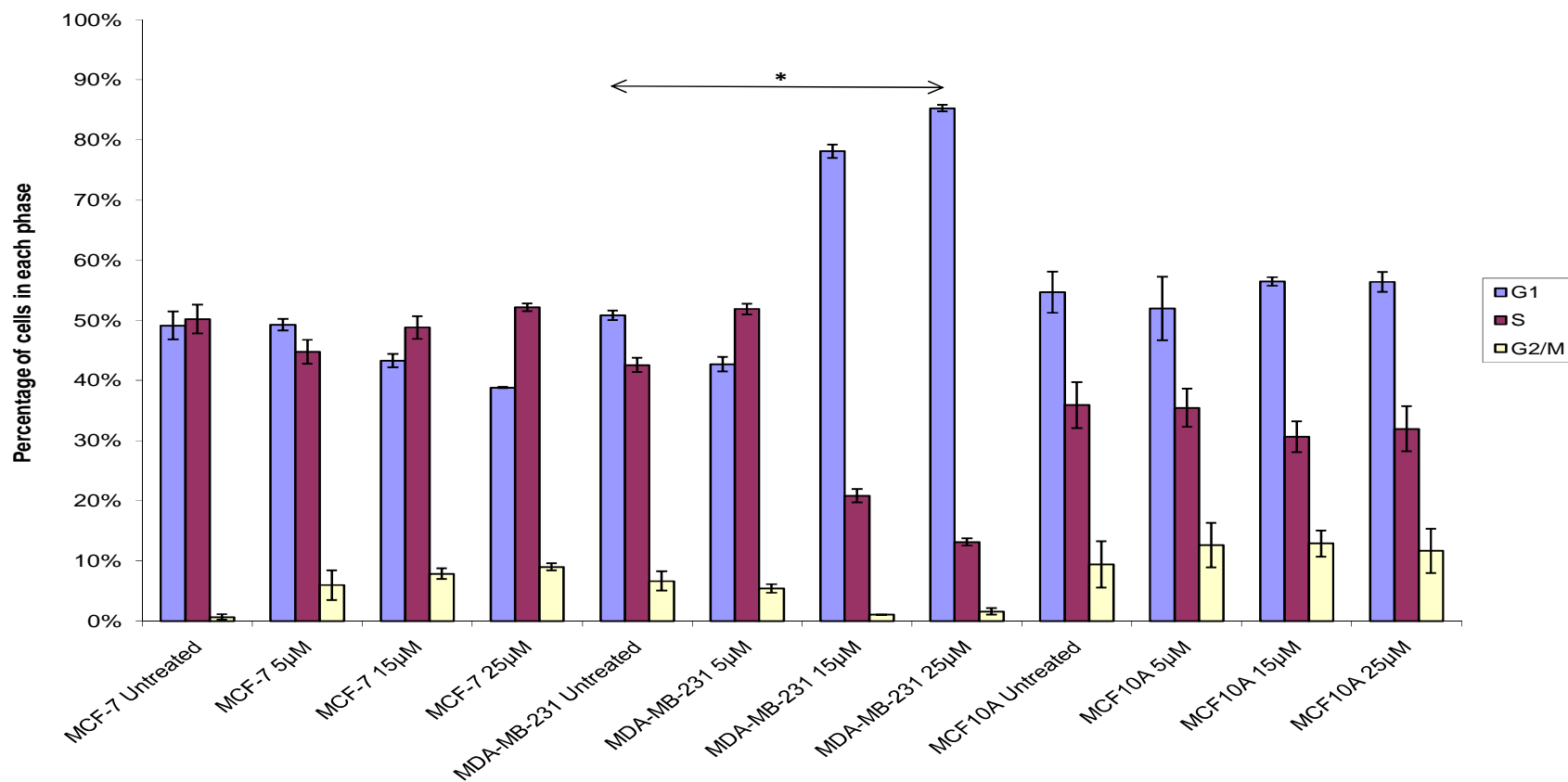


Figure 4.2.4 Percentage of MCF-7, MDA-MB-231 and MCF10A cells in G0/G1, S and G2/M phases after treated with increasing concentrations of [Co(phen)(ma)Cl] for 72 hours. * $P < 0.01$

MCF-7	Untreated	3 μ M	17 μ M	25 μ M
	^a Percentage of cells (%)			
G0/G1	49.13 \pm 2.32	49.28 \pm 0.96	43.31 \pm 1.12	38.79 \pm 0.12
G2/M	0.65 \pm 0.47	5.95 \pm 2.43	7.87 \pm 0.88	9.01 \pm 0.63
S	50.22 \pm 2.38	44.77 \pm 2.02	48.82 \pm 1.89	52.19 \pm 0.63

Table 4.2.1 Percentage of MCF-7 cells in G0/G1, S and G2/M phases after treated with increasing concentrations of [Co(phen)(ma)Cl] for 72 hours.

MDA-MB-231	Untreated	3 μ M	17 μ M	25 μ M
	^a Percentage of cells (%)			
G0/G1	50.80 \pm 0.79	42.71 \pm 1.22	78.12 \pm 1.11	85.29 \pm 0.51
G2/M	6.64 \pm 1.61	5.40 \pm 0.73	1.04 \pm 0.06	1.59 \pm 0.54
S	42.56 \pm 1.18	51.89 \pm 0.89	20.85 \pm 1.14	13.13 \pm 0.61

Table 4.2.2 Percentage of MDA-MB-231 cells in G0/G1, S and G2/M phases after treated with increasing concentrations of [Co(phen)(ma)Cl] for 72 hours.

MCF10A	Untreated	3 μ M	17 μ M	25 μ M
	^a Percentage of cells (%)			
G0/G1	54.67 \pm 3.43	51.96 \pm 5.25	56.46 \pm 0.70	56.38 \pm 1.64
G2/M	9.44 \pm 3.86	12.60 \pm 3.70	12.88 \pm 2.19	11.67 \pm 3.67
S	35.90 \pm 3.83	35.44 \pm 3.17	30.67 \pm 2.58	31.95 \pm 3.75

Table 4.2.3 Percentage of MCF10A cells in G0/G1, S and G2/M phases after treated with increasing concentrations of [Co(phen)(ma)Cl] for 72 hours.

^a Percentage of cells in G0/G1, S, G2/M phases is obtained from mean \pm standard deviation values of three independent experiments. The percentage of cells in the G0/G1, S, and G2/M phases of the cell cycle were calculated by using ModFit software.

4.2.3 Proteasome inhibition assay

MCF-7, MDA-MB-231 and MCF10A cells were treated with 3 μ M, 17 μ M and 25 μ M of [Co(phen)(ma)Cl] for 72 hours and compared with the untreated cells. Epoxomicin was used as positive control at the concentration of 5nM. After treatment period Proteasome-Glo™ Cell-Based Assays was added and incubated with the cells and medium before being analyzed using luminescence multiplate reader. The amount of luminescence emitted was directly proportional to the proteasome activity of the cells. Considering untreated cells were at the optimum level of proteasome activity the luminescence value of untreated cells were set at 100%. The luminescence values of treated cells were compared against untreated cells to obtain a relative percentage value of cell proteasome activity.

When MCF-7 was treated with 3 μ M, 17 μ M and 25 μ M of [Co(phen)(ma)Cl] the percentage of trypsin-like proteasome activity showed only minute changes with 98.62% at 3 μ M, 95.14% at 17 μ M and 92.98% at 25 μ M (Figure 4.3.1). The similar trend was observed on MCF10A cell lines too. At 3 μ M of [Co(phen)(ma)Cl] the trypsin-like proteasome activity of MCF10A was at 98.19%. Then the figure dropped to 96.83% and further down to 92.21% when the concentration of [Co(phen)(ma)Cl] increased to 17 μ M and 25 μ M respectively. The effect of [Co(phen)(ma)Cl] the trypsin-like proteasome activity of MDA-MB-231 was more apparent. The percentage of trypsin-like proteasome activity of MDA-MB-231 plummeted to 64.57% after treated with 3 μ M of [Co(phen)(ma)Cl]. The value continue to decrease to 59.89% and 52.28% when

the concentration of [Co(phen)(ma)Cl] was increased to 17 μ M and 25 μ M respectively.

The chemotrypsin-like proteasome activity of MDA-MB-231 cell line drop 66.94% when treated with 3 μ M of [Co(phen)(ma)Cl] (Figure 4.3.2). The percentage of chemotrypsin-like activity of MDA-MB-231 cells dropped further to 56.07% and 47.25% when the concentration of [Co(phen)(ma)Cl] increased to 17 μ M and 25 μ M respectively. No apparent changes of chemotrypsin-like proteasome activity of MCF-7 and MCF10A were observed when treated with [Co(phen)(ma)Cl]. For MCF-7 the percentage chemotrypsin-like proteasome activity was 99.47% at 3 μ M, 94.60% at 17 μ M and 89.67% at 25 μ M. The percentage chemotrypsin-like proteasome activity of MCF10A were at 96.88%, 94.78% and 92.96% when treated with 3 μ M, 17 μ M and 25 μ M of [Co(phen)(ma)Cl] respectively.

[Co(phen)(ma)Cl] showed to have limited effects on MCF-7 caspase-like proteasomal activity (Figure 4.3.3). When treated with 3 μ M of [Co(phen)(ma)Cl] the percentage of caspase-like proteasomal activity dropped to 95.53%. When the concentration of [Co(phen)(ma)Cl] increases the percentage of caspase-like proteasomal activity stayed almost the same with 92.95% at 17 μ M and 90.29% at 25 μ M. The same trend was observed on MCF10A cell line At 3 μ M of [Co(phen)(ma)Cl] the percentage of caspase-like proteasomal activity for MCF10A cells was 97.83%. Then it dropped to 93.04% when the concentration of

[Co(phen)(ma)Cl] increased to 17 μ M further decrease to 91.47% when it increased to 25 μ M. The caspase-like proteasomal activity for MDA-MB-231 cells showed bigger decline when treated with [Co(phen)(ma)Cl]. At 3 μ M the caspase-like proteasomal activity was at 72.28%. The value dropped to 57.83% when the concentration increased to 17 μ M. The number dropped further to 47.25% at 25 μ M.

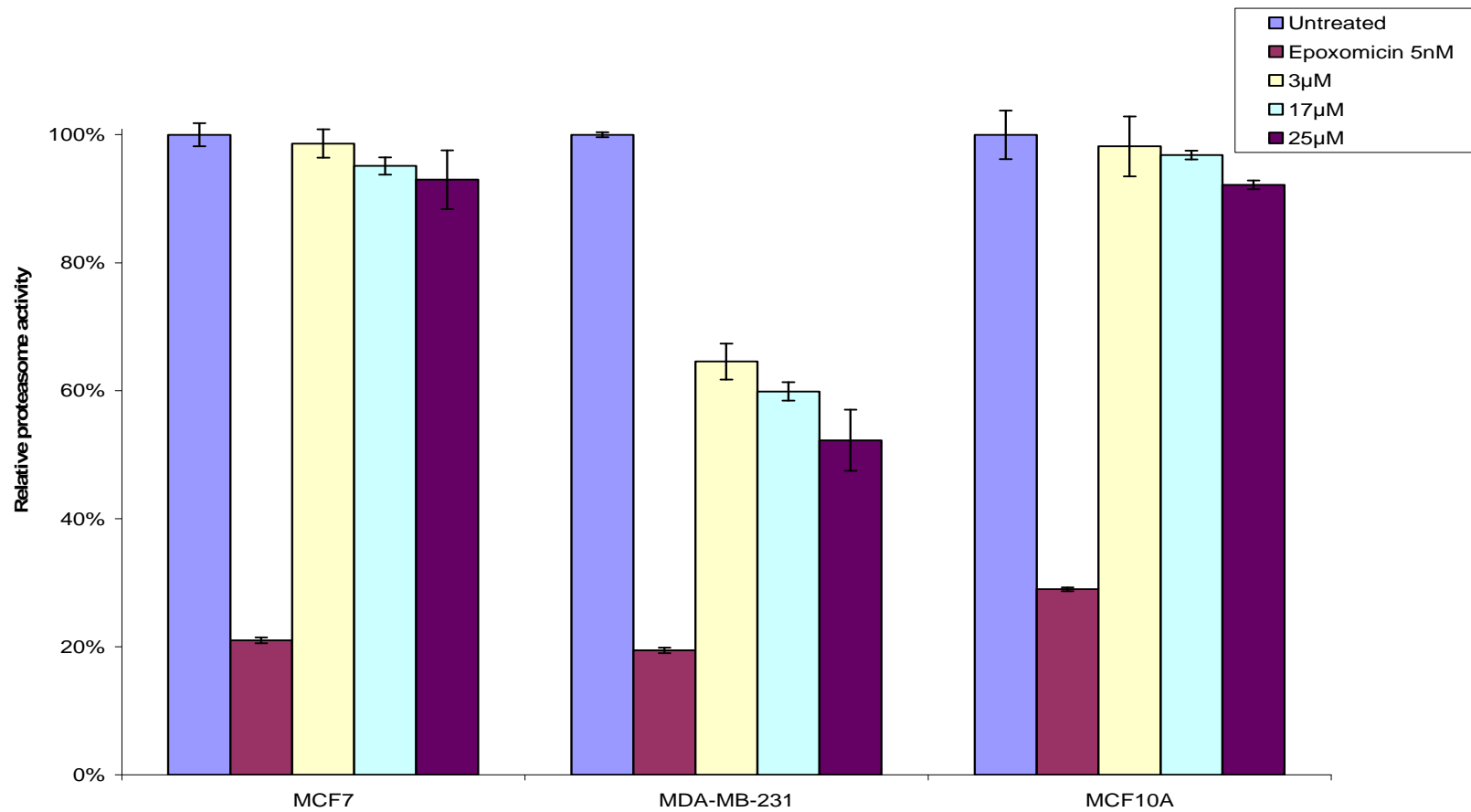


Figure 4.3.1 Percentage of trypsin-like proteasome activity of MCF-7, MDA-MB-231 and MCF10A cells after treated with increasing concentrations of [Co(phen)(ma)Cl] for 72 hours.

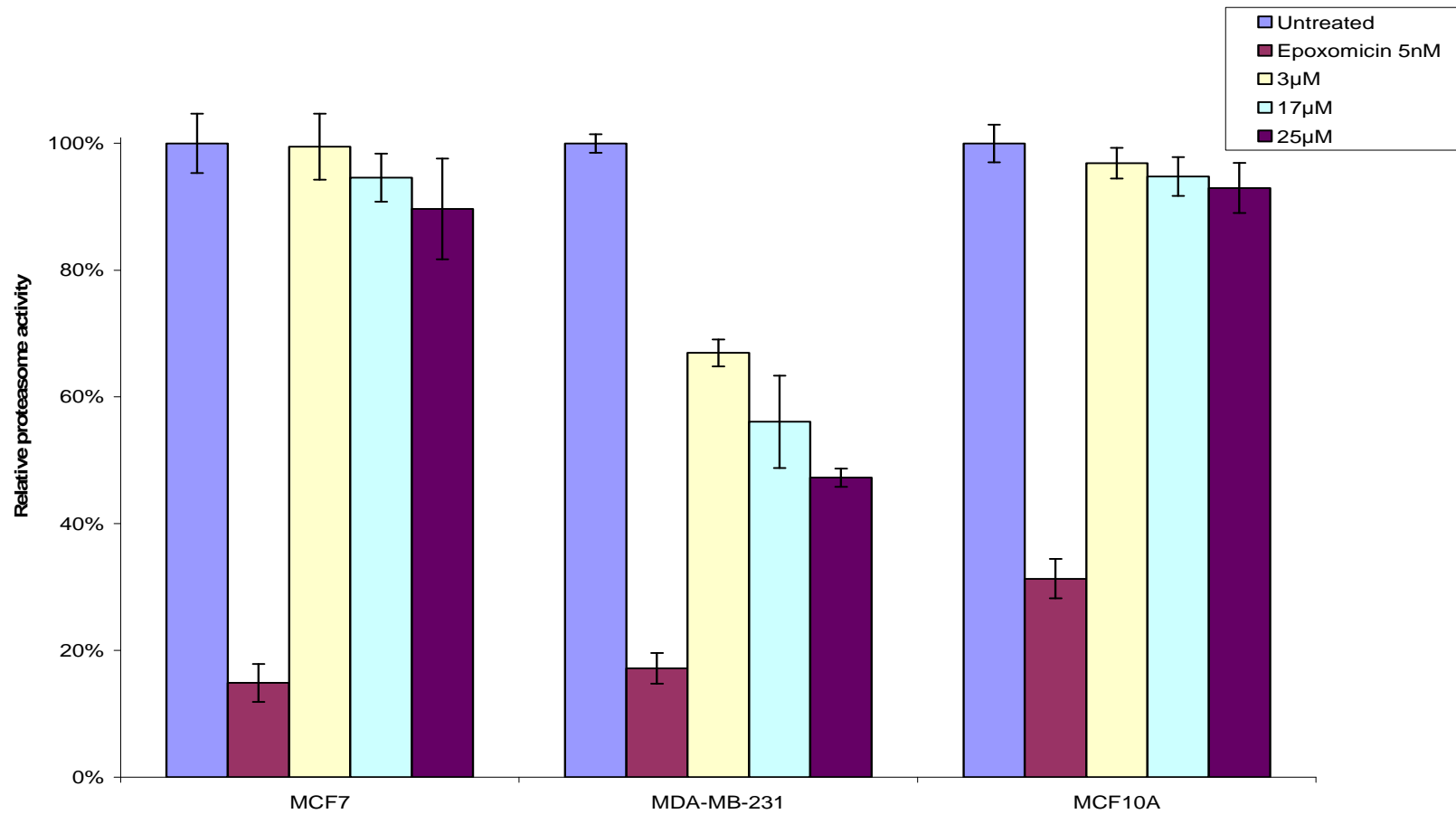


Figure 4.3.2 Percentage of chemotrypsin-like proteasome activity of MCF-7, MDA-MB-231 and MCF10A cells after treated with increasing concentrations of [Co(phen)(ma)Cl] for 72 hours.

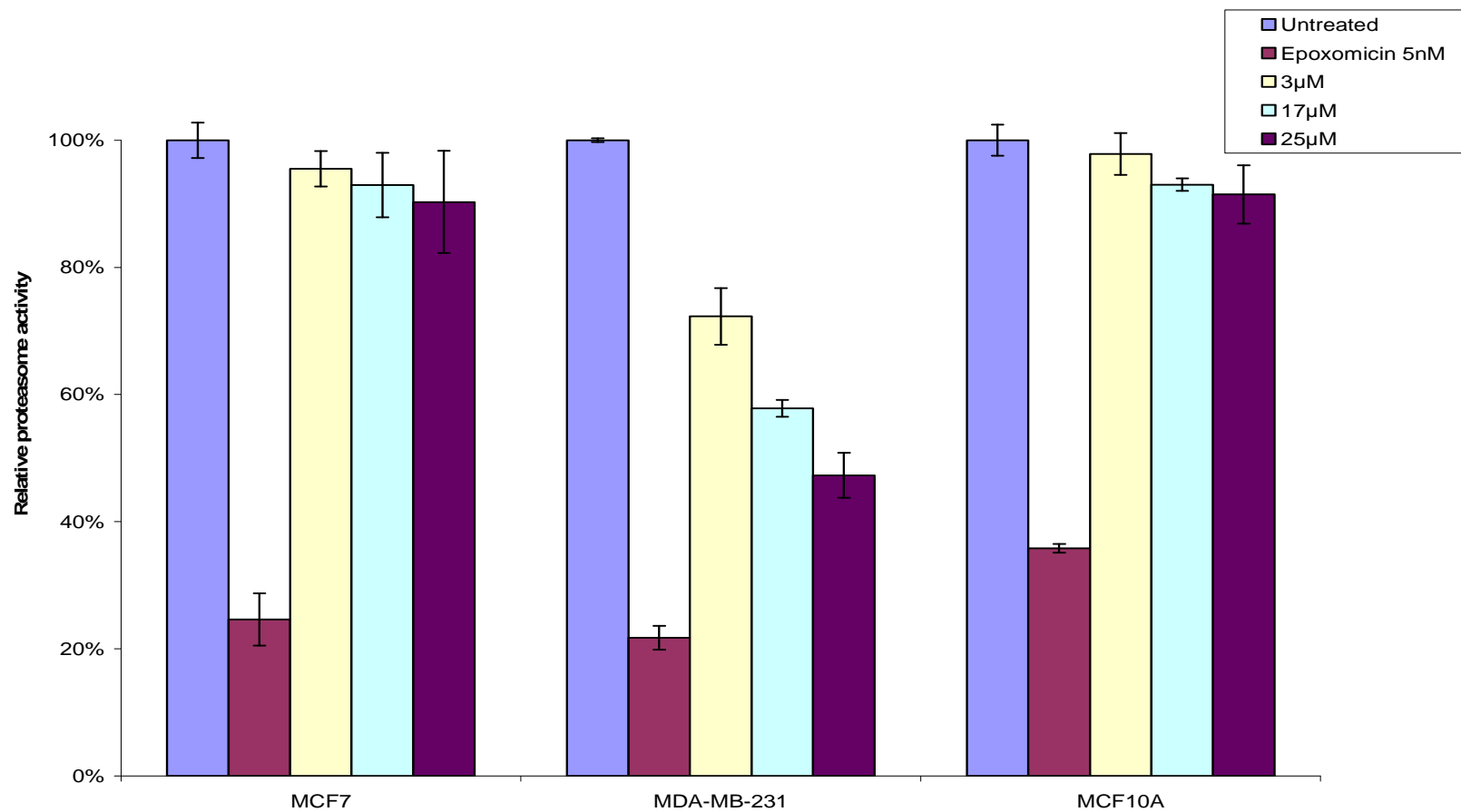


Figure 4.3.3 Percentage of caspase-like proteasome activity of MCF-7, MDA-MB-231 and MCF10A cells after treated with increasing concentrations of [Co(phen)(ma)Cl] for 72 hours.

Trypsin-like	MCF-7	MDA-MB-231	MCF10A
	^a Percentage of cells (%)	^a Percentage of cells (%)	^a Percentage of cells (%)
Untreated	100.00 ± 1.80	100.00 ± 0.38	100.00 ± 3.79
Epoxomicin 5nM	20.99 ± 0.47	19.43 ± 0.45	28.98 ± 0.29
3µM	98.62 ± 2.21	64.57 ± 2.83	98.19 ± 4.69
17µM	95.14 ± 1.36	59.89 ± 1.42	96.83 ± 0.68
25µM	92.98 ± 4.57	52.28 ± 4.76	92.21 ± 0.68

Table 4.3.1 Percentage of trypsin-like proteasome activity of MCF-7, MDA-MB-231 and MCF10A cells after treated with increasing concentrations of [Co(phen)(ma)Cl] for 72 hours.

Chemotrypsin-like	MCF-7	MDA-MB-231	MCF10A
	^a Percentage of cells (%)	^a Percentage of cells (%)	^a Percentage of cells (%)
Untreated	100.00 ± 4.67	100.00 ± 1.47	100.00 ± 2.96
Epoxomicin 5nM	14.87 ± 2.99	17.16 ± 2.44	31.31 ± 3.09
3µM	99.47 ± 5.20	66.94 ± 2.12	96.88 ± 2.42
17µM	94.60 ± 3.77	56.07 ± 7.28	94.78 ± 3.05
25µM	89.67 ± 7.97	47.25 ± 1.42	92.96 ± 3.96

Table 4.3.2 Percentage of chemotrypsin-like proteasome activity of MCF-7, MDA-MB-231 and MCF10A cells after treated with increasing concentrations of [Co(phen)(ma)Cl] for 72 hours.

Caspase-like	MCF-7	MDA-MB-231	MCF10A
	^a Percentage of cells (%)	^a Percentage of cells (%)	^a Percentage of cells (%)
Untreated	100.00 ± 2.78	100.00 ± 1.30	100.00 ± 2.45
Epoxomicin 5nM	24.60 ± 4.11	21.74 ± 1.89	35.80 ± 0.66
3μM	95.53 ± 2.78	72.28 ± 4.45	97.83 ± 3.27
17μM	92.95 ± 5.07	57.83 ± 1.32	93.04 ± 0.98
25μM	90.29 ± 8.03	47.28 ± 3.53	91.47 ± 4.58

Table 4.3.3 Percentage of caspase-like proteasome activity of MCF-7, MDA-MB-231 and MCF10A cells after treated with increasing concentrations of [Co(phen)(ma)Cl] for 72 hours.

^a Percentage of proteasomal activity is obtained from mean ± standard deviation values of three independent experiments.

4.2.4 Measurement of Reactive Oxygen Species (ROS)

MCF-7, MDA-MB-231 and MCF10A cells were treated with 3 μ M, 17 μ M and 25 μ M of [Co(phen)(ma)Cl] for 72 hours and compared with the untreated cells. Treatment with 1 μ M hydrogen peroxide served as positive control in this study. The fluorescence intensity was measured using microarray plate reader and the results were presented in relative difference between the fluorescence intensity percentage of DCF of cells incubated with [Co(phen)(ma)Cl] and untreated cells.

At 3 μ M of [Co(phen)(ma)Cl] on MCF-7 showed 5.97% minimal increase of intracellular ROS. The level of intracellular ROS level of MCF-7 increased to 8.58% and 10.93% when the concentration of [Co(phen)(ma)Cl] was increased to 17 μ M and 25 μ M respectively. The increase of intracellular ROS level of MCF-7 for positive control was marked at 89.27%.

Similar trend was observed on MCF10A cell line after treatment of [Co(phen)(ma)Cl]. Three micro molar of [Co(phen)(ma)Cl] on MCF10A only showed an increase of 2.02% of intracellular ROS level. The value increased to 4.49% at 17 μ M and raise to 8.54% at 25 μ M. The value of positive control was marked at 76.30%.

The treatment of [Co(phen)(ma)Cl] MDA-MB-231 had relatively more effect on the level of intracellular ROS level. The level of intracellular ROS level of MDA-MB-231 increased from 33.30% at 3 μ M to 68.39% at 17 μ M and

increased to 79.03% at 25 μ M. Treatment of 1 μ M hydrogen peroxide surged the level of intracellular ROS level of MDA-MB-231 to 82.98%.

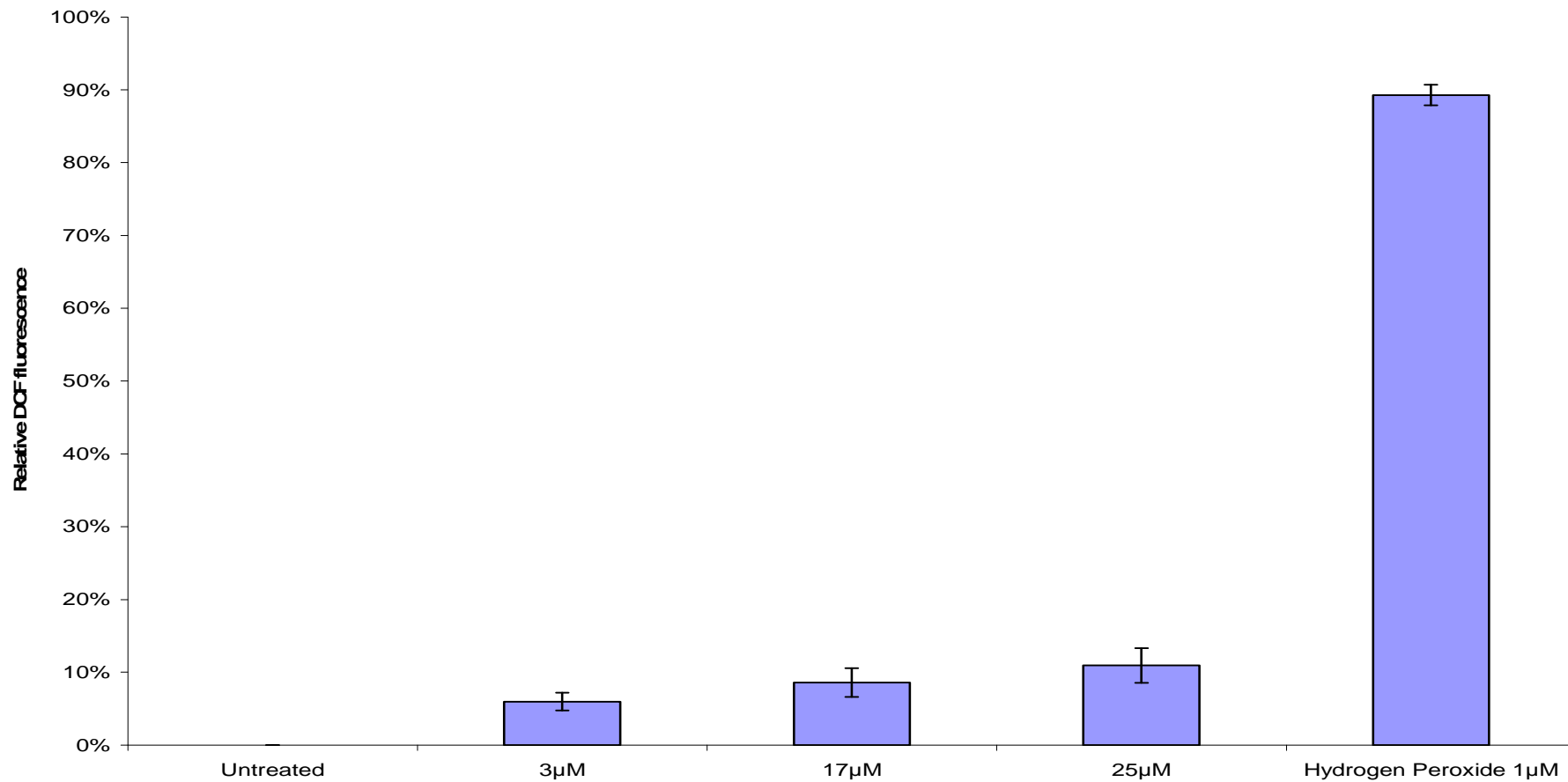


Figure 4.4.1 Relative DCF fluorescence percentage of MCF-7 cells after treated with increasing concentrations of [Co(phen)(ma)Cl] for 72 hours.

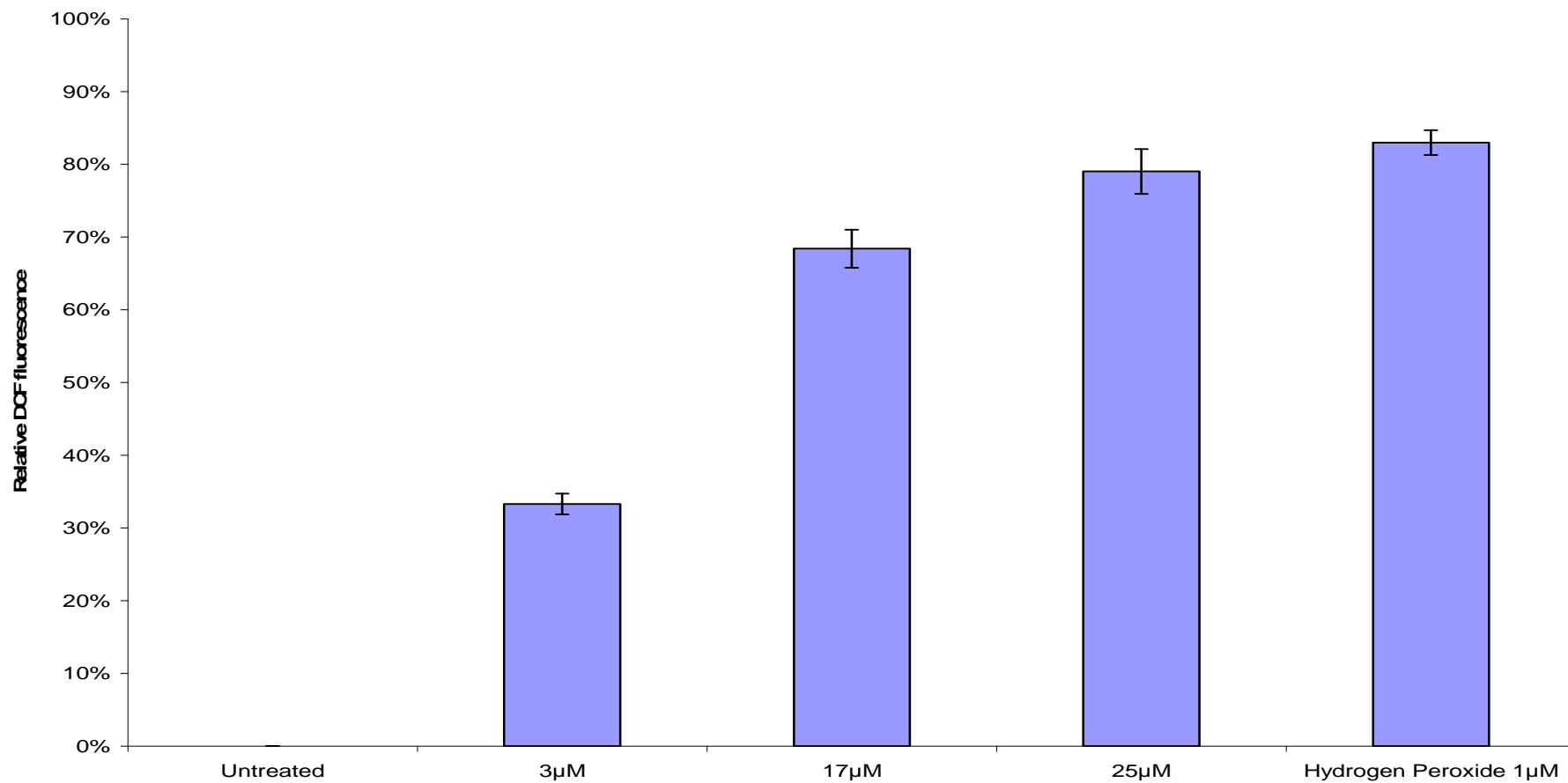


Figure 4.4.2 Relative DCF fluorescence percentage of MDA-MB-231 cells after treated with increasing concentrations of [Co(phen)(ma)Cl] for 72 hours.

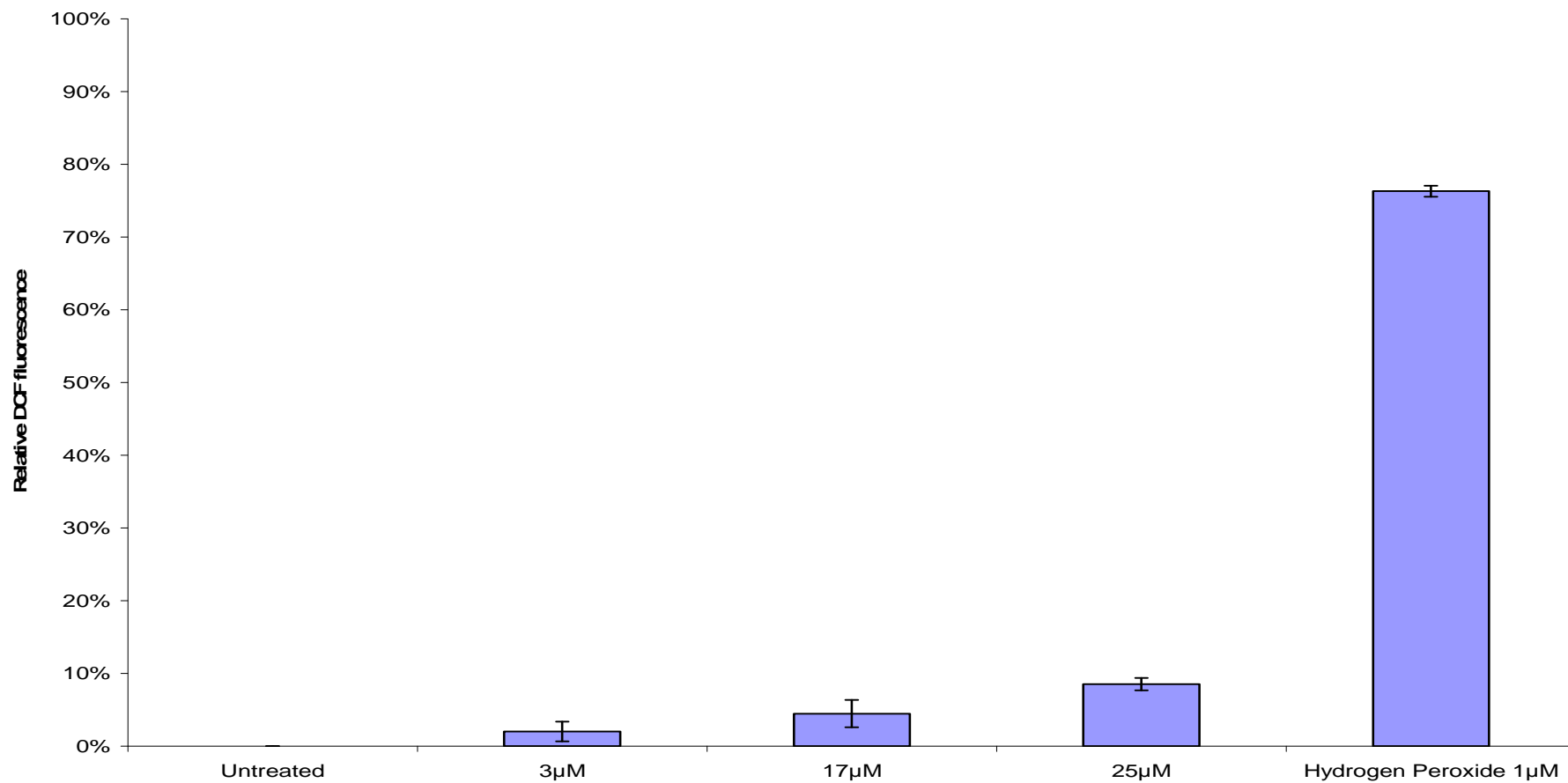


Figure 4.4.3 Relative DCF fluorescence percentage of MCF10A cells after treated with increasing concentrations of [Co(phen)(ma)Cl] for 72 hours.

Treatment \ Cell line	MCF-7	MDA-MB-231	MCF10A
	^a Relative DCF fluorescence (%)	^a Relative DCF fluorescence (%)	^a Relative DCF fluorescence (%)
Untreated	0.00 ± 0.80%	0.00 ± 0.12%	0.00 ± 1.35%
3µM	5.97 ± 1.21%	33.30 ± 1.43%	2.02 ± 1.36%
17µM	8.58 ± 1.97%	68.39 ± 2.61%	5.49 ± 1.87%
25µM	10.93 ± 2.38%	79.03 ± 3.08%	8.54 ± 0.87%
Hydrogen Peroxide 1µM	89.27 ± 1.40%	82.98 ± 1.69%	76.30 ± 0.74%

Table 4.4.1 Relative DCF fluorescence percentage of MCF-7, MDA-MB-231 and MCF10A cells after treated with increasing concentrations of [Co(phen)(ma)Cl] for 72 hours.

^a Relative DCF fluorescence percentage is obtained from mean ± standard deviation values of three independent experiments.

4.3 Discussion

The combination of annexin V-FITC and propidium iodide dye is a reliable and convenient method for quantitative apoptosis flow cytometry analysis (Kerr et. al., 1998). The test described, discriminates intact cells or healthy cells (FITC-/PI-), cells in early apoptosis (FITC+/PI-) cells in late apoptosis (FITC+/PI+) and dead cells (FITC-/PI+) (Chen et. al., 2008). The morphological studies that were discussed earlier were not substantial enough to draw a definitive conclusion. That was why annexin V-FITC/PI test were done. The results obtained from this test were corresponding to the preliminary speculation drawn from the morphological study. The amount of apoptotic cells induced by [Co(phen)(ma)Cl] on MDA-MB-231 cell line was increasing over the concentration (Figure 4.1.4). So [Co(phen)(ma)Cl] induced apoptosis on MDA-MB-231 in a dose dependent manner. The difference of the percentage of apoptotic cells between MDA-MB-231 and MCF10A was significant with $P < 0.05$. Even though the percentage of apoptotic cells of MCF-7 increased with the concentration of [Co(phen)(ma)Cl] there were substantially more dead cells compared to apoptotic cells (Figure 4.1.4). The outcome here is consistent the pictures taken in morphological study (Figure 3.2.2 b and Figure 3.2.2c).

By just looking at flow cytometry test alone it showed that [Co(phen)(ma)Cl] mostly induce death on MCF-7 cells through necrosis process. However when compared back with the photos in morphological study the cells did not show signs of necrosis (Figure 3.2.2 b and Figure 3.2.2c). The movement of the cells from Annexin V-FITC and PI negative (viable, or no measurable apoptosis),

to Annexin V-FITC positive and PI negative (early apoptosis, membrane integrity is present), Annexin V-FITC and PI positive (end stage apoptosis) and to Annexin V-FITC negative and PI positive (dead and or necrosis) suggest apoptosis (Koopman 1994). In contrast, a single observation indicating that cells are both Annexin V-FITC and PI positive, in of itself, reveals less information about the process by which the cells underwent their demise (Koopman 1994). The recommended action would be studying the compound with varying time durations and concentrations however this was not practical due to budget constrain. One of the plausible explanation would be the concentrations of the treatment used were too high for MCF-7 cell line.

The annexin V-FITC/PI test showed that [Co(phen)(ma)Cl] had limited effect towards MCF10A cell line. Even though the percentage of apoptotic and dead cells increased when the concentration of [Co(phen)(ma)Cl] increase but the figure were minute compared to the percentage of viable cells recorded (Figure 4.1.4). If the results of IC-50 value (Figure 3.1.8) and morphological study (Figure 3.2.2h and Figure 3.2.2i) were taken into account another conclusion can be drawn here. The IC-50 value of MCF10A after treated for 72 hours with [Co(phen)(ma)Cl] was 16.9 μ M which meant only 50% of the cells were viable at 16.9 μ M. However, even at 25 μ M the flow cytometry test showed that there were 94.58% of viable cells left (Table 4.1.3). The results may seem inconsistent with each other however the result of both test cannot be directly be compared with each other. The result from MTT was taking the whole population of cells and compared it with untreated cells. For annexin-V-FITC/PI test only a sample of 10 000 cells was taken. The morphological

study showed that most of the cells treated with [Co(phen)(ma)Cl] were healthy (Figure 3.2.2h and Figure 3.2.2i) compared to untreated cells (Figure 3.2.2g). The only difference was that the confluence level was noticeably lesser when the concentration of [Co(phen)(ma)Cl] increases. All these showed that [Co(phen)(ma)Cl] were not competent in killing MCF10A cells in anyway but slowed the cells growth rate instead. Since the cells treated with [Co(phen)(ma)Cl] grew slower than untreated this explains the explained the difference in the percentage of viable cells between treated and untreated cells in MTT assay result.

Faulty G2/M arrest checkpoint can permit a damaged cell to go into mitosis and undergo apoptosis, and enhancing this effect may amplify the cytotoxicity of chemotherapy (Robert 2002). Alternatively, increasing G2/M phase arrest has also been linked with enhanced apoptosis (Tyagi et. al. 2002). The treatment of [Co(phen)(ma)Cl] on MCF-7 cell line has shown to have slight arrest at G2/M phase in dose dependent manner (Figure 4.2.4). What is interesting is the effect of [Co(phen)(ma)Cl] on MDA-MB-231 on cell cycle was quite different. The results of cell cycle analysis of [Co(phen)(ma)Cl] on MCF-7 were consistent with the results of the annexin-V-FITC/PI test where G2/M arrest and increment of apoptotic cells was in dose dependent manner.

Cell cycle analysis indicated that after 72 hours of [Co(phen)(ma)Cl] treatment on MDA-MB-231 showed a considerable increase in G0/G1 phase arrest in a dose dependent manner. A significant arrest in G0/G1 at 25 μ M observed with $P < 0.01$. G0/G1 phase arrest had always been exclusively associated with

DNA damage (Linke *et al.*, 1996). So there is a high probability that [Co(phen)(ma)Cl] caused DNA damage to MDA-MB-231 which in turn caused G0/G1 arrest.

So far the cell cycle analysis test had proven that [Co(phen)(ma)Cl] causes cell death on MCF-7 and MDA-MB-231 cell lines in a completely different pathway and mode of action. However the most interesting finding obtained from this test was [Co(phen)(ma)Cl] has no effect on MCF10A, which was the non-malignant cell line. This means that [Co(phen)(ma)Cl] has a selective mode of action that targets only cancerous cells and has little effect on normal healthy cells. Further studies on [Co(phen)(ma)Cl] may lead to development of an anticancer drug that brings lesser side effects.

Proteasome-Glo™ cell-based assay showed that [Co(phen)(ma)Cl] induced cell death in a different mode of action on malignant cell lines while remains relatively ineffective on non-malignant cell line. The trend observed from the data of this assay was compliant to results obtained from previous tests. The proteasome activity of MCF-7 and MCF10A remained high and unaffected even when concentration of [Co(phen)(ma)Cl] increased. However the proteasome activity of MDA-MB-231 decreased when the concentration of [Co(phen)(ma)Cl] increased indicating [Co(phen)(ma)Cl] only inhibit the proteasome activity of MDA-MB-231 cell line among the three cell lines that were being tested.

Similar trend was also observed in the measurement of intracellular ROS level assay where the intracellular ROS level of MDA-MB-231 increased when treated with [Co(phen)(ma)Cl]. Meanwhile the intracellular ROS level of MCF-7 and MCF10A remained relatively low even after treated with [Co(phen)(ma)Cl]. This further strengthen the theory that [Co(phen)(ma)Cl] induced cell death in a different mode of mechanism on each of the malignant cell lines while remained ineffective towards non-malignant cell line.

Accumulation of intracellular ROS level can induce apoptosis by both the intrinsic and extrinsic pathway (Ozben 2007). In the extrinsic pathway, ROS generation is connected to the Fas death signalling pathway (Wang *et al.*, 2008). Fas ligands generate ROS as an upstream event for phosphorolysis of Fas to activate it. This step is imperative for following recruitment Fas-associated protein with death domain and caspase 8 as well as apoptosis induction (Gupta *et al.*, 2012). In the intrinsic pathway, ROS function to facilitate cytochrome c release by activating activating pore-stabilizing proteins like Bcl-2 and Bcl-xL as well as inhibiting pore-destabilizing proteins like Bcl-2-associated X protein, Bcl-2 homologous antagonist/killer (Martindale and Holbrook, 2002). ROS can also induce cell death through autophagy, which is a self-catabolic process involving sequestration of cytoplasmic contents (exhausted organelles and protein aggregates) for degradation in lysosomes (Shrivastava *et al.*, 2011).

Though I was still not able to pinpoint the exact mode of mechanism on the cell death induced by [Co(phen)(ma)Cl] on MCF-7 and MDA-MB-231 I was

able to narrow down the search. Clear indication was shown that [Co(phen)(ma)Cl] was capable of inducing cell death by targeting more than one pathway. Further studies are warranted to find out the details of these pathways.

CHAPTER 5

FURTHER STUDIES AND CONCLUSION

5.1 Recommendations for further studies

Further studies are needed to pinpoint the exact mechanism of action taken by [Co(phen)(mal)Cl] in killing MCF-7 and MDA-MB-231 cells. However, based on the results obtained from this study I can narrow the search to a few possible pathways. One of the most like pathways will be the inhibition of NF- κ B. One of the prominent features found in most breast cancer tumours is the constitutive activation of NF- κ B, a family of transcription factors that play critical roles in cell survival, proliferation, inflammation and immunity (Hayden and Ghosh, 2008). The importance of the NF- κ B pathway is well-known and documented. NF- κ B plays a key role in mammary epithelial proliferation, architecture and branching during early post-natal development (Brantley *et al.*, 2001; Cao *et al.*, 2001). This is the reason why constitutive NF- κ B activation detected in numerous breast tumour cell lines has weighty consequences in the initiation and progression of breast cancer (Sovak *et al.*, 1997). Studies had shown that the requirement of NF- κ B is imperative for the induction and maintenance of the epithelial-mesenchymal transition (EMT), a process that critically controls breast cancer progression (Chua *et al.*, 2004). MCF10A, an immortalized cell line which is derived from normal mammary epithelial cells, undergoes EMT which is an initiation step to metastasis when overexpressing of the NF- κ B protein occurs (Huber *et al.*, 2007). Activation of NF- κ B also blocks apoptosis in different cell types, including

human breast cancers (Barkett and Gilmore, 1999; Karin and Lin, 2002; Biswas *et al.*, 2003). So, hypothetically by inhibiting NF- κ B it will induce apoptosis and also cause cell cycle arrest. In fact this point was proven in a study when NF- κ B was selectively inhibited caused tremendous increase in the number of apoptotic cells and also induced G0/G1 arrest in an ER-negative breast cancer (Biswas *et al.*, 2004). NF- κ B can be blocked by both a signal-inducible proteasome-dependent and also a constitutive proteasome-independent calpain-dependent mechanism (Miyamoto *et al.*, 1998). Though NF- κ B is mostly activated in ER-negative cell lines like MDA-MB-231 (Biswas *et al.*, 2004; Nakshatri *et al.*, 1997) it was shown to be activated in ER-positive cell lines too like MCF-7 (Zhou *et al.*, 2005). In fact inhibition of NF- κ B has shown to induce apoptotic cell death in MCF-7 too (Shen *et al.*, 2001). Therefore NF- κ B could be a potential target for [Co(phen)(mal)Cl] in killing the malignant cell lines.

There are other feasible pathways that are more effective against highly invasive cancer cells like MDA-MB-231. For instances, inhibiting Ras and RhoA contributed to inhibition of both proliferation and invasiveness of a highly invasive and metastatic breast cancer cell line, MDA-MB-231 by inducing G0/G1 arrest (Denoyelle *et al.*, 2001, Denoyelle *et al.*, 2003; Pillé *et al.*, 2005). Another possible pathway might be upregulation of UCH-L1 gene which plays an important role in various biological processes including cell proliferation, cell cycle, apoptosis, signal transduction (Orlowski and Dees, 2003). UCH-L1 has been acknowledged as a cancer-specific methylated gene, and silenced by

promoter methylation in multiple tumors including breast cancer cells (Xiang *et al.*, 2012). Upregulation of UCH-L1 may possibly act as a tumor suppressor by inducing apoptosis and also inducing G0/G1 arrest (Wang *et al.*, 2008; Xiang *et al.*, 2012). CoCl₂, a cobalt(II) compound, was found to concomitantly upregulate UCH-L1 by mimicking hypoxia *in vitro* (Lefebvre *et al.*, 2010). Perhaps [Co(phen)(mal)Cl] also possesses the capability of upregulating UCH-L1 and induces apoptosis and cell cycle arrest on MCF-7 and MDA-MB-231.

Though there might other pathways that maybe undertaken by [Co(phen)(mal)Cl] these are few of the most probably pathways that I have narrowed down after extensive analysis of studies done by other researchers and compared with the results obtained in this study. These are the few prospective areas to look into to further narrow down the mechanism of action of [Co(phen)(mal)Cl].

5.2 Conclusion

From the results obtained from this study I found that [Cu(phen)(mal)Cl] and [Zn(phen)(mal)Cl] indiscriminately target both malignant and non-malignant breast epithelial cells alike thus were not suitable to be further studied on. [Co(phen)(mal)Cl] was found to reduce cell viability count by inducing apoptosis in both MCF-7 and MDA-MB-231 plus causing slight arrest in G2 phase on MCF-7 and G0/G1 arrest on MDA-MB-231. However [Co(phen)(mal)Cl] was shown to be targeting a proteasome-dependent and ROS-dependent pathway on MDA-MB-231 while targeting a proteasome-independent and ROS-independent

pathway on MCF-7 indicating that [Co(phen)(mal)Cl] is capable of inducing cell death with more than one mechanism of action. [Co(phen)(mal)Cl] has no apparent effect on MCF10A which could lead to developing an anticancer compound with lesser side effects. From my studies [Co(phen)(mal)Cl] has shown great potential by discriminately killing breast epithelial cells. So I suggest [Co(phen)(mal)Cl] to be further studied on not only on breast cancer cell lines but on other types of cancer cell lines too to find more on its mechanism of actions and also its efficacy on other types of cancer.

REFERENCES

- Adams, J. and Kauffman, M., 2004. Development of the Proteasome Inhibitor Velcade (Bortezomib). *Cancer Invest*, 22(2), pp. 304–311.
- Alexandre, J., Nicco, C., Chéreau, C., 2006. Improvement of the therapeutic index of anticancer drugs by the superoxide dismutase mimic mangafodipir. *Journal of the National Cancer Institute*, 98, pp. 236–244.
- Althuis, M.D. et al., 2004. Etiology of hormone receptor-defined breast cancer: a systematic review of the literature. *Cancer Epidemiol Biomarkers Prev*, 13(10), pp. 1558–1568.
- American Cancer Society [Online]. Available at <http://www.cancer.org/> [Accessed: 20 June 2013]
- Anderson, W.F., Jatoi, I. and Devesa, S.S., 2005. Distinct breast cancer incidence and prognostic patterns in the NCI's SEER program: suggesting a possible link between etiology and outcome. *Breast Cancer Research Treatment*, 90, pp. 127–137.
- Arnold, R.S. et al., 2001. Hydrogen peroxide mediates the cell growth and transformation caused by the mitogenic oxidase Nox1. *Proceedings of the National Academy of Sciences*, 98, pp. 5550–5555.
- Badie, B. et al., 1998. Adenovirus-mediated p53 gene delivery potentiates the radiation-induced growth inhibition of experimental brain tumors. *Journal of Neuro-Oncology*, 37, pp. 217–222.
- Barkett, M. and Gilmore, T.D., 1999. Control of apoptosis by Rel/NF-kappaB transcription factors. *Oncogene*, 18(49) , pp. 6910-6924.
- Barve, A. et al., 2009. Mixed-ligand copper(II) maltolate complexes: synthesis, characterization, DNA-binding and cleavage, and cytotoxicity. *Inorganic Chemistry*. 48, pp. 9120–9132.
- Bauer, J.A. et al., 2007. Nitrosylcobalamin potentiates the anti-neoplastic effects of chemotherapeutic agents via suppression of survival signaling. *PLoS One*, 2, pp. 1313–1330.
- Beltinger, C. et al., 1998. The role of CD95 (APO-1/Fas) mutations in lymphoproliferative and malignant lymphatic diseases. *Klinische Pädiatrie* , 210(4), pp. 153-158.
- Benedetti, M. et al., 2010. Water-soluble organometallic analogues of oxaliplatin with cytotoxic and anticlonogenic activity. *ChemMedChem*, 5(1), pp. 46-51.

Bernstein, L.R., Tanner, T., Godfrey, C. and Noll, B., 2000. Chemistry and pharmacokinetics of gallium maltolate, a compound with high oral gallium bioavailability. *Metal Based Drugs*, 7 (1), pp. 33–48.

Berridge, M.V., Herst, P.M. , and Tan, A.S., 2005. Tetrazolium dyes as tools in cell biology: new insights into their cellular reduction. *Biotechnology Annual Review*, 11, pp. 127-152.

Biswas, D.K. et al., 2004. NF-kappa B activation in human breast cancer specimens and its role in cell proliferation and apoptosis. *Proceedings of the National Academy of Sciences*, 101(27), pp. 10137-10142.

Biswas, G., Anandatheerthavarada, H.K., Zaidi, M. and Avadhani, N.G., 2003. Mitochondria to nucleus stress signaling: a distinctive mechanism of NFkappaB/Rel activation through calcineurin-mediated inactivation of IkappaBbeta. *Journal of Cell Biology*, 161(3), pp. 507-519.

Bjeldanes, L.F. and Chew, H., 1979. Mutagenicity of 1,2-dicarbonyl compounds: maltol, kojic acid, diacetyl and related substances. *Mutation Research*, 67, pp. 367–371.

Blum, O. et al., 1998. Isolation of a myoglobin molten globule by selective cobalt(III)-induced unfolding. *Proceedings of the National Academy of Sciences*, 95, pp. 6659–6662.

Brantley, D.M. et al., 2001. Nuclear factor-kappaB (NF-kappaB) regulates proliferation and branching in mouse mammary epithelium. *Molecular Biology of the Cell*, 12(5), pp. 1445-55.

Brewer, G.J., 2009. The risks of copper toxicity contributing to cognitive decline in the aging population and to Alzheimer’s disease. *Journal of the American College of Nutrition*, 28(3), pp. 238–242.

Cantley, L.C. and Neel, B.G., 1999. New insights into tumor suppression: PTEN suppresses tumor formation by restraining the phosphoinositide 3-kinase/AKT pathway. *Proceedings of the National Academy of Sciences*, 96, pp. 4240–4245.

Cao, Y. et al., 2001. IKK-alpha provides an essential link between RANK signaling and cyclin D1 expression during mammary gland development. *Cell*, 107, pp. 763–775.

Carter, G.E., Lieskovsky, G., Skinner, D.G. and Petrovich, Z., 1989. Results of local and/or systemic adjuvant therapy in the management of pathological stage C or D1 prostate cancer following radical prostatectomy. *Journal of Urology*, 142(5) , pp. 1266-1270.

Chen, W., Shu, X.L., Lu, X. and Li, J.R., 2008. Effects of As₂O₃ on apoptosis and Bcl-2/Bax expression of rat spermatogenic cells. *Zhongguo Zhong Yao Za Zhi*, 33(23), pp. 2823-2826.

- Chua, H.K. et al., 2004. Concurrent vs. staged colectomy and hepatectomy for primary colorectal cancer with synchronous hepatic metastases. *Diseases of the Colon & Rectum*, 47(8) , pp. 1310-6.
- Chohan, Z. H., Arif, M. and Sarfraz, M., 2007. Metal-based antibacterial and antifungal amino acid derived Schiff bases: their synthesis, characterization and *in vitro* biological activity. *Applied Organometallic Chemistry*, 21, pp. 294–302.
- Clarke, M.J., Zhu, F. and Frasca, D.R., 1999. Non-Platinum Chemotherapeutic Metallopharmaceuticals. *Chemical Reviews*, 99, pp. 2511–2533.
- Coleman, R.E. and Rubens, R.D., 1987. The clinical course of bone metastases from breast cancer. *British Journal of Cancer*, 55, pp. 61-66.
- Collins, K., Jacks, T. and Pavletich, N.P., 1997. The cell cycle and cancer. *Proceedings of the National Academy of Sciences*, 94(7) , pp. 2776-8.
- Crawford, L.J. et al., 2009. Proteasome proteolytic profile is linked to Bcr-Abl expression. *Experimental Hematology*, 37, pp. 357–366.
- Denoyelle, C. et al., 2003. New insights into the actions of bisphosphonate zoledronic acid in breast cancer cells by dual RhoA-dependent and -independent effects. *British Journal of Cancer*, 2003 May 19;88(10), pp. 1631-40.
- Denoyelle, C. et al, 2001. Cerivastatin, an inhibitor of HMG-CoA reductase, inhibits the signaling pathways involved in the invasiveness and metastatic properties of highly invasive breast cancer cell lines: an in vitro study. *Carcinogenesis*, 22(8), pp. 1139-1148.
- Devereux, M. et al., 2007. Synthesis, X-ray crystal structures and biomimetic and anticancer activities of novel copper(II)benzoate complexes incorporating 2-(4'-thiazolyl)benzimidazole (thiabendazole), 2-(2-pyridyl)benzimidazole and 1,10-phenanthroline as chelating nitrogen donor ligands. *Journal of Inorganic Biochemistry*, 101(6), pp. 881 - 892.
- Díaz, G.D., Li, Q. and Dashwood, R.H., 2003. Caspase-8 and apoptosis-inducing factor mediate a cytochrome *c*-independent pathway of apoptosis in human colon cancer cells induced by the dietary phytochemical chlorophyllin. *Cancer Research*, 63(6), pp. 1254–1261.
- Daniel, K.G. et al., 2004. Organic copper complexes as a new class of proteasome inhibitors and apoptosis inducers in human cancer cells. *Biochemical Pharmacology*, 67(6), pp. 1139–1151.

- Diel, I.J. et al., 1992. Detection of tumor cells in bone marrow of patients with primary breast cancer: a prognostic factor for distant metastasis. *Journal of Clinical Oncology*, 10, pp. 21534-21539.
- Dilda, P.J. and Hogg, P.J., 2007. Arsenical-based cancer drugs. *Cancer Treatment Reviews*, 33, pp. 542–564.
- Dong, J., Naito, M. and Tsuruo, T., 1997. c-Myc plays a role in cellular susceptibility to death receptor-mediated and chemotherapy-induced apoptosis in human monocytic leukemia U937 cells. *Oncogene*, 15, pp. 639–647.
- Drexler, H.C., 1997. Activation of the cell death program by inhibition of proteasome function. *Proceedings of the National Academy of Sciences*, 94, pp. 855–860.
- Eastman, A., 1987. Cross-linking of glutathione to DNA by cancer chemotherapeutic platinum coordination complexes. *Chemico-Biological Interactions*, 61, pp. 241–248.
- Elo, H., 2004. The antiproliferative agents trans-bis(resorcylalldoximato)copper(II) and trans-bis(2,3,4-trihydroxybenzalldoximato)copper(II) and cytopathic effects of HIV. *Zeitschrift für Naturforschung*, 59(7-8), pp. 609–611.
- Emami, S., Hosseinimehr, .S.J., Taghdisi, S.M. and Akhlaghpour, S., 2007. Kojic acid and its manganese and zinc complexes as potential radioprotective agents. *Bioorganic & Medicinal Chemistry Letters*, 1;17(1), pp. 45-8.
- Farber, S. et al., 1948. Temporary remissions in acute leukemia in children produced by folic acid antagonist, 4-aminopteroylglutamic acid (aminopterin). *The New England Journal of Medicine*, 238, pp. 787–793.
- Ferlay, J. et al., 2010. Estimates of worldwide burden of cancer in 2008: GLOBOCAN 2008. *International Journal of Cancer*, 127(12), pp. 2893-2917.
- Freier, K. et al., 2003. Tissue microarray analysis reveals site-specific prevalence of oncogene amplifications in head and neck squamous cell carcinoma. *Cancer Research*, 63, pp. 1179–1182.
- Galluzzi, L. et al., 2007. Cell death modalities: classification and pathophysiological implications. *Cell Death & Differentiation*, 14(7), pp. 1237-1243.
- Garza-Ortiz, A. et al., 2007. The synthesis, chemical and biological properties of dichlorido(azpy)gold(III) chloride (azpy=2-(phenylazo)pyridine) and the gold-induced conversion of the azpy ligand to the chloride of the novel tricyclic pyrido[2,1-c][1,2,4]benzotriazin-11-ium cation. *Journal of Inorganic Biochemistry*, 101(11-12), pp. 1922-1930.

- Ghosh, S. and Hayden, M.S., 2008. New regulators of NF-kappaB in inflammation. *Nature Reviews Immunology*, 8(11), pp. 837-48.
- Gielen, M. and Tiekink, E.R., 2005. *Metallotherapeutic Drugs and Metal-Based Diagnostic Agents*. Wiley.
- Gokhale, N.H. et al., 2001. Copper complexes of carboxamidrazone derivatives as anticancer agents. 3. Synthesis, characterization and crystal structure of [Cu(appc)Cl₂], (appc=N1-(2- acetylpyridine)pyridine-2- carboxamidrazone). *Inorganica Chimica Acta*, 319(1-2), pp. 90-94.
- Gralla, E.J., Stebins, R.B., Coleman, G.L. and Delahunt, C.S., 1969. Toxicity studies with ethyl maltol. *Toxicology and Applied Pharmacology*, 15, pp. 604-613.
- Gupta, K.J., Igamberdiev, A.U. and Mur, L.A.J., 2012. NO and ROS homeostasis in mitochondria: a central role for alternative oxidase. *New Phytologist*, 196 (1), pp. 1-3.
- Gupta, Y., Kohli, D.V. and Jain, S.K., 2008. Vitamin B12-mediated transport: a potential tool for tumor targeting of antineoplastic drugs and imaging agents. *Critical Reviews in Therapeutic Drug Carrier Systems*, 25, pp. 347-379.
- Hanley, C. et al., 2008. Preferential killing of cancer cells and activated human T cells using ZnO nanoparticles. *Nanotechnology*, 19, pp. 295103.
- Harbour, J.W. and Dean, D.C., 2000. The Rb/E2F pathway: expanding roles and emerging paradigms. *Genes & Development*, 14, pp. 2393-2409.
- Hayden, M.S. and Ghosh, S., 2008. Shared principles in NF-kappaB signaling. *Cell*, 132(3), pp. 344-362.
- Hileman, E.O., Liu, J., Albitar, M., Keating, M.J. and Huang, P., 2004. Intrinsic oxidative stress in cancer cells: a biochemical basis for therapeutic selectivity. *Cancer Chemotherapy and Pharmacology*, 53, pp. 209-219.
- Hindo, S.S. et al., 2009. Metals in anticancer therapy: copper(II) complexes as inhibitors of the 20S proteasome. *European Journal of Medicinal Chemistry*, 44(11), pp. 4353-4361.
- Hironishi, M., Kordek, R., Yanagihara, R. and Garruto, R.M., 1996. Maltol (3-hydroxy-2-methyl-4-pyrone) toxicity in neuroblastoma cell lines and primary murine fetal hippocampal neuronal cultures. *Neurodegeneration*, 5, pp. 325-329.
- Ho, J.J. et al., 2003. Methylation status of promoters and expression of MUC2 and MUC5AC mucins in pancreatic cancer cells. *International Journal of Oncology*, 2003;22, pp. 273-279.

Huang, Q. et al., 2006. Zinc(II) and copper(II) complexes of beta-substituted hydroxylporphyrins as tumor photosensitizers. *Bioorganic & Medicinal Chemistry Letters*, 1;16(11), pp. 3030-3.

Huang, Z.Y. et al., 2002. Astrocyte-specific expression of CDK4 is not sufficient for tumor formation, but cooperates with p53 heterozygosity to provide a growth advantage for astrocytes in vivo. *Oncogene*, 21, pp. 1325–1334.

Huber, A.V. et al., 2007. Human chorionic gonadotrophin attenuates NF-kappaB activation and cytokine expression of endometriotic stromal cells. *Molecular Human Reproduction*, 13(8), pp. 595-604.

IARC, 2012, *GLOBOCAN 2012: Estimated Cancer Incidence, Mortality and Prevalence Worldwide in 2012* [Online]. Available at http://globocan.iarc.fr/Pages/fact_sheets_cancer.aspx [Accessed: 20 June 2013]

Im, J.S. and Lee, J.K., 2008. ATR-dependent activation of p38 MAP kinase is responsible for apoptotic cell death in cells depleted of Cdc7. *Journal of Biological Chemistry*, 283, pp. 25171–25177.

Imajoh-Ohmi, S. et al., 1995. Lactacystin, a specific inhibitor of the proteasome, induces apoptosis in human monoblast U937 cells. *Biochemical and Biophysical Research Communications*, 217, pp. 1070–1077.

Ishikawa, K. et al., 2008. ROS-generating mitochondrial DNA mutations can regulate tumor cell metastasis. *Science*, 320:661–664.

Jakupec, M.A. and Keppler, B.K., 2004. Gallium in cancer treatment. *Current Topics in Medicinal Chemistry*, 4, pp. 1575–1583.

Jiang, Q., Zhu, J., Zhang, Y., Xiao, N. and Guo, Z., 2008. DNA binding property, nuclease activity and cytotoxicity of Zn(II) complexes of terpyridine derivatives. *Biometals*, (2), pp. 297-305.

Jing, Y., Dai, J., Chalmers-Redman, R.M., Tatton, W.G. and Waxman, S., 1999. Arsenic trioxide selectively induces acute promyelocytic leukemia cell apoptosis via a hydrogen peroxide-dependent pathway. *Blood*. 94, pp. 2102–2111.

Jung, M., Kerr, D.E. and Senter, P.D., 1997. Bioorganometallic chemistry—synthesis and antitumor activity of cobalt carbonyl complexes. *Archiv der Pharmazie (Weinheim)*, 330, pp. 173–176.

Kaneko, N. et al., 2004. Orally administrated aluminum-maltolate complex enhances oxidative stress in the organs of mice. *Journal of Inorganic Biochemistry*, 98 (12), pp. 2022–2031.

- Kandioller, W. et al., 2009. Tuning the anticancer activity of maltol-derived ruthenium complexes by derivatization of the 3-hydroxy-4-pyrone moiety. *Journal of Organometallic Chemistry*, 694, pp. 922–929.
- Karin, M. and Lin, A., 2002. NF-kappaB at the crossroads of life and death. *Nature Immunology*, 3(3), pp. 221-7.
- Kawanishi, S., Hiraku, Y., Pinlaor, S. and Ma, N., 2006. Oxidative and nitrative damage in animals and patients with inflammatory diseases in relation to inflammation-related carcinogenesis. *Biological Chemistry*, 387(4), pp. 365–372.
- Kelland, L., 2007. The resurgence of platinum-based cancer chemotherapy. *Nature Reviews Cancer*, 7, pp. 573–584.
- Kemp, S. et al., 2007. Encapsulation of platinum(II)-based DNA intercalators within cucurbit[6,7,8]urils. *Journal of Biological Inorganic Chemistry*, 12, pp. 969-979.
- Kerr, J.F., Wyllie, A.H. and Currie, A.R., 1972. Apoptosis: a basic biological phenomenon with wide-ranging implications in tissue kinetics. *British Journal of Cancer*, 26, pp. 239–257.
- Kerr, J.F.R., Winterford, C.M. and Harmon, B.V., 1994. Apoptosis—its significance in cancer and cancer therapy. *Cancer*, 73, pp. 2013–2026.
- Kerr, R.O., Cardamone, J., Dalmaso, A.P. and Kaplan, M.E., 1972. Two mechanisms of erythrocyte destruction in penicillin-induced hemolytic anemia. *The New England Journal of Medicine*, 287(26), pp. 1322-1325.
- Kim, J.M. et al., 2008. Cdc7 kinase mediates Claspin phosphorylation in DNA replication checkpoint. *Oncogene*, 27, pp. 3475–3482.
- King, M.S., Sharpley, M.S. and Hirst, J., 2009. Reduction of hydrophilic ubiquinones by the flavin in mitochondrial NADH: ubiquinone oxidoreductase (complex I) and production of reactive oxygen species. *Biochemistry*, 48, pp. 2053–2062.
- Koopman, W.J., 1994. The future of biologics in the treatment of rheumatoid arthritis. *Seminars in Arthritis and Rheumatism*, 23(6), pp. 50-58.
- Köpf, H. and Köpf-Maier, P., 1979. Titanocene dichloride--the first metallocene with cancerostatic activity. *Angewandte Chemie International Edition*, 18(6), pp. 477-478.
- Korde, L.A. et al., 2010. Gene expression pathway analysis to predict response to neoadjuvant docetaxel and capecitabine for breast cancer. *Breast Cancer Research Treatment*, 119, pp. 685–699.

- Kostova, I., 2006. Gold coordination complexes as anticancer agents. *Anti-Cancer Agents in Medicinal Chemistry*, 6, pp. 19–32
- Koutsilieris, M. et al., 1999. Chemotherapy cytotoxicity of human MCF-7 and MDA-MB 231 breast cancer cells is altered by osteoblast-derived growth factors. *Molecular Medicine*, 5(2), pp. 86–97.
- Larsen, J.F., Walter, S. and Krarup, T., 1990. Complete androgen blockade as primary treatment for advanced metastatic cancer of the prostate. *International Urology and Nephrology*, 22(3), pp. 249-55.
- Lefebvre, B. et al, 2010. Proteasomal degradation of retinoid X receptor alpha reprograms transcriptional activity of PPARgamma in obese mice and humans. *Journal of Clinical Investigation*, 120(5), pp. 1454-1468.
- Liboiron, B.D. et al., 2005. New Insights into the Interactions of Serum Proteins with Bis(maltolato)oxovanadium(IV): Transport and Biotransformation of Insulin-Enhancing Vanadium Pharmaceuticals. *Journal of the American Chemical Society*, 127 (14), pp. 5104–5115.
- Linke, S.P. et al., 1996. A reversible, p53-dependent G0/G1 cell cycle arrest induced by ribonucleotide depletion in the absence of detectable DNA damage. *Genes Development*, 10(8), pp. 934-47.
- Malumbres, M. and Barbacid, M., 2001. To cycle or not to cycle: a critical decision in cancer. *Nature Reviews Cancer*, 1, pp. 222–231.
- Malumbres, M. and Barbacid, M., 2009. Cell cycle, CDKs and cancer: a changing paradigm. *Nature Reviews Cancer*, 9, pp. 153–166.
- Mani, A. and Gelmann, E.P., 2005. The ubiquitin-proteasome pathway and its role in cancer. *Journal of Clinical Oncology*, 23(21), pp. 4776-4789.
- Marte, B.M. and Downward, J., 1997. PKB/Akt: connecting phosphoinositide 3-kinase to cell survival and beyond. *Trends in Biochemical Sciences*, 22, pp. 355–358.
- Marzano, C. et al, 2002. Cytotoxicity and DNA damage induced by a new platinum(II) complex with pyridine and dithiocarbamate. *Chemico-Biological Interactions*, 140(3), pp. 215-29.
- Mathew, R. et al., 2001. Esophageal squamous cell carcinomas with DNA replication errors (RER+) are associated with p16/pRb loss and wild-type p53. *Journal of Cancer Research and Clinical Oncology*, 127(10), pp. 603-12.
- Matsumoto, S. et al., 2010. Hsk1 kinase and Cdc45 regulate replication stress-induced checkpoint responses in fission yeast. *Cell Cycle*, 9, pp. 4627–4637.

- McConkey, D.J. and Zhu, K., 2008. Mechanisms of proteasome inhibitor action and resistance in cancer. *Drug Resist Update*, 11, pp. 164–179.
- McFadyen, W.D., Wakelin, L.P., Roos, I.A. and Leopold, V.A., 1985. Activity of platinum(II) intercalating agents against murine leukemia L1210. *Journal of Medical Chemistry*, 28(8), pp. 1113-6.
- Mirabelli, C.K. et al., 1986. Cellular pharmacology of mu-[1,2-bis(diphenylphosphino)ethane]bis[(1-thio-beta-D-glucopyranosato-S)gold(I)]: a novel antitumor agent. *Anti-cancer Drug Design*, 1(3), pp. 223-34.
- Miyamoto, S., Seufzer, B.J. and Shumway, S.D., 1998. Novel IkappaB alpha proteolytic pathway in WEHI231 immature B cells. *Molecular Cell Biology*, 18(1), pp. 19-29.
- Martindale, J.L. and Holbrook, N.J., 2002. Cellular response to oxidative stress: signaling for suicide and survival. *Journal of Cell Physiology*, 192(1), pp. 1-15.
- Miyajima, A. et al., 1997. Role of reactive oxygen species in cis-dichlorodiammineplatinum-induced cytotoxicity on bladder cancer cells. *British Journal of Cancer*, 76, pp. 206–210.
- Montagnoli, A. et al., 2004. Cdc7 inhibition reveals a p53-dependent replication checkpoint that is defective in cancer cells. *Cancer Research*, 64, pp. 7110–7116.
- Montagnoli, A et al., 2008. A Cdc7 kinase inhibitor restricts initiation of DNA replication and has antitumor activity. *Nature Chemical Biology*, 4, pp. 357–365.
- Montagnoli, A., Moll, J. and Colotta, F., 2010. Targeting cell division cycle 7 kinase: a new approach for cancer therapy. *Clinical Cancer Research*, 16, pp. 4503–4508.
- Motegi, A., Murakawa, Y. and Takeda, S., 2009. The vital link between the ubiquitin-proteasome pathway and DNA repair: impact on cancer therapy. *Cancer Letters*, 283, pp. 1–9.
- Morgillo, F. et al., 2010. Antitumor activity of bortezomib in human cancer cells with acquired resistance to anti-epidermal growth factor receptor tyrosine kinase inhibitors. *Lung Cancer*, 71(3), pp. 283-290.
- Nagaraja, G.M. et al., 2006. Gene expression signatures and biomarkers of noninvasive and invasive breast cancer cells: comprehensive profiles by representational difference analysis, microarrays and proteomics. *Oncogene*, 13;25(16), pp. 2328-2338.
- Nakshatri, H. et al., 1997. Constitutive activation of NF-kappaB during progression of breast cancer to hormone-independent growth. *Molecular Cell Biology*, 17(7), pp. 3629-3639.

- Narla, R.K., Chen, C.L., Dong, Y. and Uckun, F.M., 2001. In vivo antitumor activity of bis(4,7-dimethyl-1,10-phenanthroline) sulfatooxovanadium(IV) (METVAN [VO(SO₄)(Me₂-Phen)₂]). *Clinical Cancer Research*, 7(7), pp. 2124-2133.
- Nasmyth, K., 1996. Viewpoint: putting the cell cycle in order. *Science*, 274(5293), pp. 1643-1645.
- Nawrocki, S.T. et al., 2008. Myc regulates aggresome formation, the induction of Noxa, and apoptosis in response to the combination of bortezomib and SAHA. *Blood*. 2008;112, pp. 2917–2926.
- Orlowski, R.Z. and Dees, E.C., 2003. The role of the ubiquitination-proteasome pathway in breast cancer: applying drugs that affect the ubiquitin-proteasome pathway to the therapy of breast cancer. *Breast Cancer Research*, 5(1), pp. 1-7.
- Osinsky, S. et al., 2004. Selectivity of effects of redox-active cobalt(III) complexes on tumor tissue. *Experimental oncology*, 26, pp. 140–144.
- Osinsky, S.P. et al., 2003. Redox-active cobalt complexes as promising antitumor agents. *Russian Chemical Bulletin*, 52, pp. 2636–2645.
- Ostrovsky, S., Kazimirsky, G., Gedanken, A. and Brodie, C., 2009. Selective cytotoxic effect of ZnO nanoparticles on glioma cells. *Nano Research*, 2, pp. 882–890.
- Ott, I. and Gust, R., 2007. Non platinum metal complexes as anti-cancer drugs. *Archiv der Pharmazie (Weinheim)*, 340, pp. 117–126.
- Ott I. et al., 2005. Synthesis, cytotoxicity, cellular uptake and influence on eicosanoid metabolism of cobalt-alkyne modified fructoses in comparison to auranofin and the cytotoxic COX inhibitor Co-ASS. *Organic & Biomolecular Chemistry*, 3(12), pp. 2282-2286.
- Ozben, T., 2007. Oxidative stress and apoptosis: impact on cancer therapy. *Journal of Pharmaceutical Sciences*, 96(9), pp. 2181-2196.
- Paola, F.,I. et al., 2010. Non-classical anticancer agents: synthesis and biological evaluation of zinc(II) heteroleptic complexes. *Dalton Transactions*, 39, pp. 4205-4212.
- Pelicano, H. et al., 2003. Inhibition of mitochondrial respiration: a novel strategy to enhance drug-induced apoptosis in human cells by a reactive oxygen species-mediated mechanism. *The Journal of Biological Chemistry*, 278, pp. 37832–37839.

- Pillé, J.Y. et al., 2005. Anti-RhoA and anti-RhoC siRNAs inhibit the proliferation and invasiveness of MDA-MB-231 breast cancer cells in vitro and in vivo. *Molecular Therapy*, 11(2), pp. 267-74.
- Premanathan, M., Karthikeyan, K., Jeyasubramanian, K. and Manivannan, G., 2011. Selective toxicity of ZnO nanoparticles toward Gram positive bacteria and cancer cells by apoptosis through lipid peroxidation. *Nanomedicine*, 7, pp. 184–192.
- Reffitt, D.M. et al., 2000. Assessment of iron absorption from ferric trimaltol. *Annals of Clinical Biochemistry*, 37 (4), pp. 457–66.
- Roccaro, A.M. et al., 2006. Bortezomib mediates antiangiogenesis in multiple myeloma via direct and indirect effects on endothelial cells. *Cancer Research*, 66, pp. 184–191.
- Rosenberg, B., VanCamp, L., Trosko, J.E. and Mansour, V.H., 1969. Platinum compounds: a new class of potent antitumour agents. *Nature*, 222, pp. 385–386.
- Ruiz-Sanchez, P., Konig, C., Ferrari, S. and Alberto, R., 2011. Vitamin B(12) as a carrier for targeted platinum delivery: *in vitro* cytotoxicity and mechanistic studies. *Journal of Biological Inorganic Chemistry*, 16, pp. 33–44.
- Samuelson, A.V. and Lowe, S.W., 1997. Selective induction of p53 and chemosensitivity in RB-deficient cells by E1A mutants unable to bind the RB-related proteins. *Proceedings of the National Academy of Sciences*, 94, pp. 12094–12099.
- Schein, P.S. et al., 1980. Phase I clinical trial of spirogermanium. *Cancer Treatment Report*, 64(10-11), pp. 1051-6.
- Schwartzmann, G. et al., 2002. Anticancer drug discovery and development throughout the world. *Journal of Clinical Oncology*, 20(18), pp. 47S-59S.
- Shaw, I.C., 1999. Gold-based therapeutic agents. *Chemical Reviews*, 99, pp. 2589–2600.
- Shen, J., Channavajhala, P., Seldin, D.C. and Sonenshein, G.E., 2001. Phosphorylation by the protein kinase CK2 promotes calpain-mediated degradation of IkappaBalpha. *Journal of Immunology*, 167(9), pp. 4919-25.
- Sherr, C.J. and Roberts, J.M., 1999. CDK inhibitors: positive and negative regulators of G1-phase progression. *Genes & Development*, 13, pp. 1501–1512.
- Sherry, M.M., Greco, A.F., Johnson, D.H. and Hainsmorth, J.D., 1986. Metastatic breast cancer confined to the skeletal system. *American Journal of Medicine*, 81, pp. 381-386.
- Shinohara, K. et al., 1996. Apoptosis induction resulting from proteasome inhibition. *Biochemical Journal*, 317, pp. 385–388.

- Shrivastava, A. et al., 2011. Cannabidiol Induces Programmed Cell Death in Breast Cancer Cells by Coordinating the Cross-talk between Apoptosis and Autophagy. *Molecular Cancer Therapeutics*, 10, pp. 1161-1172.
- Shrivastava, H.Y., Kanthimathi, M. and Nair, B.U., 2002. Copper(II) complex of a tridentate ligand: an artificial metalloprotease for bovine serum albumin. *Biochimica et Biophysica Acta*, 1573(2), pp. 149–155.
- Sovak, M.A. et al., 1997. Aberrant nuclear factor-kappaB/Rel expression and the pathogenesis of breast cancer. *The Journal of Clinical Investigation*, 100(12) , pp. 2952-2960.
- Schumacker, P.T., 2006. Reactive oxygen species in cancer cells: live by the sword, die by the sword. *Cancer Cell*. 10, pp. 175–176.
- Spitz, F.R. et al., R.J., 1996. In vivo adenovirus-mediated p53 tumor suppressor gene therapy for colorectal cancer. *Anticancer Research*, 16, pp. 3415–3422.
- Szatrowski, T.P. and Nathan, C.F., 1991. Production of large amounts of hydrogen peroxide by human tumor cells. *Cancer Research*, 51, pp. 794–798.
- Swords, R. et al., 2010. Cdc7 kinase—a new target for drug development. *European Journal of Cancer*, 46, pp. 33–40.
- Tai, Y.T., Strobel, T., Kufe, D. and Cannistra, S.A., 1999. In vivo cytotoxicity of ovarian cancer cells through tumor-selective expression of the BAX gene. *Cancer Research*, 59, pp. 2121–2126.
- Takimoto, C.H. and Calvo, E., 2008. *Cancer Management: A Multidisciplinary Approach*. 11 ed.
- Tamura, D. et al., 2010. Bortezomib potentially inhibits cellular growth of vascular endothelial cells through suppression of G2/M transition. *Cancer Science*, 2010;101, pp. 1403–1408.
- Thati, B. et al., 2007. Apoptotic cell death: a possible key event in mediating the in vitro anti-proliferative effect of a novel copper(II) complex, [Cu(4-Mecdoa)(phen)(2)] (phen=phenanthroline, 4-Mecdoa=4-methylcoumarin-6,7-dioxactetate), in human malignant cancer cells. *European Journal of Pharmacology*, 569(1-2), pp. 16-28.
- Theriault, R.L. and Hortobagyl, G.N., 1992. Bone metastasis in breast cancer. *Anticancer Drugs*, 3, pp. 455-462.
- Thompson, C.B., 1995. Apoptosis in the pathogenesis and treatment of disease. *Science*, 267, pp. 1456–1462.

- Thorp, H.H., 1998. Bioinorganic Chemistry and Drug Design: Here Comes Zinc Again (Crosstalk). *Chemistry & Biology*, 5, pp.R125-R127.
- Toyokuni, S., Okamoto, K., Yodoi, J. and Hiai, H., 1995. Persistent oxidative stress in cancer. *Federation of European Biochemical Societies Letters*, 358, pp. 1–3.
- Traenckner, E.B., Wilk, S. and Baeuerle, P.A., 1994. A proteasome inhibitor prevents activation of NF-kappa B and stabilizes a newly phosphorylated form of I-kappa B-alpha that is still bound to NF-kappa B. *European Molecular Biology Organization Journal*, 15, pp. 5433–5441.
- Trachootham, D. et al., 2006. Selective killing of oncogenically transformed cells through a ROS-mediated mechanism by beta-phenylethyl isothiocyanate. *Cancer Cell*, 10, pp. 241–252.
- Tripathi A. et al., 2007. Complexity in modeling and understanding protonation states: computational titration of HIV-1-protease-inhibitor complexes. *Chemistry & Biodiversity*, 4(11), pp. 2564-2577.
- Tripathi, L., Kumar, P. and Singhai, A.K., 2007. Role of chelates in treatment of cancer. *Indian Journal of Cancer*, 44(2), pp. 62–71.
- Tsang, W.P., Chau, S.P., Kong, S.K. and Kwok, T.T., 2003. Reactive oxygen species mediate doxorubicin induced p53-independent apoptosis. *Life Sciences*, 73, pp. 2047–2058.
- Tsujimoto, Y., Cossman, J., Jaffe, E. and Croce, C.M., 1985. Involvement of the bcl-2 gene in human follicular lymphoma. *Science*, 228, pp. 1440–1443.
- Tsujimoto, Y et al., 1984. Cloning of the chromosome breakpoint of neoplastic B cells with the t(14;18) chromosome translocation. *Science*, 226, pp. 1097–1099.
- Tudzarova, S. et al., 2010. Molecular architecture of the DNA replication origin activation checkpoint. *European Molecular Biology Organization Journal*, 29, pp. 3381–3394.
- Tyagi, A., Agarwal, C. and Agarwal, R., 2002. The cancer preventive flavonoid silibinin causes hypophosphorylation of Rb/p107 and Rb2/p130 via modulation of cell cycle regulators in human prostate carcinoma DU145 cells. *Cell Cycle*, 1(2), pp. 137-142.
- Vol'pin, M.E., Levitin, I. and Osinsky, S.P., 1999. pH-dependent organocobalt sources for active radical species: a new type of anticancer agents. *MedSci entry for metal ions in biological systems*, 36, pp. 485–519.
- Wang, J. and Yi, J., 2008. Cancer cell killing via ROS: to increase or decrease, that is the question. *Cancer Biology & Therapy*, 7, pp. 1875–1884.

- Wang, X. et al., 2009. 1-Oxo-3-substitute-isothiochroman-4-carboxylic acid compounds: synthesis and biological activities of FAS inhibition. *Bioorganic & Medicinal Chemistry Letters*, 1;19(3), pp. 770-772.
- Wallace-Brodeur, R.R. and Lowe, S.W., 1999. Clinical implications of p53 mutations. *Cellular and Molecular Life Sciences*, 55, pp. 64–75.
- Waris, R., Turkson, J., Hassanein, T. and Siddiqui, A., 2005. Hepatitis C virus constitutively activates STAT-3 via oxidative stress: Role of STAT-3 in HCV replication. *Journal of Virology*, 79, pp. 1569–1580.
- Weder, J.E. et al., 2002. Copper complexes of non-steroidal anti-inflammatory drugs: an opportunity yet to be realized. *Coordination Chemistry Reviews*, 232(1-2), pp. 95–126.
- Weiss, R.B. and Christian, M.C., 1993. New cisplatin analogues in development. A review. *Review. Erratum in: Drugs*, 46(3), pp. 377.
- Wernyj, R.P. and Morin, P.J., 2004. Molecular mechanisms of platinum resistance: still searching for the Achilles' heel. *Drug Resistance Updates*, 7(4-5), pp. 227-232.
- Williams, G. and Stoeber, K., 1999. Clinical applications of a novel mammalian cell-free DNA replication system. *British Journal of Cancer*, 80(1), pp. 20–24.
- Wold, W.S., 1993. Adenovirus genes that modulate the sensitivity of virus-infected cells to lysis by TNF. *Journal of Cellular Biochemistry*, 53, pp. 329–335.
- Wong, E. and Giandomenico, C.M., 1999. Current status of platinum-based antitumor drugs. *Chemical Reviews*, 99, pp. 2451–2466.
- World Health Organization, 2014, *Cancer* [Online]. Available at <http://www.who.int/mediacentre/factsheets/fs297/en/> [Accessed: February 2014]
- Wyllie, A.H., Kerr, J.F. and Currie, A.R., 1980. Cell death: the significance of apoptosis. *International Review of Cytology*, 68, pp. 251–306.
- Xiang, M., Zhou, W., Gao, D., Fang, X. and Liu, Q., 2012. Inhibitor of apoptosis protein-like protein-2 as a novel serological biomarker for breast cancer. *International Journal of Molecular Sciences*, 13(12), pp. 16737-16750.
- Yang, X.R. et al., 2011. Associations of breast cancer risk factors with tumor subtypes: a pooled analysis from the Breast Cancer Association Consortium studies. *Journal of the National Cancer Institute*, 103, pp. 250–263.
- Yasumoto, E. et al., 2004. Cytotoxic activity of deferiprone, maltol and related hydroxyketones against human tumor cell lines. *Anticancer Research*, 24, pp. 755–762.

Yoon, C., Kuwabara, M.D., Spassky, A. and Sigman, D.S., 1990. Sequence specificity of the deoxyribonuclease activity of 1,10-phenanthroline-copper ion. *Biochemistry*, 27;29(8), pp. 2116-21.

Zhang, H. et al., 2011. A strategy for ZnO nanorod mediated multi-mode cancer treatment. *Biomaterials*, 32, pp. 1906–1914.

Zhou, X.F. et al., 2005. Effects of dihydropyridines and pyridines on multidrug resistance mediated by breast cancer resistance protein:in vitro and in vivo studies. *Drug Metabolism and Disposition*, 33(8), pp. 1220-1228.

Zhu, J., Chen, Z. and Lallemand-Breitenbach, V.H., 2002. How acute promyelocytic leukaemia revived arsenic. *Nature Reviews. Cancer* 2 (9), pp. 705–714.

APPENDIX A

Anova: One way for Figure 3.1.8

Cell line	IC-50 value		
MCF-7	2.9	3.2	3.8
MCF10A	17.8	16.8	18.2

Anova: Single
Factor

SUMMARY

<i>Groups</i>	<i>Count</i>	<i>Sum</i>	<i>Average</i>	<i>Variance</i>
MCF7	3	9.89	3.296667	0.214033333
MCF10A	3	52.8	17.6	0.52

ANOVA

<i>Source of Variation</i>	<i>SS</i>	<i>df</i>	<i>MS</i>	<i>F</i>	<i>P-value</i>	<i>F crit</i>
Between Groups	306.878	1	306.878	836.14191	8.51E-06	7.708647
Within Groups	1.468067	4	0.367017			
Total	308.3461	5				

$P < 0.05$

APPENDIX B

Anova: One way for Figure 4.1.4

Cell line	Percentage of apoptotic cells at 25µM		
MDA-MB-231	68.75%	69.63%	76.35%
MCF10A	4.51%	0.02%	5.04%

Anova: Single Factor

SUMMARY

<i>Groups</i>	<i>Count</i>	<i>Sum</i>	<i>Average</i>	<i>Variance</i>
MDA-MB-231	3	2.1473	0.715767	0.001728
MCF10A	3	0.0957	0.0319	0.000761

ANOVA

<i>Source of Variation</i>	<i>SS</i>	<i>df</i>	<i>MS</i>	<i>F</i>	<i>P-value</i>	<i>F crit</i>
Between Groups	0.70151	1	0.70151	563.7105	1.87E-05	7.708647
Within Groups	0.004978	4	0.001244			
Total	0.706488	5				

$P < 0.05$

APPENDIX C

Anova: One way for Figure 4.2.4

Concentration of [Co(phen)(ma)Cl]	Percentage of MDA-MB-231 cells in G1 phase		
	0 μ M	84.97%	85.01%
25 μ M	50.82%	51.58%	50.00%

Anova: Single
Factor

SUMMARY

<i>Groups</i>	<i>Count</i>	<i>Sum</i>	<i>Average</i>	<i>Variance</i>
0 μ M	3	2.5586	0.85286 7	2.64E-05
25 μ M	3	1.524	0.508	6.24E-05

ANOVA

<i>Source of Variation</i>	<i>SS</i>	<i>df</i>	<i>MS</i>	<i>F</i>	<i>P-value</i>	<i>F crit</i>
Between Groups	0.1784	1	0.1784	4014.24	3.72E-07	7.70864 7
Within Groups	0.00017 8	4	4.44E-05			
Total	0.17857 7	5				

$P < 0.01$